CHALMERS
UNIVERSITY OF TECHNOLOGY

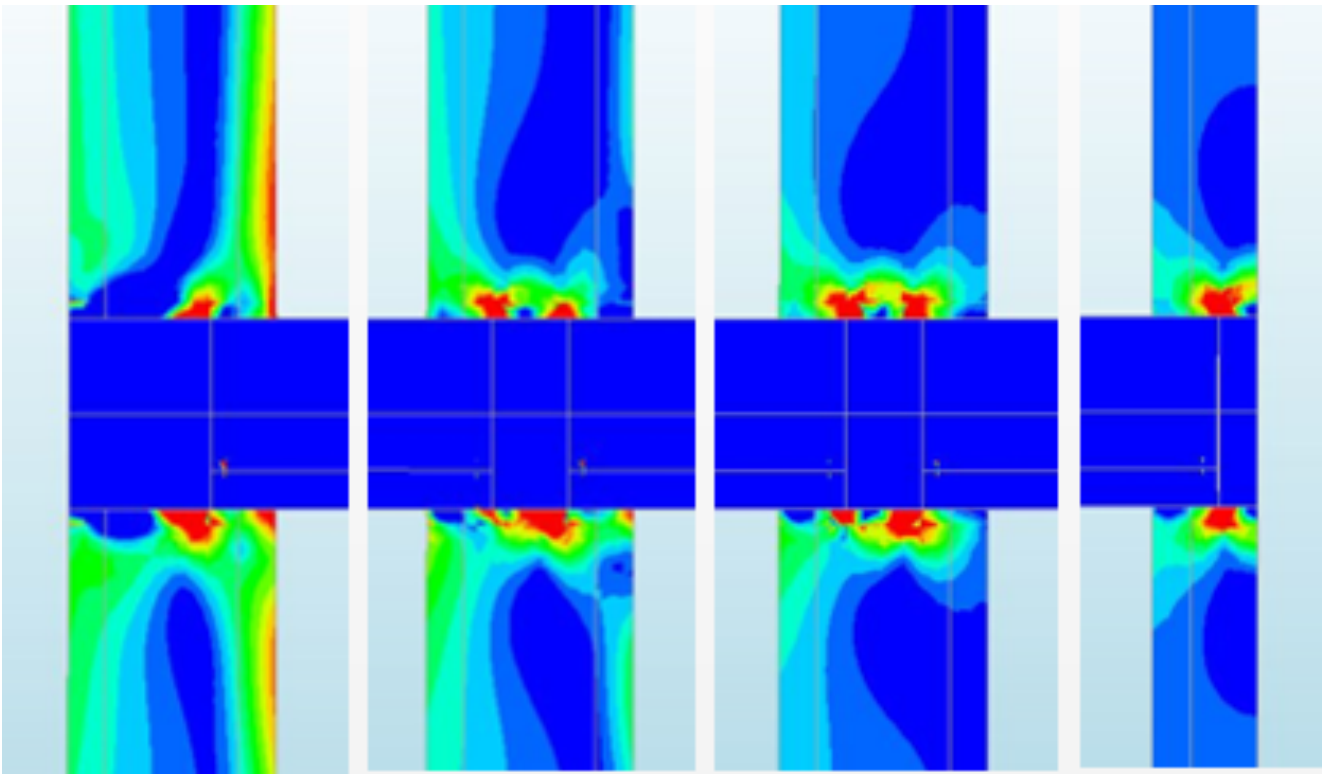

Restraint induced damage in prefabricated concrete element buildings due to long-term effects

Master's thesis in the Master's Programme Structural Engineering and Building Technology

SEBASTIAN JERNBERG
JOHANNES TISELL

Department of Architecture and Civil Engineering
Division of Structural Engineering
Concrete structures
CHALMERS UNIVERSITY OF TECHNOLOGY
Master's Thesis ACEX30-19-7

MASTER'S THESIS ACEX30-19-7

Restraint induced damage in prefabricated concrete element buildings due to long-term effects

Master's Thesis in the Master's Programme Structural Engineering and Building Technology

SEBASTIAN JERNBERG
JOHANNES TISELL

Department of Architecture and Civil Engineering
Division of Structural Engineering
Concrete structures
CHALMERS UNIVERSITY OF TECHNOLOGY
Göteborg, Sweden 2019

Restraint induced damage in prefabricated concrete element buildings due to long-term effects

Master's Thesis in the Master's Programme Structural Engineering and Building Technology

SEBASTIAN JERNBERG

JOHANNES TISELL

© SEBASTIAN JERNBERG, JOHANNES TISELL, 2019

Examensarbete ACEX30-19-7
Institutionen för arkitektur och samhällsbyggnadsteknik
Chalmers tekniska högskola, 2019

Department of Architecture and Civil Engineering
Division of Structural Engineering
Concrete Structures
Chalmers University of Technology
SE-412 96 Göteborg
Sweden
Telephone: + 46 (0)31-772 1000

Cover:
Figure which illustrates the development of strains for the reference object after approximately 50 years of service life
Department of Architecture and Civil Engineering
Göteborg, Sweden, 201

Restraint induced damage in prefabricated concrete element buildings due to long-term effects

Master's thesis in the Master's Programme Structural Engineering and Building Technology

SEBASTIAN JERNBERG

JOHANNES TISELL

Department of Architecture and Civil Engineering
Division of Structural Engineering
Concrete Structures
Chalmers University of Technology

ABSTRACT

An important aspect to include in the design of structures is the materials' behaviour during service life. In addition to external loading, concrete will deform due to long-term effects such as shrinkage and creep. These effects cause a need for movements within the material and if these movements are prevented by the structural system either by internal restraint, e.g. reinforcement, or external restraint, e.g. clamping, restraint forces will appear. The restraint forces induce stresses which can cause damages and reduce the capacity of the structure. This study aims to investigate where damages such as cracks and spalling occur in long and narrow buildings consisting of prestressed prefabricated concrete slab elements subjected to long-term effects.

Since an important aspect is to understand how and why these damages appear, a parametric study was performed, and the individual influences of various parameters were investigated with respect to the cracking behaviour. The parameters included in the parametric study were storage time for the elements, number of stories, total length of the building and span lengths. DIANA, a finite element (FE) software, was used to model the building in two dimensions, assuming plane stress state. Different models were analysed, and the results were examined in order to predict crack patterns in future designs. To increase the credibility of the results from the FE analysis, different verification analyses were made such as simplified FE analysis and hand-calculations.

The result clearly shows that storage time for the concrete elements is an important factor to include in design with respect to cracks and restraint forces. They also indicate that increased number of stories and longer spans increase the restraint forces and could therefore induce cracks. If these restraint forces are large enough they could affect the structural behaviour of the building and need therefore be taken into account in design.

After the results have been investigated, the origin of restraint forces is associated with storage time. Longer storage time before use, results in less restraint forces within the construction. Except for longer storage time, the effect of clamping is a relevant parameter to consider when designing long and narrow buildings. The effect of clamping in combination with long-term effects are critical when buildings exceed more than five stories.

Key words: Restraint forces, restraint, cracking, clamping, tie reinforcement, DIANA

Tvångskrafter i prefabricerade betongelementbyggnader påverkade av långtidseffekter

Examensarbete inom masterprogrammet Structural Engineering and Building Technology

SEBASTIAN JERNBERG

JOHANNES TISELL

Institutionen för arkitektur och samhällsbyggnadsteknik
Avdelningen för Konstruktionsteknik
Betongbyggnad
Chalmers tekniska högskola

SAMMANFATTNING

Materialens beteende under en konstruktions livslängd är en viktig aspekt som bör beaktas vid projektering av byggnader. I tillägg till yttre belastningar så deformeras betongen på grund av långtidseffekter såsom krympning och krypning. Effekten av krympning och krypning orsakar ett rörelsebehov inom materialet och om dessa rörelser är förhindrade antingen genom internt mothåll, armering, eller externt mothållet, klämmande effekt, så kommer tvångskrafter att uppstå. Tvångskrafterna kommer inducera spänningar i byggnaden vilket skulle kunna resultera i skador och därmed reducera byggnadens kapacitet. Denna studies målsättning är att undersöka var dessa skador i form av sprickor och spjälkning av betong uppstår i långsmala byggnader då konstruktionen är långsträckt och där förspända prefabricerade betongplattor utsätts för långtidseffekter.

En viktig aspekt är att förstå hur och varför dessa skador uppstår, därför har en parametrisk studie genomförts där varje parameters påverkan undersökts men hänsyn till sprickbildning. Parametrarna som inkluderas i studien omfattas av lagringstid, totalt antal våningar, total byggnadslängd och spannlängd. DIANA är en programvara som hanterar finita element beräkningar och det användes för att modellera objektet i 2D. En mängd olika modeller analyserades och resultaten undersöktes för att kunna förutse sprickbildning i framtida konstruktioner. För att öka trovärdigheten av resultaten från DIANA så har olika verifieringsverktyg såsom andra finita element program och handberäkningar använts.

Resultatet visar tydligt att lagringstiden för betongelementen är av stor vikt gällande uppkomsten av sprickor och tvångskrafter. De indikerar också att antalet våningar och spannlängder spelar roll gällande tvångskrafter och sprickor. Om tvångskrafterna blir tillräckligt stora så kan det påverka det bärande systemet och måste därför beaktas i dimensioneringen.

Efter att resultaten undersökts så kan slutsatsen gällande uppkomsten av tvångskrafter associeras till lagringstid. Längre lagringstid innan användning resulterar i mindre tvångskrafter inom konstruktionen. Bortsett från längre lagringstider är den klämmande effekten en relevant parameter att ha i åtanke vid dimensionering av långsmala byggnader. Den klämmande effekten kombinerat med långtidseffekter är kritiska då byggnader överstiger fem våningar.

Nyckelord: Tvångskrafter, tvång, sprickbildning, klämning, raskopplingsarmering, DIANA

Contents

Preface

This master thesis corresponds to 30 credits at University level and has been performed during the spring semester of 2018 in cooperation with COWI, Göteborg.

The study has increased our knowledge regarding concrete's behaviour when exposed to long-term effects and provided a deeper understanding concerning FE-modelling. This process has required a strict and structured working schedule and has prepared us for future challenges.

We would like to thank everyone at COWI for their hospitality over the last months. Especially, we would like to thank our supervisors Oscar Pagrotsky and Elias Fritzson for their guidance and patience with us as they always have been available to answer questions.

At Chalmers University of Technology, we would like to thank our examiner Mario Plos for his guidance.

Göteborg January 2019

Sebastian Jernberg & Johannes Tisell

Notations

Roman upper case letters

A_c	Concrete cross section area
A_{ef}	Effective concrete area
A_{hole}	Area where the tendon profile is placed
A_I	Transformed cross sectional area of state I
$A_{I,ef}$	Effective transformed cross sectional area of state I
A_{net}	Net concrete area
A_s	Cross sectional area of reinforcement steel
A_{trans}	Area of transformed concrete section
A_p	Cross sectional area of prestressing steel
E_c	Young's modulus for concrete
$E_{c,ef}$	Effective Young's modulus of concrete
E_{cm}	Mean value of Young's modulus of concrete
E_p	Young's Modulus for prestressing steel
E_s	Young's modulus for reinforcement steel
F_{cs}	Shrinkage force
I_c	Second moment of inertia of concrete
I_{trans}	Transformed second moment of inertia
I_I	Second moment of inertia state I
N	Normal force
P_i	Tendon force in the prestressing steel after short-term, i.e. before long term effects
P_{0i}	Effective prestressing force, initial value, i.e. before any long-term effects have occured
R	Restraint degree
S	Support stiffness

Roman lower case letters

e	Eccentricity
f_c	Compressive strength
f_{cc}	Cube compressive strength
f_{ck}	Characteristic concrete compression strength
f_{cm}	Mean concrete compressive strength
f_{ct}	Tensile strength of concrete
$f_{ctk.0,05}$	Lower characteristic value
$f_{ctk.0,95}$	Upper characteristic value
f_{ctm}	Mean tensile strength of concrete
f_t	Maximum tensile strength
f_y	Yield strength
f_{yd}	Design yield stress for reinforcement steel
f_{yk}	Characteristic yield stress for reinforcement steel
f_{pud}	Design value of tensile strength
f_{puk}	Characteristic value of tensile strength
$f_{p0.1k}$	Characteristic 0,1% proof-stress
k	Hardening ratio, between steel tensile strength and yield point
k_h	Coefficient depending on the size of the section
l	Length of element
s	Slip & spacing of ties

t	Time at the considered moment or time after tensioning
t_I	Width of the interface zone, or element length
t_0	Age of the concrete when it is loaded
u	Total displacement of the support
v	Effectiveness factor for the concrete
z_{cp}	Distance between the centre of gravity of the concrete section and the tendons
ΔT	Change in temperature

Greek lower case letters

$\beta(f_{cm})$	Factor that consider the concrete strength
$\beta(t_0)$	Factor that consider the age of concrete when it is loaded
$\beta_{as}(t)$	Time function for autogenous shrinkage
β_c	Coefficient for the strength of the compression strut
$\beta_c(t,t0)$	Coefficient that describe the development of creep during a time
$\beta_{ds}(t)$	Time function for drying shrinkage
β_H	Factor considering both relative humidity and notional size
β_{RH}	Factor that consider the ambient relative humidity
ε_c	Concrete strain
ε_{ca}	Autogenous strain
ε_{cc}	Creep strain
ε_{cd}	Drying shrinkage strain
ε_{cdi}	Starting value to determine the drying shrinkage
ε_{cs}	Total shrinkage strain
$\varepsilon_{c.el}$	Elastic concrete strain
ε_s	Total steel strain
ε_{sud}	Strain limit
ε_{syd}	Strain in steel at design yield strength
ε_{suk}	Strain at maximal stress
ε_p	Strain in prestressing steel
ε_{p0i}	Strain difference between steel and concrete
κ_1	Interaction “effectiveness” factor
κ_2	Interaction coefficient for flexural resistance at slip
μ	Friction coefficient
ρ	Ratio of reinforcement crossing the interface
σ_c	Concrete stress or compressive stress
σ_{ct}	Concrete tensile stress
σ_n	Lowest compressive stress resulting from normal force acting on the interface
σ_s	Stress in ordinary reinforcement steel
σ_p	Stress in prestressing steel
τ_a	Shear resistance from adhesion/mechanical interlocking
τ_b	Bond stress
τ_u	Ultimate shear stress
χ_t	Relaxation factor
$\varphi(t,t_0)$	Creep coefficient
φ_0	Notional creep coefficient
φ_{ef}	Effective creep coefficient
φ_{RH}	Factor that consider the relative humidity in creep

1 Introduction

1.1 Background

Building with prefabricated elements has a long tradition in Sweden, but has increased rapidly during recent years as a result of population growth and urbanization. Some reasons for its increase regarding concrete structures is that prefabrication provides advantages compared to in situ concrete. Some advantages are that longer spans can be obtained with prefabricated prestressed elements, it provides a more efficient work at the construction site and it reduces the construction time (Betongelementföreningen, 1998). However, for prefabricated concrete structures, there are some uncertainties concerning the consequences of long-term effects.

A common method to make the construction phase more efficient for long and narrow buildings, is to span the slab elements in the same direction as the length of the building. Regardless of how the slabs are positioned, Eurocode states that the elements of the floor need to be connected to each other so that local failure of a structural member does not lead to progressive collapse. However, this section in Eurocode, section 9.10 (CEN, 2004), may not be sufficient with respect to the effect of restraint forces since it has been derived without taking restraint into account. The part of Eurocode which regulates design against progressive collapse treats different tying systems of steel reinforcement, to increase the structures' ductility and integrity. The ties act as restraints which prevents free movement of the structural member (CEN, 2004). Due to uncertainties, how to interpret the code regarding restraints, questions have been raised regarding how long-term effects should be treated.

In the structural system, load distribution from the upper walls and the support from lower structural walls could clamp the slab and act as a restraint. Other restraints that could affect the response are friction between interfaces and adhesive forces between elements. When restraints and long-term effects, such as shrinkage and creep, are present restraint forces are induced within the element.

The longer the building is, the more restraint forces are induced in the structure. The need for movement due to long-term effects increases in magnitude with the length. Since concrete has low tensile strength, tensile stresses due to restraint forces could eventually cause cracking of a concrete element. The concrete is supposed to crack to a certain degree but cracking and crack widths must be limited due to aesthetics and with respect to large cracks by the integrity and capacity of the structural system. Furthermore, if cracks become visible, the residents may feel uncomfortable and unsure regarding the safety of the building. An investigation concerning restraint forces in long prefabricated prestressed concrete structures is therefore needed to gain an increased understanding of how and where cracks occur, in order to minimize maintenance and repair.

1.2 Aim and objectives

The aim of this project was to understand the consequences from shrinkage and creep in the structural system with regard to restraints. Furthermore, by adopting a parametric study, the aim was also to predict crack patterns and reduce cracking in future designs. This was done in order to illustrate the impact each variable have on the final design.

Questions treated in the study were:

- How to model and evaluate the results from an FE-analysis with regard to restraints?
- How does different parameters affect the structural response and where does cracks occur?
- Could the cracks create a structural problem?
- How could the development of cracks be prevented in future designs?

1.3 Scope and limitations

The scope of this study is to provide knowledge concerning:

- Structural system arranged with prestressed prefabricated massive slabs.
- Long-term effects, such as shrinkage and creep.
- The restraint effect due to ties and magnitude of clamping.

To limit the study certain decisions and restrictions has been made:

- All variable loads will be disregarded.
- Restraint forces due to thermal effect is not a part of this study.
- Adhesive restraints will be included in the FE-model but not further investigated in the parametric study.
- No stabilizing units in the horizontal direction is included in the structural system studied.

1.4 Method

A literature study was performed to acquire sufficient background information and increase understanding about material behaviour, restraint forces and long-term effects. Various sources such as research publications, standards, guidelines and textbooks were used. The knowledge from the literature study acted as a base for the analytical and numerical investigation.

In order to study the behaviour of long-term effects in buildings with prestressed prefabricated concrete slab elements a parametric study was performed. The parametric study was performed in accordance with different design codes in Eurocode (CEN, 2002) (CEN, 2006) (CEN, 2004) and Model Code 2010 (fib, 2013). The results were compared and evaluated in order to demonstrate the impact various parameters have on the risk of damages occurring. Selected parameters in this study were storage time, number of storeys, number of spans and span length.

The parametric study was made with the Finite Element Method (FEM) using the software DIANA (release 10.2) (DIANA fea, 2017). DIANA was chosen for this study since it is a general finite element software that can handle complex nonlinear models and has good capabilities for modelling of concrete structures. It is reliable regarding long-term effects because of its extensive material models and libraries, and can also handle the different phases in the service life with its specific analysis procedures. To confirm the FE-model, the modelling procedure was verified with both hand-calculations and another FEM software, PRE-Stress 6.5.

2 Problem description

2.1 Introduction

A common method when constructing buildings is to use prefabricated concrete elements. Compared to in-situ cast concrete it improves the efficiency and productivity at the construction site. The need for labour and construction time will decrease, which will reduce expenses for the contractor, and fewer injuries and accidents occur due to less moments performed on site (Betongelementföreningen, 1998). However, the method puts high demands on the design, especially in the early phases, since an error is difficult to adjust afterwards.

For slabs, prefabricated prestressed concrete elements are beneficial in order to obtain longer spans and to dispose the area as required, e.g. if the plan is unsymmetrical (Betongelementföreningen, 1998). For long and narrow buildings, it is favourable to place all slab elements in the same direction as the length of the building, see Figure 2.1. This simplifies the construction of the structure. With regard to safety, each element needs to be connected to both the adjacent slabs and to the structural walls to prevent the risk for progressive collapse in case one element should fail. To further increase the efficiency, prestressing can be used. This will also increase the possibility to have a variety of even longer span lengths. The prestressing effect is also favourable in the serviceability limit state with regard to cracks and deformation (Betongelementföreningen, 1998).

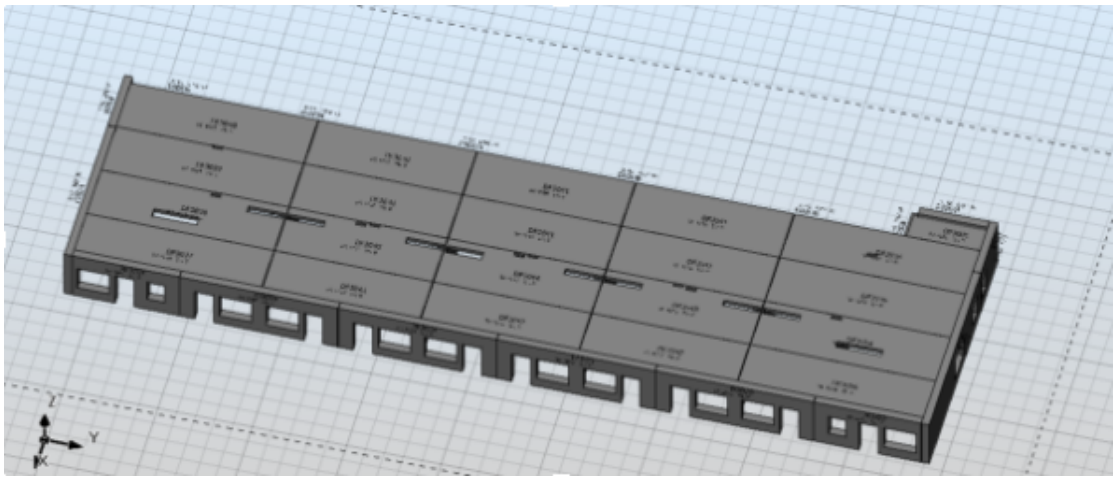

Figure 2.1 An illustration of a long and narrow building with slab elements placed in the longitudinal direction of the building.

Before regulations regarding prevention of progressive collapse was implemented each unit was, depending on the magnitude of the clamping force, able to move and deform freely. However, after some serious accidents, measures were taken to avoid progressive collapse by applying reinforcement ties between the elements so it would act more as one unit, see Figure 2.2 (Danielsson & Malmgren, 2006).

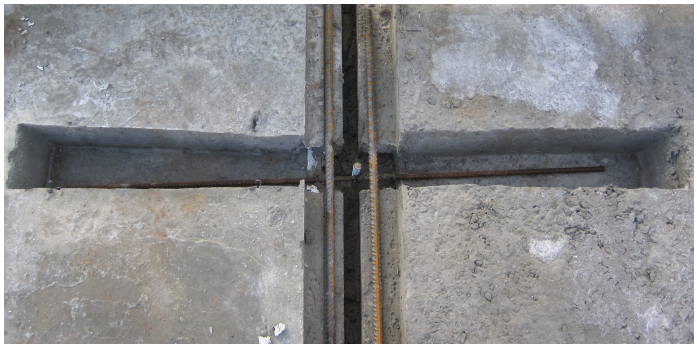

Figure 2.2 An example of a tying system with both horizontal and vertical reinforcement.

When applying this method to larger buildings with several spans, more restraint forces will be induced and this could eventually cause damage that affect the structural system.

2.2 Restraint forces

When concrete structures are loaded, tensile stresses might appear and cracks are almost inevitable due to the low tensile strength of concrete. The stresses originate from either external loads or restraint forces. The external loads are imposed displacements or loads that are directly applied at the boundaries of a structural concrete member (Antona & Johansson, 2011). When a prestressed prefabricated concrete slab is part of a structural system, it will be restrained and restraint forces will emerge due to different intrinsic deformations and loads which the element is subjected to. Restraint forces appear when a concrete member has a need to move but the movement is prevented due do external or internal restraints, e.g. boundary conditions or reinforcing steel (Eriksson & Fritzson, 2014). This study focuses on movement which originates from self-weight, shrinkage and creep.

The process of shrinkage starts already during storage. The storage time can vary between one week and several months and during this time the prefabricated concrete slab is able to deform without any restraints. The advantage with longer storage time is that the structure can deform more without any restraint and smaller restraint forces is obtained when the structure is mounted. However, the problem of shrinkage and creep remains since it acts over a long period of time (Al-Emrani, Engström, Johansson, & Johansson, Bärande konstruktioner Del 1, 2013).

In design, it is important to recognize and to account for the effect of restraint forces and not only design with regard to external loads. CEN (2004) states that this needs to be taken into account in design but it is not fully explained how and where these restraint forces appear in concrete structures and what consequences it might entail.

2.3 Damages

The prestressed prefabricated concrete slab elements are connected by a tying system. Since the tying system connects the slab elements, several elements will act as one unit. When the concrete slabs are mounted and partially fixed to the structural walls it will induce restraint forces within each element due to long-term effects. These restraint forces increase with the length of the building and could eventually cause cracks or

spalling of concrete. The damages are usually not critical for the structural system but could create a sense of discomfort and are not aesthetically pleasing.

The effect of shrinkage and creep deforms the concrete slab and causes tensile stresses due to restraints. If these stresses exceed the tensile strength cracking occurs which decreases the restraint forces and allows the slab to deform. An indication that cracking has occurred and that the slab is deformed is if an unpainted concrete surface has been revealed in the ceiling, where the slab and the structural wall meets. Support rotation occur due to the load acting on the structure and could eventually cause crushing of the top corner of the supporting wall. Also, if the slab deforms over the support and causes the joint to "open", it will create a tensile force in the upper edge of the wall and it could cause spalling of concrete in this area, see Figure 2.3 and Figure 2.4. According to [1]Fritzson these damages occur after about 5 years depending on the design of the structure.

Figure 2.3 Spalling of concrete wall. Photo: Elias Fritzson. (Reproduced with permission from the photographer.)

[1] Elias Fritzson, COWI, 2018-05-18

Figure 2.4 Spalling of concrete wall with visible reinforcement. Photo: Elias Fritzson. (Reproduced with permission from the photographer.)

3 Material behaviour

3.1 Concrete

Concrete is a composite material with material behaviour depending on the loading condition. An important difference in property of concrete is that its tensile strength is significantly lower than its compressive strength; a typical assumption is that the tensile strength is approximately a tenth of the compressive strength (Al-Emrani, Engström, Johansson, & Johansson, Bärande konstruktioner Del 1, 2013). In Figure 3.1, a typical uni-axial stress-strain relation for concrete is shown, illustrating the difference between tensile and compressive strength for concrete.

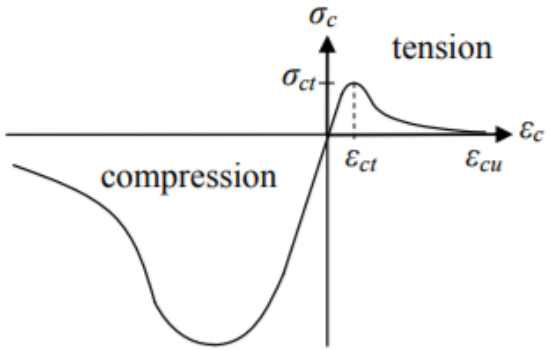

Figure 3.1 Typical uni-axial stress-strain relation for concrete (Eriksson & Fritzson, 2014).

The failure modes will differ depending on whether the stress state is in compression or tension (Plos, 2000). In this thesis focus will be on the tensile strength of concrete and therefore the compressive strength will not be further explained. When a concrete specimen is subjected to tensile stresses, micro-cracks will form at local weak points in the material. If the tensile stress is increased the micro-cracks will connect to each other and eventually form a real crack. Before cracking starts, the concrete can be assumed to have a linear elastic material behaviour, but this is not the case after cracking (Plos, 2000).

Concrete is highly dependent on imperfections in the material. This means that each specimen is unique even though it has been manufactured in the same way. Because of this, the mechanical properties do not have an absolute value, illustrated in Figure 3.2. It describes the mean tensile strength, its lower and upper characteristic value for a strength class according to Eurocode 2 (Engström, Restraint cracking of reinforced concrete structures, 2014).

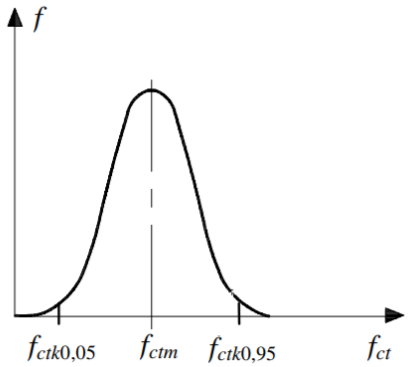

Figure 3.2 Fundamental distribution of the mean tensile strength f_{ctm}, lower characteristic value $f_{ctk.0,05}$ (5 %-fractile) and upper characteristic value $f_{ctk.0,95}$ (95 %-fractile) (Engström, Restraint cracking of reinforced concrete structures, 2014).

As Figure 3.2 indicates, the tensile strength of concrete is highly unpredictable and this should be taken into account in design. Depending the purpose of the design, it could be favourable to use either the lower or upper characteristic value. When designing against restraint forces, a high tensile strength is unfavourable since the restraint force will be allowed to increase, as long as the member is uncracked. However, if the purpose is to design a member with a crack limit, the lower characteristic value should be used (Al-Emrani, Engström, Johansson, & Johansson, Bärande konstruktioner Del 1, 2013).

3.2 Steel reinforcement

Steel reinforcement combined with plain concrete provides additional tensile strength. Classification of reinforcement is influenced by parameters specified as yield strength, fatigue strength, bond strength and tolerances. One of the most common processing methods is to hot-roll the reinforcement bars. A general stress-strain relation for hot-rolled reinforcement is shown in Figure 3.3 (Al-Emrani, Engström, Johansson, & Johansson, Bärande konstruktioner Del 1, 2013).

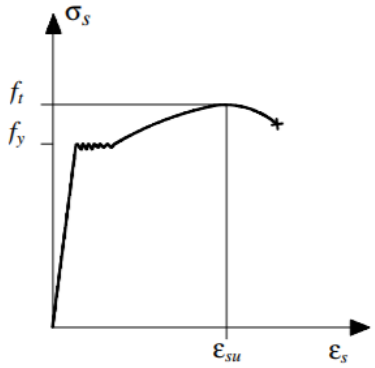

Figure 3.3 Stress-strain relation for hot-rolled reinforcement (Al-Emrani, Engström, Johansson, & Johansson, Bärande konstruktioner Del 1, 2013).

In Figure 3.3 a linear relation between stress and strain is assumed up to yield strength f_y and the elastic deformation is reversible. The inclination of the linear behaviour is dependent of Young's Modulus of Elasticity E_s. When the stress is increased over the

yield strength plastic irreversible deformations will arise. A phase of strain hardening occurs until maximum stress f_t is reached.

Eurocode 2 (CEN, 2004), contains a simplified and an idealised stress-strain curve. Both can be applicable for calculations in the ultimate limit state regarding dimensioning or verification of resistance capacity. The two dimensioning curves is presented in Figure 3.4.

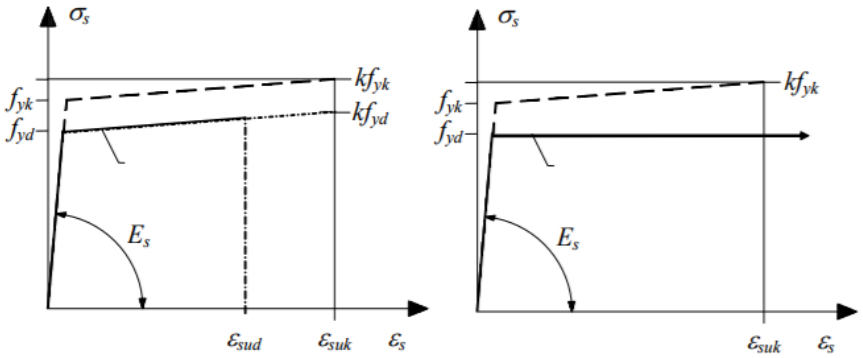

Figure 3.4 Simplified and idealised design stress-strain relations according to Eurocode 2, a) Idealised curve with an inclined upper branch and a strain limit, b) Design curve with an horizontal upper branch (Al-Emrani, Engström, Johansson, & Johansson, Bärande konstruktioner Del 1, 2013).

Curve a) in Figure 3.4 has an upper branch defined with regard to a strain limit ε_{sud} and design values. Corresponding steel stress equation for curve a) is presented in (3-2). Curve b) in Figure 3.4 also has an upper branch without a strain limitation and corresponding steel stress equation is presented in (3-1).

$$\sigma_s = E_s * \varepsilon_s \quad \text{for} \quad \varepsilon_s \le \varepsilon_{syd} = \frac{f_{yd}}{E_s} \tag{3-1}$$

$$\sigma_s = f_{yd} + \frac{\varepsilon_s - \varepsilon_{syd}}{\varepsilon_{suk} - \varepsilon_{syd}}(k * f_{yd} - f_{yd}) \quad \text{for} \quad E_{c,ef}(t, t_0) = \frac{E_{cm}}{1 + \varphi_{ef}(t, t_0)} \tag{3-2}$$

where
ε_s = strain in steel
ε_{syd} = strain in steel at design yield strength
ε_{suk} = strain at maximal stress
ε_{sud} = strain limit, ε_{sud}=0,9* ε_{suk} (recommended value 0,9)
E_s = Young's modulus for reinforcement steel
E_{cm} = mean value of Young's modulus pf concrete
$E_{c,ef}$ = effective Young's modulus of concrete
f_{yd} = design yield stress for reinforcement steel
k = hardening ratio, quota between steel tensile strength and yield point
t = actual time considered
t_0 = concrete age when load was applied

$$\sigma_s = E_s * \varepsilon_s \quad \text{for} \quad \varepsilon_s \le \varepsilon_{syd} = \frac{f_{yd}}{E_s} \tag{3-3}$$

$$\sigma_s = f_{yd} \quad \text{for} \quad \varepsilon_s \geq \varepsilon_{syd} \tag{3-4}$$

3.3 Prestressing steel

Plain and reinforced concrete structural members have a problem with cracking, causing the stiffness of the structural member to decrease. The maximum allowed deformation will therefore often be decisive. Another disadvantage with cracked reinforced concrete sections is the increased risk of corrosion and fatigue of the reinforcing steel. Cracking occur due to high tensile stresses in the structural member and the phenomena of prestressing could partly or fully prevent cracks to take place under service condition according to Engström (2011). This study only treats slabs with prestressing, which distributes load in one direction only and could therefore be treated using beam theory.

The stress-strain relationship for prestressing steel is based on the characteristic tensile strength and the characteristic 0,1% proof-stress $f_{p0.1k}$. Two alternative design stress-strain diagrams according to Eurocode 2 is shown in Figure 3.5**.**

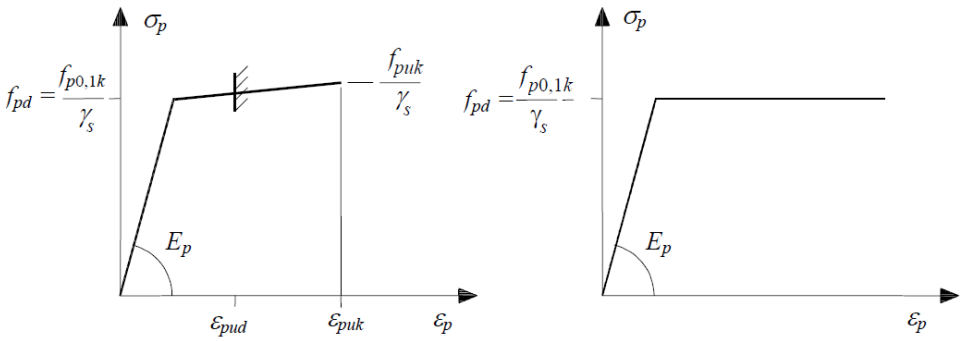

Figure 3.5 Two alternative design stress-strain diagrams (Engström, Design and analysis of prestressed concrete structures, 2011).

The prestressing steel does not have a pronounced yield stress. As seen in Figure 3.5, the breakpoint between the two branches is determined by the characteristic 0,1% proof-stress and the slope of the first branch, which is defined by Young's modulus of prestressing steel E_p. The shape of curve a with a maximum value determined by the characteristic value of ultimate strain ε_{puk} and the design value of the tensile strength f_{pud} represent the real properties of prestressing steel in the best way but, since the rupture is more brittle than for ordinary reinforcement, the maximum strain the design curve is limited to ε_{pud}. A comparison of general stress-strain relationship between ribbed reinforcing steel and prestressing steel is shown in Figure 3.6 (Engström, Design and analysis of prestressed concrete structures, 2011).

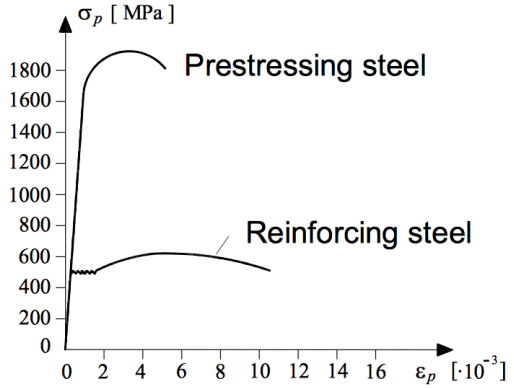

Figure 3.6 Comparison of stress-strain relation for prestressing steel and reinforcing steel (Engström, Design and analysis of prestressed concrete structures, 2011).

Prestressed prefabricated slabs are concrete element with constant cross-section. During the production, tendons are prestressed in a tensioning bed before the concrete is casted. After hardening of concrete, the tensioning force in the tendons embedded within the concrete is released. This means that the structural member is subjected to compressive axial forces before any variable load is applied. Due to prestressing, the structure will not be subjected to tensile stresses before a substantial load is applied and as the load increases the compressive effect of prestressing is reduced. As a result, the response of cracking is delayed in comparison to an ordinary reinforced concrete member. To fully prevent cracking in the serviceability limit state the prestressed member need a large enough axial compressive force. Stress distribution for a fully prestressed structural member is shown in Figure 3.7.

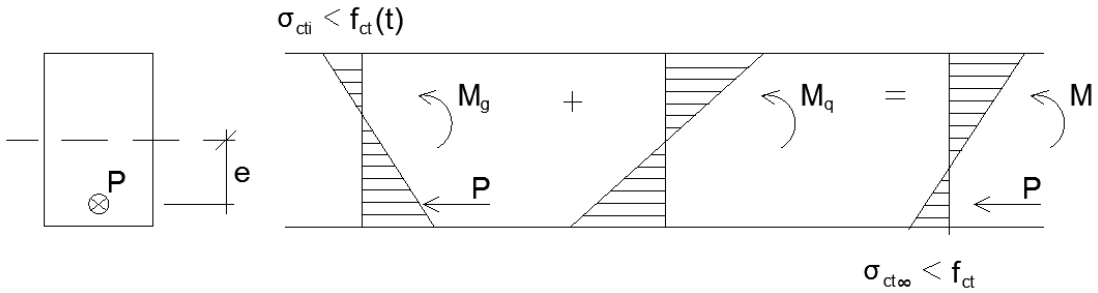

Figure 3.7 Example of stress distribution for a fully prestressed beam (Engström, Design and analysis of prestressed concrete structures, 2011).

In a partially prestressed member cracking is accepted but crack widths need to be controlled in the serviceability limit state. Stress distribution for a limited acceptable amount of cracking is presented in Figure 3.8.

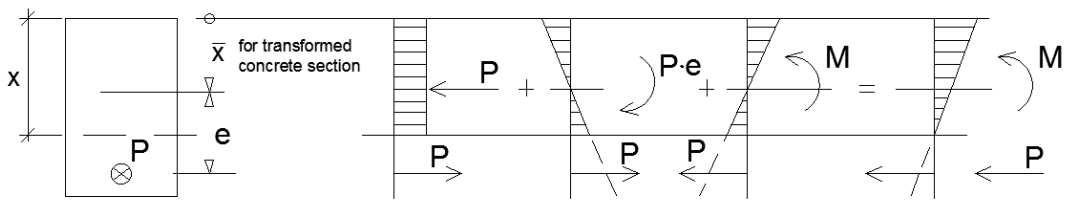

Figure 3.8 Example of stress distribution for a partially prestressed beam (Engström, Design and analysis of prestressed concrete structures, 2011).

There is no general requirement on the prestressing degree in to Eurocode 2. In Eurocode 2 there is a recommendation with regard to corrosion that the concrete at the level of the prestressing steel should not have tensile stresses, or a limitation of crack width. When corrosion is no longer a factor, Eurocode 2 recommends that the concrete tensile stresses during quasi-permanent load combination should be avoided at the level of prestressing steel (Engström, Design and analysis of prestressed concrete structures, 2011).

Prestressing is also influenced by time dependent effects such as shrinkage, creep and relaxation. Shrinkage and creep is further explained in Section 4.5 and 4.6.

Relaxation is an effect due to prestressing, which result in a decrease of the prestressing force over time when the tendon is subjected to constant strain. The initial stress in the prestressing tendon is expressed as

$$\sigma_p(t) = \sigma_{pi} - \Delta\sigma_{pr}(t) \tag{3-5}$$

where σ_{pi} = initial steel stress
$\Delta\sigma_{pr}$ = relaxation loss at time t

The magnitude of relaxation effect varies according to Eurocode 2 depending on the type of prestressing steel and the three relaxation classes is presented in Table 3.1.

Table 3.1 Type of prestressing steel and basic relaxation factor χ_{1000} (CEN, 2004)

Relaxation class	**Prestressing steel**	**χ_{1000}**
1	Wire and strand with ordinary relaxation	0,08
2	Wire and strand with low relaxation	0,025
3	Hot-rolled and processed bars	0,04

The final relaxation factor for a certain class and time *t* can be obtained from following equations:

Class 1 $$\chi_t = 5{,}39 * \chi_{1000} e^{6{,}7\mu} * \left(\frac{t}{1000}\right)^{0{,}75(1-\mu)} * 10^{-3} \tag{3-6}$$

Class 2 $$\chi_t = 0{,}66 * \chi_{1000} e^{9{,}1\mu} * \left(\frac{t}{1000}\right)^{0{,}75(1-\mu)} * 10^{-3} \tag{3-7}$$

Class 3 $$\chi_t = 1{,}98 * \chi_{1000} e^{8\mu} * \left(\frac{t}{1000}\right)^{0{,}75(1-\mu)} * 10^{-3} \tag{3-8}$$

where t = time after tensioning in hours
μ = σ_{pi}/f_{puk}
f_{puk} = characteristic value of tensile strength

The remaining effect of prestressing after relaxation at a certain time can be explained in Figure 3.9 and (3-9).

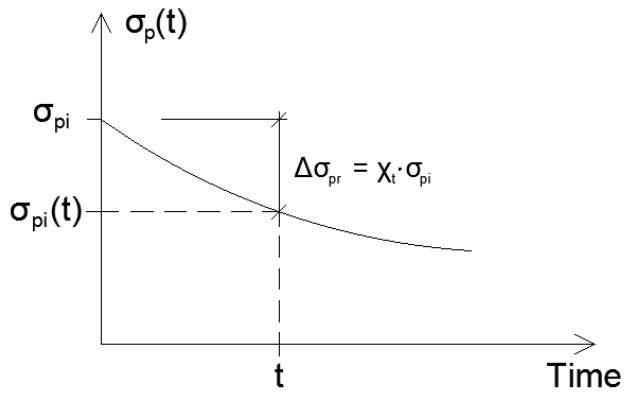

Figure 3.9 Relaxation of prestressing steel with constant imposed strain (Engström, Design and analysis of prestressed concrete structures, 2011).

$$\sigma_p(t) = \sigma_{pi} - \Delta\sigma_{pr}(t) \tag{3-9}$$

The influence of shrinkage and creep also decrease the effect of prestressing. The prestressing compressive force *P* cause an initial elastic strain in the concrete, see (3-10). The initial strain will increase with time due to effect of creep and how the total strain increase in the concrete after long time is stated in (3-11).

$$\varepsilon_{ci} = \frac{\sigma_c}{E_{cm}} = \frac{P}{A_c * E_{cm}} \tag{3-10}$$

$$\Delta\varepsilon = \varphi(t, t_0)\varepsilon_{ci} + \varepsilon_{cs}(\infty) \tag{3-11}$$

The loss in prestressing effect due to shrinkage and creep depends on the concrete strain since the length between the prestressed tendon and concrete member is equal. Concrete strain correlates to the change in steel strain after long time. The magnitude of the loss of prestressing effect is stated as

$$\Delta\sigma_p = E_s * \Delta\varepsilon_p = E_s * \Delta\varepsilon \tag{3-12}$$

For the remaining prestressing effect, the steel stress can be expressed as

$$\sigma_p = \sigma_{pi} - \Delta\sigma_p \tag{3-13}$$

The total loss of prestressing stress when creep, shrinkage and relaxation is combined could according to Heinrich (1991) and CEN (2004) be determined as

$$\Delta\sigma_{p,c+s+r} = \frac{\varepsilon_{cs}E_p + 0{,}8\Delta\sigma_{pr} + \frac{E_p}{E_{cm}}\varphi(t, t_0).\sigma_{c,QP}}{1 + \frac{E_p}{E_{cm}}\frac{A_p}{A_c}(1 + \frac{A_c}{I_c}z_{cp}^2)[1 + 0{,}8\varphi(t, t_0)]} \tag{3-14}$$

where $\Delta\sigma_{p,c+s+r}$ = absolute value of the variation of stress in the tendons due to creep, shrinkage and relaxation
ε_{cs} = shrinkage strain
E_p = modulus of elasticity for the prestressing steel

$\Delta\sigma_{pr}$ = variation of stress in the tendons due to relaxation
$\varphi(t,t_0)$ = creep coefficient at t and load application at t_0
$\sigma_{c,QP}$ = stress in concrete adjacent to the tendons due to self-weight and initial prestress and other quasi-permanent actions where relevant
A_p = area of prestressing tendon
A_c = area of concrete section
I_c = second moment of inertia of concrete
z_{cp} = distance between the centre of gravity of the concrete section and the tendons

3.4 Interaction between concrete and steel reinforcement

The reinforcement is first anchored to the concrete through a chemical bond. A chemical bond is usually a relative weak connection according to Burström (2007). A new anchorage between concrete and reinforcement will arise through friction when the chemical bond breaks. The surface properties of reinforcement is therefore of great importance and ribbed bars could be used to increase the friction bond capacity.

The stress in the interface between concrete and reinforcement is called bond stress. Bond stress τ_b is a shear stress which depends on surface properties of reinforcement bars. An increase in bond stress can induce a slip *s* between the steel and the concrete. The general relation between bond stress and slip *s* can be studied based on the results from pull-out tests with short embedment length presented in Figure 3.10 (Engström, Restraint cracking of reinforced concrete structures, 2014). Illustration of pull-out test is shown in Figure 3.11.

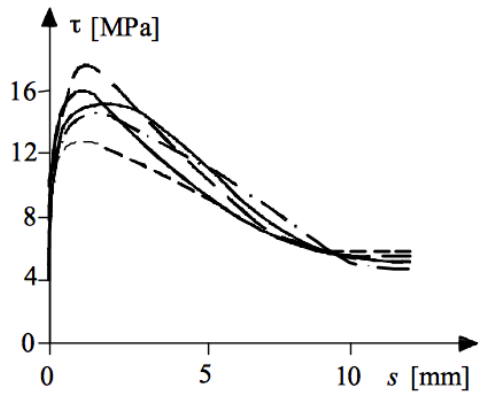

Figure 3.10 Results from pull-out tests with short embedment length (Engström, Restraint cracking of reinforced concrete structures, 2014).

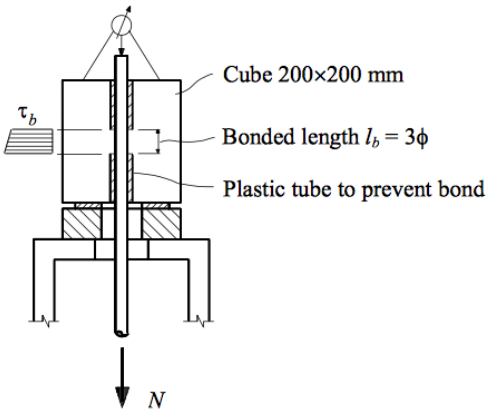

Figure 3.11 Illustration of pull-out test (Engström, Restraint cracking of reinforced concrete structures, 2014).

A general relation between bond stress τ_b and slip s for ribbed bars is explained with different mechanisms in Figure 3.12.

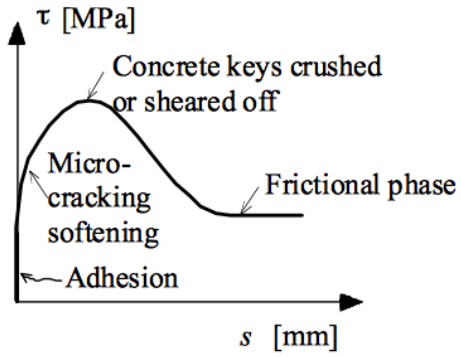

Figure 3.12 Different mechanisms which is developed in relation to bond stress and slip (Engström, Restraint cracking of reinforced concrete structures, 2014).

A schematic relation between bond stress and local slip is proposed in fib (2013) based on results from pull-out tests with short embedment length. The proposal is shown in Figure 3.13 (Engström, Restraint cracking of reinforced concrete structures, 2014).

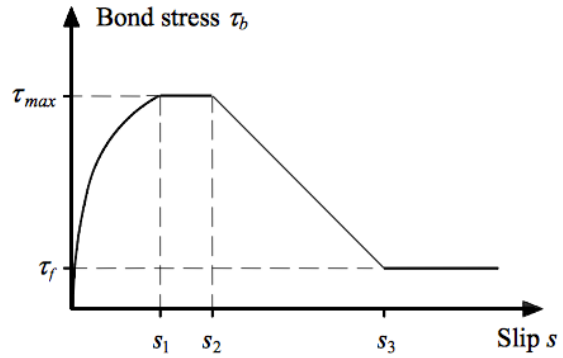

Figure 3.13 Schematic relation between bond stress and local slip (Engström, Restraint cracking of reinforced concrete structures, 2014).

The schematic relation between bond stress and local slip can be used to predict how steel stress, bond stress and slip varies along the reinforcement bar (Al-Emrani, Engström, Johansson, & Johansson, Bärande konstruktioner del 2, 2011). Local slip is

usually smaller than the value s_1 in serviceability limit state where the maximum bond strength is reached. The first branch can therefore be expressed as (3-15) according to Engström (2014).

$$\tau_b(s) = 0{,}22 * f_{cm} * s^{0{,}21} \qquad s < s_1 \qquad (3\text{-}15)$$

where f_{cm} = concrete compression strength, mean value
s = slip, should be inserted in mm

3.5 Interaction between concrete cast at different times

Prefabricated elements normally have an uneven surface and because of this an additional layer of concrete is cast at site. The additional layer of concrete also allows the elements covered by the additional concrete layer to interact. The connection between two concrete bodies cast at different times can be exposed to shear forces (parallel to the interface), normal forces (perpendicular to the interface) or a combination of both. A variety of tests identifies interface roughness, cleanliness of surface, concrete strength and concrete quality, eccentricity or inclination of shear force, interface condition with respect to bond (strong bond/pre-cracking/debonding) and ratio of reinforcement crossing the interface as main parameters influencing the load bearing capacity according to fib (2013).

Interface roughness, cleanliness of interface, concrete strength and quality influence the mechanisms of adhesive bonding and mechanical interlocking. Adhesive bonding can develop along even interfaces whilst mechanical interlocking requires a rougher interface surface. The effects of adhesive bonding and mechanical interlocking is simplified in Figure 3.14.

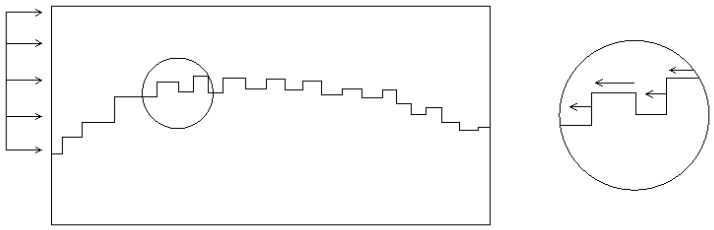

Figure 3.14 Mechanism of adhesive bonding and mechanical interlocking (fib, 2013).

Another mechanism affecting the capacity of the connection between the concrete materials is shear friction. Shear friction is developed when the structure is exposed to both shear force and a compressive force, see Figure 3.15. A rougher intersection surface induces larger capacity in shear friction.

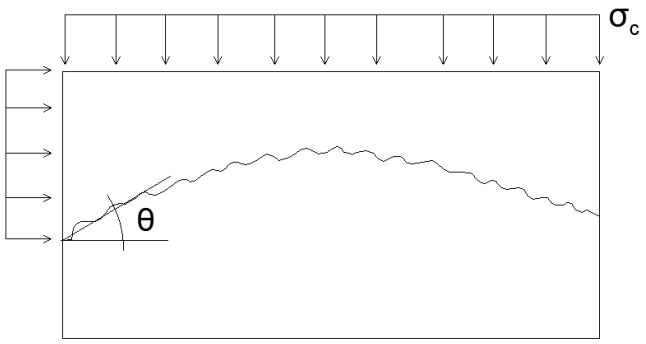

Figure 3.15 Mechanism of shear friction (fib, 2013).

The illustration of Figure 3.15 can be used to calculate the shear resistance for a smooth interface area according to equation (3-16). In case there is a change in interface roughness, equation (3-17) is more suitable. Values of the friction coefficient μ is stated in Table 3.2 depending on the interface roughness.

$$\tau = \sigma_c * tan\,\theta \tag{3-16}$$

$$\tau = \tau_a + \mu * \sigma_c \tag{3-17}$$

where σ_c = compressive stress perpendicular to the surface
θ = angle between surfaces
τ_a = shear resistance from adhesion/interlocking
μ = friction coefficient

Table 3.2 Coefficient of friction for concrete grades ≤ C50 according to fib (2013)

Interface roughness	**Coefficient of friction μ**
Smooth interface	0.5-0.7
Rough interface	0.7-1.0
Very rough interface	1.0-1.4

Dowel action of reinforcement is a mechanism affected by connectors crossing the interface. A shear slip between the concrete materials results in a lateral displacement between the top and bottom part of the connectors. When a shear slip occur, bending stresses is induced in the connectors. Maximum bending resistance of the mechanism is of interest when the maximum shear slip takes place with an approximate value of 0.1-0.2 times the diameter of the connector. Effect of large slips is called kinking and the principle of dowel action for both bending stresses and kinking is illustrated in Figure 3.16.

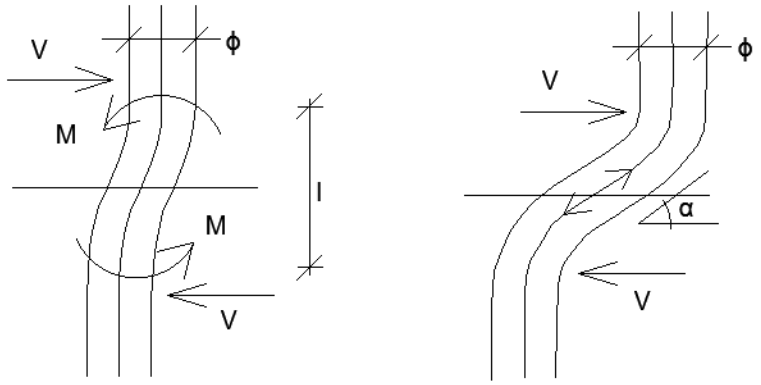

Figure 3.16 Mechanism of dowel action (fib, 2013).

The lateral displacement which arise due to shear slip also generates an axial tensile force as a result of the opening of the joint. The proportion of the tensile force depends on roughness of the interaction surface. With regard to tensile stresses full bending resistance cannot be achieved. With all mentioned mechanisms combined, each mechanism will reach its maximum allowable shear resistance at a different shear slip and it is not a possibility to add the maximum values together. The ultimate shear resistance can, according to fib (2013), be expressed as

$$\tau_u = \tau_a + \mu\left(\rho * \kappa_1 * f_y * \sigma_n\right) + \kappa_2 * \rho * \sqrt{f_y * f_{cc}} \leq \beta_c * \nu * f_{cc} \tag{3-18}$$

where
- ρ = ratio of reinforcement crossing the interface ($\rho=A_s/A_c$)
- κ_1 = interaction "effectiveness" factor
- κ_2 = interaction coefficient for flexural resistance at slip
- σ_n = lowest compressive stress resulting from normal force acting on the interface
- f_{cc} = cube compressive strength
- β_c = coefficient for the strength of the compression strut – see Table 7.3-2 in fib (2013)
- ν = effectiveness factor for the concrete

4 Restraint

4.1 Restraint degree

When a member is prevented from "free" movement there is a restraint. The most obvious way to restraint a member is by adding an external-restraint in the boundary condition e.g. where the structural member is fixed to the support. The other way is to add an internal-restraint where stresses within the structural member emerge e.g. through bond interaction between reinforcement and concrete (Engström, Restraint cracking of reinforced concrete structures, 2014). A restraints' influence on a member is defined by the restraint degree *R* which describes to what extent a structural member is prevented to move freely depending on both the external and the internal restraint. Equation (4-1) - (4-4) determines whether the member has full restraint, no restraint, or partial restraint, $0 \leq R \leq 1$ (Engström, Restraint cracking of reinforced concrete structures, 2014).

$$R = \frac{actual\ imposed\ strain}{imposed\ strain\ in\ case\ of\ full\ restraint} \tag{4-1}$$

$$R = \frac{actual\ stress\ dependent\ strain}{-(stress\ independent\ strain)} \tag{4-2}$$

$$R = \frac{\varepsilon_c}{-\varepsilon_{cs}} \tag{4-3}$$

$$R = \frac{\frac{\sigma_c}{E_c}}{\sigma_c\left(\frac{1}{E_c} + \frac{A_c}{S * l}\right)} \tag{4-4}$$

where ε_c = stress dependent strain
ε_{cs} = stress independent strain
σ_c = concrete stress
S = total stiffness of the supports S=N/u
N = normal force
u = total displacement of the supports
l = length of element

A general statement is that real structures are exposed to internal and external restraint at the same time (Eriksson & Fritzson, 2014). Some restraint could also act as both an internal as an external restraint depending on the circumstances. However, to understand the general picture of how a structural member responds to a certain situation it is first essential to understand the concept of external and internal restraint.

4.2 Stress-dependent strain and stress-independent strain

When considering strain with regard to cracking it is important to understand that it can occur two types of strains, stress-dependent and stress-independent strain. The strains

can be separated depending on whether the strain is a result from imposed load or not. The sum of these two strains gives the total deformation.

When a structural member is exposed to an external loading which will cause a deformation it will result in stress-dependent strains. This type of strain occurs both in short and long-term. For short-term, the stress-strain relation can be found by Hooke's law and will give rise to an elastic strain expressed as

$$\varepsilon_{c,el} = \frac{\sigma_c}{E_c} \tag{4-5}$$

For long-term response, the stress-dependent strain will increase with time due to creep. The strain is highly dependent on the concrete stress for short-term response but also with the load duration. The development of creep is largest in the beginning and will after a certain time reach its final value, see Section 4.6. If constant stress is applied then the stress-dependent strain can be expressed as (4-6) (Engström, Restraint cracking of reinforced concrete structures, 2014).

$$\varepsilon_c(t) = \varepsilon_{c,el} + \varepsilon_{c,el} * \big(\varphi(t, t_0)\big) = \varepsilon_{c,el}(1 + \varphi(t, t_0) \tag{4-6}$$

Stress-independent strains is a result from when a structural member is allowed to deform freely without an applied stress. This deformation does not induce any stresses within the member. If a structural member is restrained and no longer allows free movement stresses will appear and cause stress-dependent strains. Shrinkage or thermal expansion or contraction are such factors which result in stress-independent strains. Stress-independent strain can vary with time similar to long-term response for stress-dependent strain. Thermal concrete strain will not be included in this study and therefore not further explained. Shrinkage will be explained further in Section 4.5.

4.3 External restraint

According to Engström (2014) a general statement regarding external restraint is that the extent of restraint in a structural member increases with the number of fixed boundaries. This relation is explained in Figure 4.1 where a member is subjected to different number and position of the fixed boundaries.

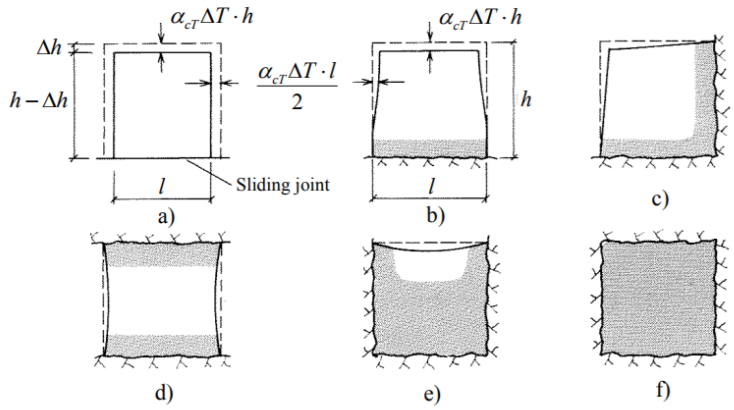

Figure 4.1 Different boundary conditions for a strucural member (Engström, Restraint cracking of reinforced concrete structures, 2014).

Figure 4.1 clearly shows that the extent of the restraint increases with number of fixed boundaries and position. A member with no fixed boundaries is totally free to move and a member with only one fixed boundary can still move rather free. When increasing the number of fixed edges the freedom of movement is decreased and it is also affected by the positions of the fixed boundaries. If all boundaries are fixed the whole structure is considered to have full restraint.

As mentioned earlier in this section, external restraint is when a structural member to some extent is fixed to its support or boundaries to prevent free movement. A slab which is fixed in the short ends between either structural walls or beams by bond in the joints have an external restraint, see Figure 4.2. When full restraint occurs, the boundaries are very stiff and will prevent the slab to move in the longitudinal direction. High stresses will occur close to the supports and cracks are likely to form in this area. If the boundaries are more flexible then the restraint will not be completely stiff and the need for movements can to some extent be fulfilled. In general, movements in the transverse direction is more likely to occur even though the short ends are fixed to some degree, see Figure 4.2 (Engström, Restraint cracking of reinforced concrete structures, 2014).

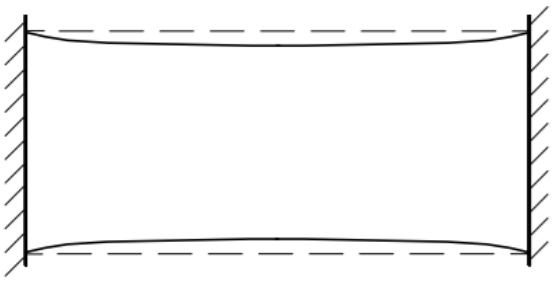

Figure 4.2 Slab element that is attached to structural members at the shorter ends (Engström, Restraint cracking of reinforced concrete structures, 2014).

4.4 Internal restraint

Internal restraint is when a structural member is subjected to different stress-independent strains within the member and these strains prevent each other from moving freely. The stresses that occurs from this phenomenon is called eigenstresses

and could cause cracking of the concrete. Reinforcement is a common type of internal restraint which prevents the concrete to shrink freely.

Depending on whether the stress-independent strains within the cross-section have a linear or non-linear variation this will give different results. Because the free movements within the section will fit each other there will be no need for eigenstresses in the linear variation, only curvature. However, if the curvature is prevented by an external restraint, corresponding stresses will arise. However internal restraint and eigenstresses will always be the result with regard to a non-linear variation of stress-independent strains (Engström, Restraint cracking of reinforced concrete structures, 2014).

This study will consider a concrete slab with eccentric prestressed reinforcement, but to fully understand the problem, first a structural member of concrete with symmetrically arranged reinforcement is explained in Section 4.4.1.

4.4.1 Reinforced concrete member with symmetrically arranged reinforcement exposed to uniform shrinkage

According to Engström (2014) the total strain and corresponding stresses can be derived from Figure 4.3 and the equations (4-7) - (4-11).

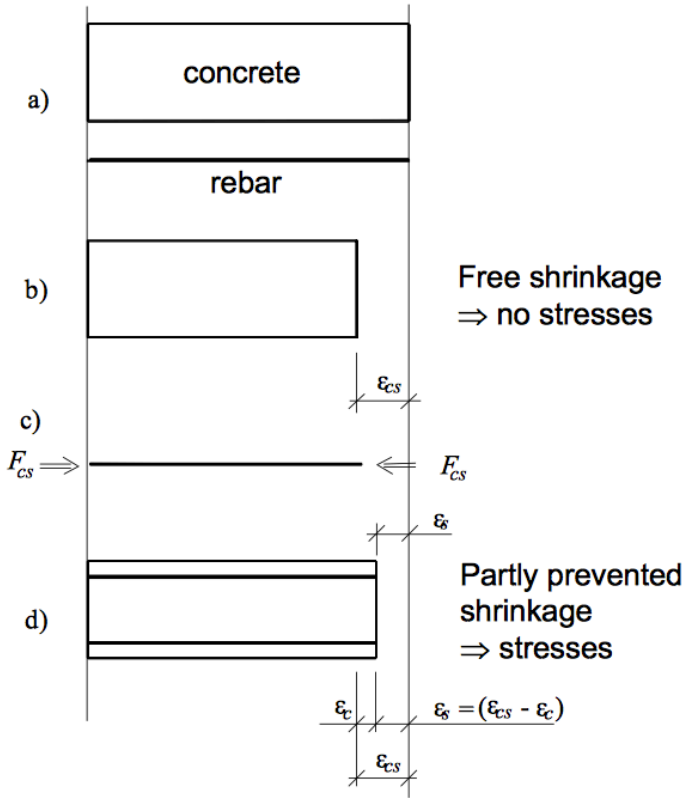

Figure 4.3 Stress and strain development over time (Engström, Restraint cracking of reinforced concrete structures, 2014).

In the first step a) when time is equal to zero and no loading is applied, both concrete and reinforcement are without any initial stresses. In step b) after a certain time t, the concrete has shrinked freely without any stresses and resulting in a shrinkage strain ε_{cs}.

The reinforcement is compressed in step c) with a shrinkage force F_{cs} in order to achieve the same length as the concrete after free shrinkage. The concrete and reinforcement are still coupled together under the influence of the compressive force acting on the steel.

$$F_{cs}(t) = E_s * \varepsilon_{cs} * A_s \tag{4-7}$$

In step d) the shrinkage force in the steel is removed and the steel tries to go back to its original length. When removing the compressive force the concrete member is subjected to a tensile force equal to the shrinkage force F_{cs} that wants to elongate the reinforced concrete member, leading to a concrete strain ε_c. ε_s is the total strain of the steel which is a result of the total strain of the concrete, both stress-independent and stress-dependent strains, since full interaction is assumed. As full interaction between the concrete and reinforcement is assumed the concrete stress can be solved from Navier's formula for the transformed concrete section stated as

$$\sigma_c(t) = \frac{F_{cs}(t)}{A_{I,ef}} \tag{4-8}$$

where $A_{I,ef} = A_c + (\alpha_{ef} - 1) * A_s$

$\alpha_{ef} = \frac{E_s}{E_c(1+\varphi(t,t_0))}$

The steel stress is determined by adding the concrete stress with a factor α_{ef} as (4-9). This is illustrated in Figure 3.3 step c) and d).

$$\sigma_s(t) = \frac{-F_{cs}}{A_s} + \alpha_{ef} * \sigma_c(t) \tag{4-9}$$

The total shortening of the reinforced concrete member is expressed by the strain in the concrete and reinforcement after the compressive force F_{cs} is removed and can be determined as

$$\varepsilon_c - |\varepsilon_{cs}(t)| = \varepsilon_s \tag{4-10}$$

The restraint force as a result from the imposed strain can be determined by the means of eigenstresses according to

$$\sigma_c(t) * A_{net} = \sigma_s(t) * A_s \tag{4-11}$$

where $A_{net} = A_c - A_s$

4.4.2 Reinforced concrete member with eccentric arranged reinforcement exposed to uniform shrinkage

If the internal restraint in case of reinforcement is only placed in either the upper or lower section or in another way not placed symmetrically the shrinkage force F_{cs} will act with an eccentricity. The internal restraint acts in the interface between the concrete and reinforcement, in other words at the level of the reinforcement. As an effect from

the unsymmetrically placed reinforcement, the restraint situation will be a result from an average stress-independent strain, uniform shrinkage, and an irregular stress-dependent strain from reinforcement.

If an external moment is acting on a structural member with eccentric reinforcement the stress in the concrete will be determined as

$$\sigma_c(z) = \frac{\sum F_{cs}}{A_{trans}} + \frac{\sum(F_{cs} * e_s) + M}{I_{trans}} * z \tag{4-12}$$

where $A_{trans}, I_{trans} = A_I, I_I$ in uncracked section
$A_{trans}, I_{trans} = A_{II}, I_{II}$ in cracked section
$e_s = d - x_i$ in uncracked section
$e_s = d - x_{II}$ in cracked section

Figure 4.4 illustrates a case with one reinforcement layer placed in the lower section with an external moment acting is shown.

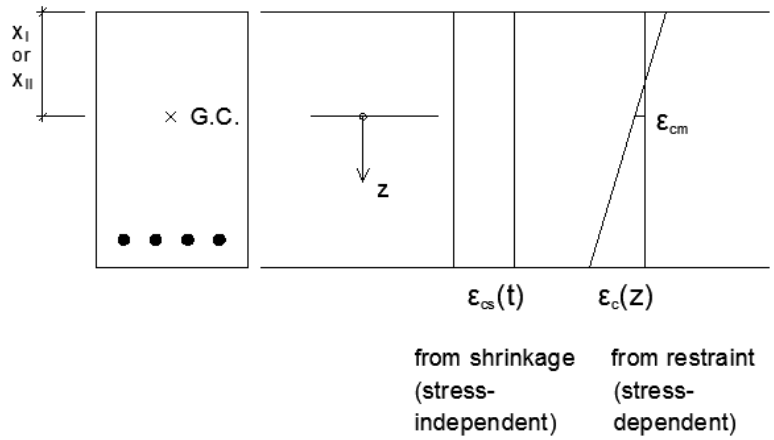

*Figure 4.4 Reinforce*d concrete section with eccentric reinforcement and uniform shrinkage. The restraint from the steel results in both a stress-dependent average strain ε_{cm} and curvature *(Engström, Restraint cracking of reinforced concrete structures, 2014)*.

An average strain is found by combining the stress-dependent and stress-independent deformation shown as

$$\varepsilon_{cm,tot} = \varepsilon_{cs}(t) + \frac{F_{cs}(t)}{E_{c,ef} * A_{trans}} \tag{4-13}$$

4.4.3 Prestressed concrete member with symmetrically arranged prestressing tendons exposed to uniform shrinkage

Prestressing of tendons in relation to concrete cause a strain difference between concrete and steel. The strain difference varies with time and is dependent on shrinkage strain, see Figure 4.5.

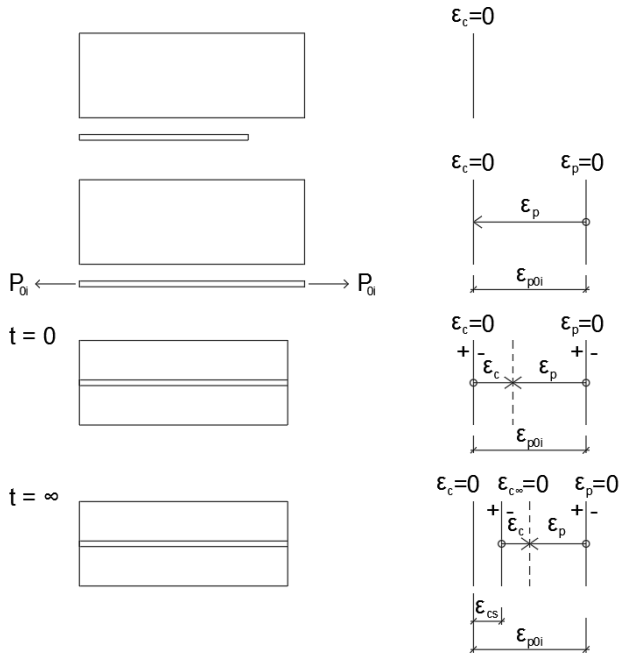

Figure 4.5 Strain conditions due to shrinkage of a prestressed concrete prismatic member. The effect of prestrain and shrinkage (Engström, Design and analysis of prestressed concrete structures, 2011).

In the first step a) the concrete and the tendon has no initial stresses. In the second step b) the prestressing tendon is loaded with a tensile force to compensate the length difference between the materials. The applied tensile force can be expressed as (4-14) and is defined as effective prestressing force and causes an internal restraint.

$$P_{0i} = E_p * \varepsilon_{p0i} * A_p \tag{4-14}$$

where ε_{p0i} = strain difference between steel and concrete

The tensile force causes a total strain difference ε_{p0i} in the prestressing tendon and after release of tensile force, step c), a compatibility condition can be established as (4-15) from the strain diagram, see Fel! Det går inrte att hitta någon referenskälla..

$$\varepsilon_p + (-\varepsilon_c) = \varepsilon_{p0i} \tag{4-15}$$

In the last step d) long-term effect i.e. shrinkage causes the compatibility condition in (4-15) to change due to a decrease of the initial prestrain. Compatibility condition for long-term effect is expressed as

$$\varepsilon_p + (-\varepsilon_c) = \left(\varepsilon_{p0i} - \varepsilon_{cs}\right) \tag{4-16}$$

The internal restraint force can now be determined as

$$E_p * \left(\varepsilon_{p0i} - \varepsilon_{cs}\right) * A_p = P_{0i} - F_{cs} \tag{4-17}$$

4.5 Shrinkage

Concrete shrinks when it is dehydrated. This could lead to damage on the structural member in forms of cracks or a need for curvature upwards along the edges of the slab. The shrinkage is a result of water leaving the pore system causing a contraction of the cement paste that starts already during hardening, but the final value $\varepsilon_{cs}(\infty)$ is obtained first after a long time (Burström, 2007). The final shrinkage strain has large influence on stresses in concrete and the risk of cracking. According to Engström (2014) can the final value of shrinkage for concrete be in the magnitude of $0{,}1*10^{-3}$ - $0{,}5*10^{-3}$ depending on the relative humidity, see Figure 4.6. The horizontal axis represents relative humidity in percent and the vertical axis represent shrinkage in per mille.

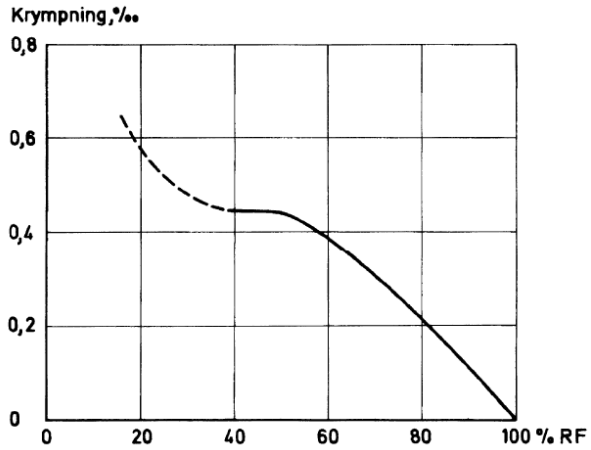

Figure 4.6 Shrinkage of concrete as a function of relative humidity (Burström, 2007).

Shrinkage strain is a stress-independent deformation which can be divided into two main parts, drying shrinkage and autogenous shrinkage (Engström, Restraint cracking of reinforced concrete structures, 2014). Eurocode 2 states that the shrinkage strain at a certain time [days] can be expressed as

$$\varepsilon_{cs}(t) = \varepsilon_{cd}(t) + \varepsilon_{ca}(t) \tag{4-18}$$

where $\varepsilon_{cd}(t)$ = drying shrinkage strain
$\varepsilon_{ca}(t)$ = autogenous shrinkage strain

The degree of which shrinkage is acting on a structural concrete member is highly dependent on the water cement-ratio. If the relation between the water and cement is low the majority of the water will react with the cement and the concrete will have a low permeability. If this is the case, drying shrinkage will only affect the surface of the concrete member and the autogenous shrinkage will be the dominating part of the shrinkage. On the contrary, drying shrinkage will be the main part of the total shrinkage if the concrete has a high water cement relation (Engström, Restraint cracking of reinforced concrete structures, 2014).

4.5.1 Drying shrinkage

Drying shrinkage occurs when the moisture inside the concrete evaporates to the surrounding environment causing a decrease in volume. The process goes as follows: As the concrete is mixed and hardened, a significant part of the water will be stored in

the pore system and if placed in a dry environment this amount of water will evaporate with time and cause shrinkage. The process depends on various factors such as relative humidity, temperature, wind speed, thickness and surface area of the element (Brattström & Hagman, 2017). In general, the permeability of concrete is low and the drying process therefore develops under long period of time.

The final drying shrinkage can be determined as (4-19) according to CEN (2004).

$$\varepsilon_{cd}(t) = \beta_{ds}(t) * \varepsilon_{cd}(\infty) \quad (4\text{-}19)$$

where $\beta_{ds}(t)$ = time function of drying shrinkage
$\varepsilon_{cd}(\infty)$ = final value of drying shrinkage

The final value of drying shrinkage can be stated as

$$\varepsilon_{cd}(\infty) = k_h * \beta_{RH} * \varepsilon_{cdi} \quad (4\text{-}20)$$

where k_h = coefficient that depends on the size of the section
β_{RH} = factor that considers the ambient relative humidity
ε_{cdi} = starting value to determine the drying shrinkage strain

4.5.2 Autogenous shrinkage

Autogenous shrinkage takes place under the hardening process of concrete and is a type of chemical shrinkage caused under the hydration process. When the concrete has hardened there is still some moisture and cement left within the member and these will react with each other under the early days after casting. This will cause a "chemical shrinkage" which is not dependent on the exchange of moisture between concrete and the surrounding environment. A beneficial part of autogenous shrinkage is that it develops a lot faster than drying shrinkage, which leads to a drier concrete during the first period of casting (Engström, Restraint cracking of reinforced concrete structures, 2014).

According to CEN (2004) the final autogenous shrinkage can be determined as

$$\varepsilon_{ca}(t) = \beta_{as}(t) * \varepsilon_{ca}(\infty) \quad (4\text{-}21)$$

where β_{as} = time function of autogenous shrinkage
$\varepsilon_{ca}(\infty)$ = final value of autogenous shrinkage

4.6 Creep

When a structural concrete member is subjected by stress it will deform. The total deformation can be divided into two parts, an immediate elastic deformation and a creep deformation. The elastic deformation is time-independent and will occur in accordance to Hooke's law independently of creep. The creep deformation will develop with time until it reaches its final value after approximately 70 years (Engström, Restraint cracking of reinforced concrete structures, 2014). If the stress on the member is removed the elastic deformation will regress but the creep deformation will remain, see Figure 4.7.

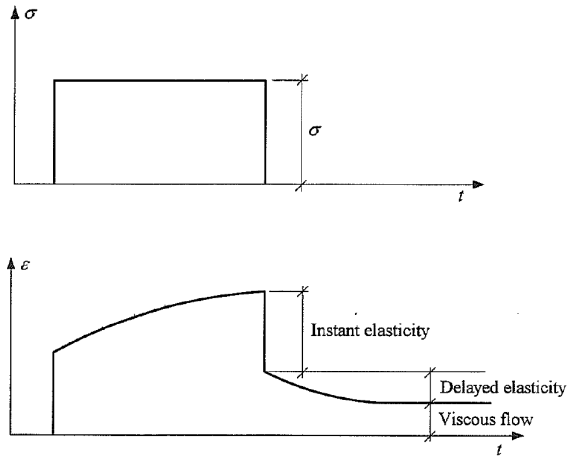

Figure 4.7 Deformation of concrete over time due to loading and unloading (Engström, Restraint cracking of reinforced concrete structures, 2014).

The creep strain could be found by multiplying a time-dependent factor to the elastic strain as follow

$$\varepsilon_{cc}(t) = \varphi(t, t_0) * \frac{\sigma_c}{E_c} \tag{4-22}$$

The creep coefficient can be calculated as

$$\varphi(t, t_0) = \beta_c(t, t_0) * \varphi_0 \tag{4-23}$$

where β_c = time function of the creep coefficient
(t,t_0) = notional creep coefficient
φ_0

The notional creep coefficient can be expressed as (4-24) and usually gives a value between 1 and 3 under normal service conditions. Lower strength class for concrete, drier climate and early loading age result in a higher notional creep coefficient.

$$\varphi_0 = \varphi_{RH} * \beta(f_{cm}) * \beta(t_0) \tag{4-24}$$

where φ_{RH} = factor that considers the relative humidity
$\beta(f_{cm})$ = factor that considers the concrete strength
$\beta(t_0)$ = factor that considers the age when the concrete was loaded

The creep coefficient develops in time and a short load duration results in a reduced creep coefficient dependent on the time function $\beta_c(t,t_0) < 1$ stated as

$$\beta_c(t, t_0) = \left[\frac{(t - t_0)}{\beta_H + (t - t_0)}\right]^{0,3} \tag{4-25}$$

where β_H = coefficient depending on the ambient relative humidity and the notional size of the section

The creep deformation is of great importance and needs to be taken into account in the design. In comparison to the elastic deformation the final creep value could be up to three times as large. As (4-25) states, the creep is highly dependent on the concrete age when loaded. If the concrete is loaded at a very early age compared to being loaded after hardening at 28 days, the final creep coefficient could be more than doubled. Except from concrete age the same factors as influence drying shrinkage of concrete also influence creep. This means that the moisture content is also very important when considering creep effect (Engström, Restraint cracking of reinforced concrete structures, 2014). When designing with respect to long-time effects, an elastic modulus of elasticity can be used.

Creep will, except from deforming the concrete member, make the concrete "softer" with time. This will cause a redistribution of stresses from the concrete to the reinforcement. It will also reduce restraint stresses since the concrete will adapt itself to the constraints over time, Engström (2014). As a result, creep will decrease the internal stresses caused by shrinkage.

If a constant stress is smaller than half of the compressive strength the creep deformation is expected to be proportional to the stress, if higher stress is applied the creep will increase non-linearly.

4.6.1 Different approaches for effective modulus of elasticity

When designing for creep one has to take into account that the concrete stress is generally not constant over time. The stress can either decrease or increase during service life and this variation needs to be considered. An example could be that the effect of shrinkage, creep and relaxation causes a decrease of the prestressing force in a prestressed member which decreases the compressive stress in the concrete. For each different portion of the stress one unique creep factor can be determined reflecting how this part of the stress varies over time. Four different approaches can be used to account for stress that varies during time, Engström (2014).

4.6.1.1 Effective modulus of elasticity based on the first creep function

This is the first and most simple approach. It does not take the loading history into account and calculates only one creep function based on when the first load is applied. This creep function is then combined with the load stress applied after a certain time and can be determined as

$$\varepsilon_c(t) = \left(1 + \varphi(t, t_0)\right) * \frac{\sigma_c(t)}{E_{cm}} \tag{4-26}$$

or

$$\varepsilon_c(t) = \frac{\sigma_c(t)}{E_{c,ef}(t, t_0)} \quad \text{with} \quad E_{c,ef}(t, t_0) = \frac{E_{cm}}{1 + \varphi(t, t_0)} \tag{4-27}$$

This is a very approximate method and if the concrete stress is increased with time then will the creep deformation will be overestimated. In the same way the creep deformation will be underestimated if the stress will decrease with time.

4.6.1.2 Effective modulus of elasticity based on the first creep function with a modified creep coefficient

The second approach is similar to the first approach but with a modified creep coefficient. Since the first approach is very approximate and gives an overestimation or an underestimation of the creep deformation depending on the loading history, an adjustment is needed. The creep coefficient is determined as in the first approach but modified with regard to relaxation χ (Engström, Restraint cracking of reinforced concrete structures, 2014). The second approach can be determined as

$$\varepsilon_c(t) = \left(1 + \chi * \varphi(t, t_0)\right) * \frac{\sigma_c(t)}{E_{cm}} \tag{4-28}$$

or

$$\varepsilon_c(t) = \frac{\sigma_c(t)}{E_{c,ef}(t, t_0)} \qquad \text{with} \qquad E_{c,ef}(t, t_0) = \frac{E_{cm}}{1 + \chi * \varphi(t, t_0)} \tag{4-29}$$

where χ = relaxation factor

4.6.1.3 Effective modulus of elasticity with an effective creep coefficient based on several creep functions

The third approach takes each unique creep function in consideration by calculating an average effective creep coefficient as

$$\varphi_{ef}(t, t_0) = \frac{\sum_i \varphi_i(t, t_i) * \sigma_{ci}}{\sum_i \sigma_i} \tag{4-30}$$

where φ_{ef} = effective creep coefficient

The effective creep coefficient can then be used to calculate the effective modulus of elasticity and the stress-dependent strain is still based on the stress acting at age *t*. The strain acting at age *t* can then be expressed as

$$\varepsilon_c(t) = \left(1 + \varphi_{ef}(t, t_0)\right) * \frac{\sigma_c(t)}{E_{cm}} \tag{4-31}$$

or

$$\varepsilon_c(t) = \frac{\sigma_c(t)}{E_{c,ef}(t, t_0)} \qquad \text{with} \qquad E_{c,ef}(t, t_0) = \frac{E_{cm}}{1 + \varphi_{ef}(t, t_0)} \tag{4-32}$$

4.6.1.4 Superposition method

The fourth approach is the most accurate since it assumes that each stress component results in one unique creep function. By superposition these creep functions can be combined with the stress applied at the same time. If the concrete stress is decrease at a certain time it will be added in the equation with a negative sign. This will result in different time step which corresponds more to reality than the previous three approaches. The stress is considered to be constant for each time step and a higher number of time steps gives a more precise calculation. The stress dependent strain can be determined as

$$\varepsilon_c(t) = \left(1 + \varphi(t, t_1)\right) * \frac{\sigma_1}{E_{cm}} + \left(1 + \varphi(t, t_2)\right) * \frac{\sigma_2}{E_{cm}} + \left(1 + \varphi(t, t_3)\right) * \frac{\sigma_3}{E_{cm}} \tag{4-33}$$

4.6.2 Superposition method with regard to shrinkage of a prestressed concrete member

In a concrete member, the prestressing force will decrease with time due to shrinkage. A consequence will be that the initial strain will decrease causing a continuous redistribution of steel and concrete stresses. The magnitude of the redistribution will also be influenced by relaxation of prestressing steel and creep of concrete. The development of the redistribution can be determined numerically by the superposition.

Engström (Engström, Restraint cracking of reinforced concrete structures, 2014) provides an example where a short post-tensioned concrete element is studied. The beam has no external load, relaxation is not taken into account and it is arranged with symmetrical tendons which provides a uniformly distributed stress across the section. The change of stresses in concrete and steel can then be determined from the following reasoning.

The initial stresses are stated as

$$\sigma_{ci} = \frac{P_i}{A_{net}} \qquad \sigma_{pi} = \frac{P_i}{A_p}$$

where P_i = initial prestressing force

$A_{net} = A_c - A_{hole}$

The following conditions of equilibrium, compatibility and constitutive relations must all be satisfied with regard to shrinkage and creep.

$$\sigma_c * A_{net} + \sigma_p * A_p = 0 \qquad \text{(equilibrium)} \tag{4-34}$$

$$\varepsilon_p - \varepsilon_c = \varepsilon_{p0i} - \varepsilon_{cs} \qquad \text{(compatibility)} \tag{4-35}$$

$$\Delta\varepsilon_p = \Delta\varepsilon_c - \Delta\varepsilon_{cs} \tag{4-36}$$

$$\varepsilon_c = f(\sigma_{ci}, \Delta\sigma_i, \varphi_i) \qquad \text{(constitutive, concrete)} \qquad (4\text{-}37)$$

$$\Delta\varepsilon_p = \frac{\Delta\sigma_p}{E_p} \qquad \text{(constitutive, steel)} \qquad (4\text{-}38)$$

The development of concrete strain is increased with small steps over time. The corresponding stress are determined by a combination of these conditions

$$\Delta\sigma_c = \frac{-E_p(\Delta\varepsilon_c - \Delta\varepsilon_{cs})A_p}{A_{net}} \qquad (4\text{-}39)$$

$$\Delta\sigma_p = E_p(\Delta\varepsilon_c - \Delta\varepsilon_{cs}) \qquad (4\text{-}40)$$

5 Restraint in prefabricated element buildings

5.1 Progressive collapse

When a local collapse occurs due to failure in one or a few structural elements and then propagates to other components causing a global collapse, a progressive collapse is a fact. The triggering event is assumed to have a very low probability of occurrence and can evolve due to local action or lack of resistance. Until a few decades ago, progressive collapse has only been designed for in certain buildings, such as embassy's or very long bridges and, according to Starossek (2014), the codes regarding progressive collapse today lack general applicability. However, due to certain events such as the partial collapse of Ronan Point in 1968, the codes have been reviewed and harder restrictions has been taken to prevent progressive collapse.

5.1.1 Ronan point

Ronan Point was a prefabricated 22-storey tower block in East London that partially collapsed due to a gas explosion. At the explosion, some of the load bearing walls lost their structural function and due to bad coherence between elements it forced the slabs above to collapse. The weight from the rubble, caused by the collapse, was too heavy to support for the exposed storey and progressive collapse was initiated, see Figure 5.1 and Figure 5.2.

Figure 5.1 Partial collapse of the corner of Ronan Point in East London as a result of a gas explosion in 1968 (The Daily Telegraph, 1968).

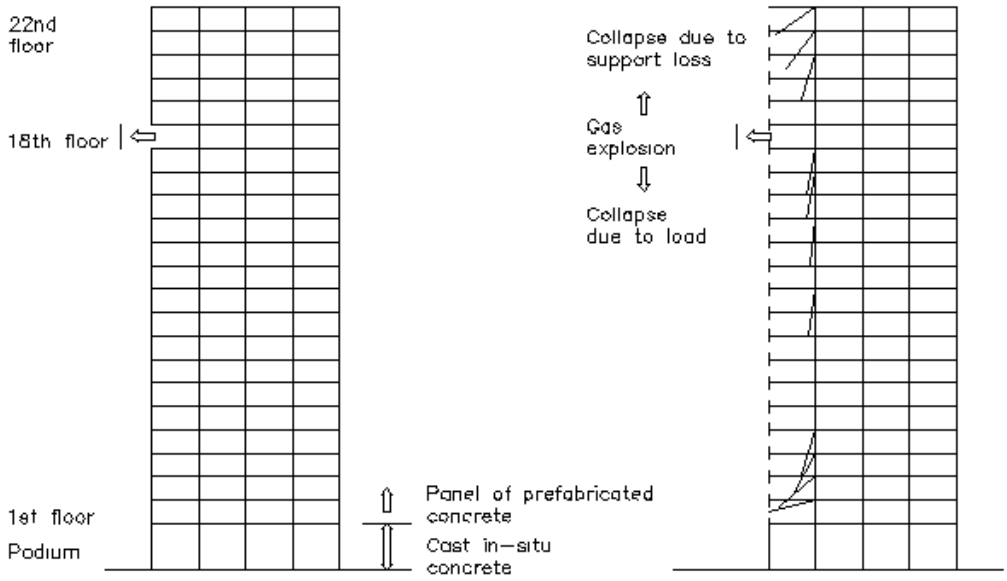

Figure 5.2 The progress of the progressive collapse in Ronan Point in London 1968 after a gas explosion at the 18th floor.

5.1.2 Accidental design situations

The event at Ronan Point initiated a discussion on how robustness should be considered in the design and the possibility of progressive collapse. The codes were first developed in England and later implemented to Eurocode. CEN (2006) states that structures shall be designed for the relevant accidental design situations in accordance with EN 1990, 3.2(2)P (CEN, 2002). This means that different accidental design situations need to be accounted for, see Figure 5.3. If the accidental action is known, the left-hand side of the flowchart is applicable. However, this study will focus on the right-hand side of the flowchart based on strategies on limiting the extent of localised failure. The right-hand side is interesting since it considers failure from loading and long-term effects rather than from unpredictable actions and are therefore more applicable to this study.

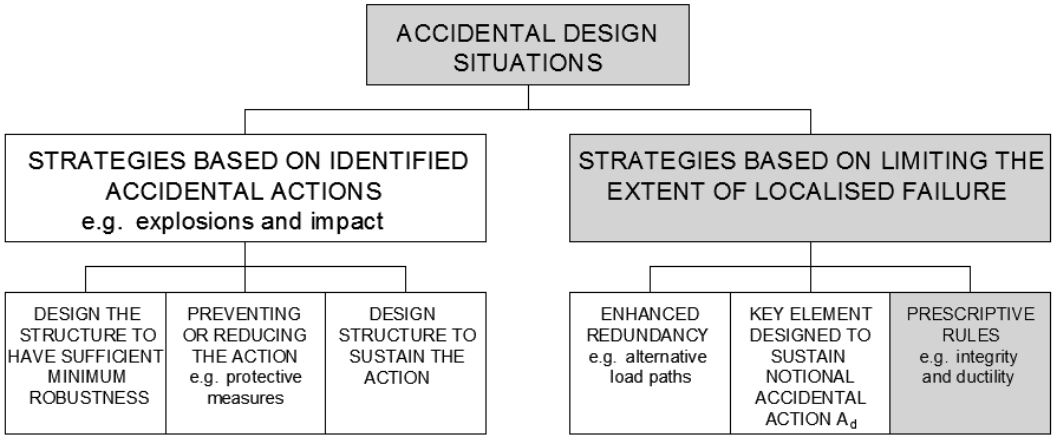

Figure 5.3 Accidental design situations (CEN, 2006).

In design, the most common method is to use prescriptive rules such as integrity and ductility. The purpose is to give sufficient robustness for actions both accidental and unspecified e.g. three-dimensional tying for extra integrity or a limited deformation for structural members subjected to impact. Prefabricated elements, which this study will focus on, are depending on the design of the connection and function in the serviceability limit state. To prevent a progressive collapse the connection needs to have a ductile behaviour and a proper tying system.

5.2 Tying system and consequence class

According to CEN (2004) the suitable tying system shall be able to provide alternative load paths to prevent progressive collapse, see Figure 5.4. The ties that should be used are:

a) Peripheral ties (red)
b) Internal ties (blue)
c) Horizontal column or wall ties (yellow)
d) Depending on the consequence class, vertical ties (green)

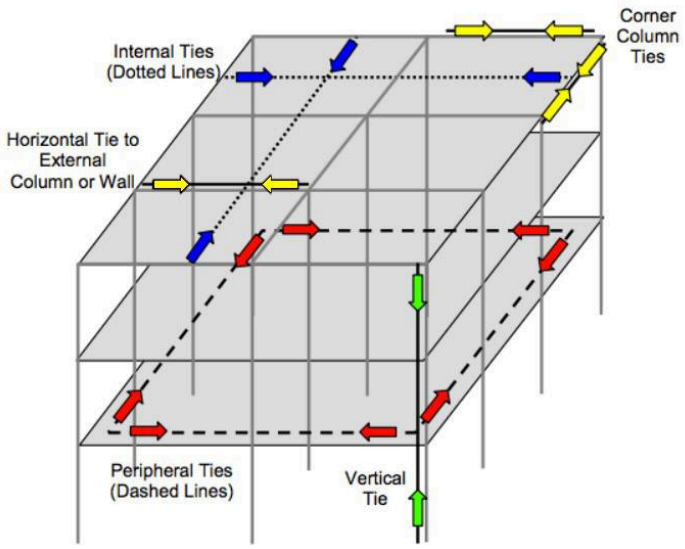

Figure 5.4 Different types of ties incorporated to provide structural integrity (Department of Defense (DOD), 2016).

The peripheral ties were not included in this study. Focus was on the internal, horizontal and vertical ties.

5.2.1 Horizontal ties for frame structures

Internal ties are horizontal ties which should be arranged in each floor and roof level of the building. The internal ties need to be organized in two directions perpendicular to each other in order to connect the walls and columns with the structural system. The horizontal ties should be arranged as close to the slabs edge as possible and over the grid lines without disruption, i.e. the horizontal ties are continuous. At least 30% of the ties needs to be placed on the grid lines.

The horizontal ties for this study consist of ordinary reinforcement and prestressed steel. In design, each tie should be able to resist a tensile load determined accordingly

For internal ties $T_i = \max(0{,}8(g_k + \psi q_k)s * L, 75kN)$ (5-1)

For perimeter ties $T_p = \max(0{,}4(g_k + \psi q_k)s * L, 75kN)$ (5-2)

where s = spacing of ties
L = span of the tie
ψ = relevant factor in the expression for combination of action effects for the accidental design situation (i.e. ψ_1 or ψ_2 in accordance with expression (6.11b) of EN 1990. Recommended values for ψ-factor is found in table A.1.1 in CEN (2002)

5.2.2 Vertical ties

Each structural wall needs to be anchored continuously from the foundation to the roof level according to CEN (2002). The structural walls should have the capacity to resist an accidental tensile force equal to the largest vertical permanent and variable load from any storey. An accidental load is not considered to act at the same time as the vertical load case including permanent and variable load. However, vertical ties will be included in this study.

5.2.3 Consequence class

It is the consequence class that determine the amount and type of tying system. Depending on the consequence of failure, building type and occupancy, a consequence class can be chosen, see Table 5.1.

Table 5.1 Consequence class (CEN, 2006).

CONSEQUENCE CLASS	EXAMPLE OF CATEGORISATION OF BUILDING TYPE AND OCCUPANCY
1	Single occupancy houses not exceeding 4 storeys. Agricultural buildings. Buildings into which people rarely go, provided no part of the building os closer to another building, or area where people do go, than a distance of 1.5 times the building height.
2a Lower Risk Group	5 storey single occupancy houses. Hotels not exceeding 4 storeys. Flats, apartments and other residential buildings not exceeding 4 storeys. Offices not exceeding 4 storeys. Industrial buildings not exceeding 3 storeys. Retailing premises not exceeding 3 storeys of less than 1000 m^2 floor area in each storey. Single storey educational buildings. All buildings not exceeding two storeys to which the public are admitted and which contain floor areas not exceeding 2000 m^2 at each storey.
2b Upper Risk Group	Hotels, flats, apartments and other residential buildings greater than 4 storeys but not exceeding 15 storeys. Educational buildings greater than single storey but not exceeding 15 storeys. Retailing premises greater than 3 storeys but not exceeding 15 storeys. Hospitals not exceeding 3 storeys. Offices greater than 4 storeys but not exceeding 15 storeys. All buildings to which the public are admitted and which contain floor areas exceeding 2000 m^2 but not exceeding 5000 m^2 at each storey. Car parking not exceeding 6 storeys.
3	All buildings defined above as Class 2 Lower and Upper Consequence Class that exceed the limits on area and number of storeys. All buildings to which members of the public are admitted in significant numbers. Stadia accommodating more than 5000 spectators. Buildings containing hazardous substances and / or processess

5.3 Components of the joints

To prevent damages and to improve the structural system the design of the connection between the slab and the wall is essential. The main objective of the connection is to conjoin each structural element and distribute the loads to the foundation. To achieve this, the connection needs to be designed to work as a structural integration for the various part of the structure.

A connection can be designed in different ways but a vital part of the connections is that it should obtain enough capacity to prevent progressive collapse. Appropriate ductility and deformation resistance during loading is required so that a suitable load distribution can be achieved.

A connection consists of different components such as joints and reinforcing steel, see Figure 5.5 - Figure 5.7. The void in between the structural elements is filled with concrete and reinforcing steel. The combination and configuration of the concrete and reinforcing steel merge the structural elements together which allow forces to be transferred. The reinforcing steel is anchored in the elements in each side through embedment in the joints, chases or recesses.

In the connection zone, it is vital to design the geometry and the tying system so that it can resist compression-, tensile-, shear- and bending stresses that act independently or at the same time.

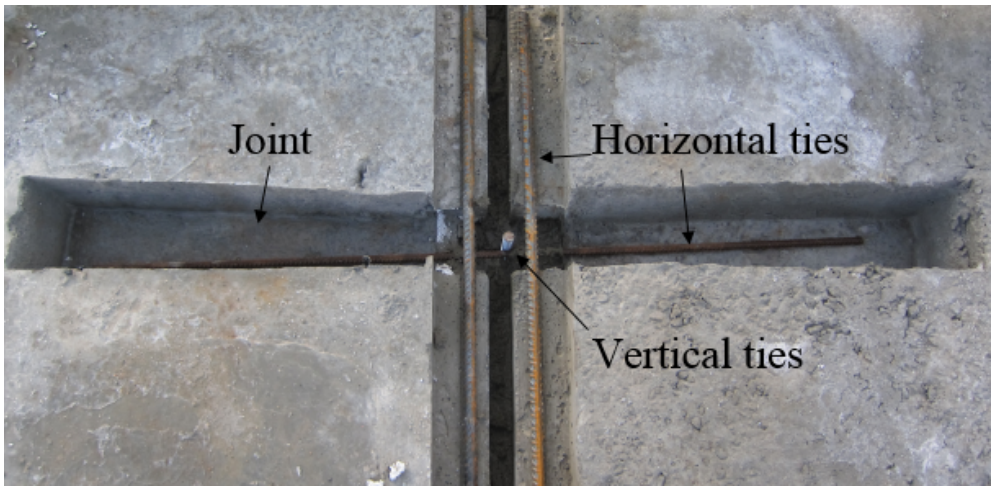

Figure 5.5 Components of an intermediate joint.

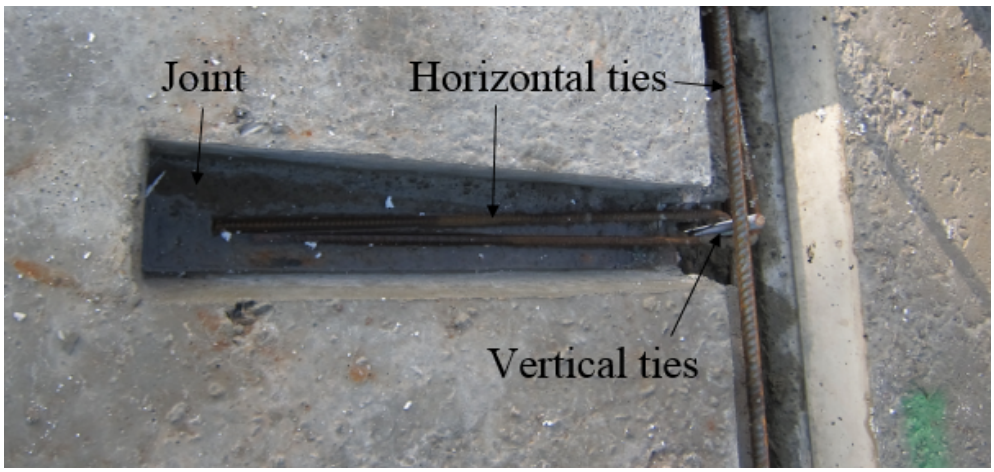

Figure 5.6 Components of an end joint.

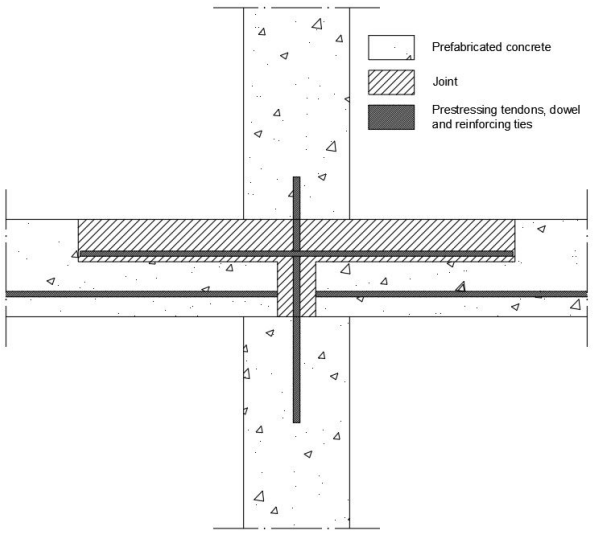

Figure 5.7 Section presenting the lay-out of prestressing tendon, tie reinforcement and the dowel.

A connection should be designed with regard to following requirements (Hermodsson, 1992);

- connect the slab with the supporting structure
- transmit tensile forces to the structural system
- achieve enough shear capacity at longitudinal and transverse joint movements
- reduce the risk of spalling
- take care of long-term effects such as shrinkage, creep and thermal effects
- prevent horizontal movements of the slab element in both longitudinal and transverse direction
- distributes vertical loads down to the foundation

5.4 Force transmitting mechanisms

5.4.1 Compressive transfer

Compressive force is transferred through adhesion in the joint. The magnitude of forces which can be transmitted depends on the concrete strength, steel reinforcement and material properties of the filling and padding. If the compressive forces exceed the capacity there is a risk of spalling and it therefore needs to be accounted for in the design (Hermodsson, 1992).

5.4.2 Tensile transfer

A requirement for the connection zone is that certain ties are needed to transmit tensile forces. The connectors are either anchored directly in the connection zone by casting, or indirect to the elements by concrete filling, joints or chases. The concrete needs to harden before an indirect anchorage is able to transmit forces. Stirrups, screws and reinforcing steel from the elements are example of direct connectors while reinforcement steel between the elements is a typical indirect connector, see Figure 5.5 and Figure 5.6.

Anchorage of the reinforcing steel and other connectors are normally achieved through bond and to obtain its full function certain requirements such as concrete filling length (transmission length), cross-section dimensions and detailing of anchorage regions needs to be taken into account. When a ductile behaviour in the ultimate limit state is requested, the demands with regard to anchorage could be stricter (Hermodsson, 1992).

5.4.3 Shear transfer

Shear is transferred either by friction or dowel action by reinforcing steel, screw or dowel. Betongelementföreningen (1998) states that when the horizontal forces are transferred through friction, the magnitude will be decided by acting normal forces and interface or the padding's friction coefficient. These forces cause horizontal displacements which will give rise to displacements perpendicular to the interface. Simultaneously, the connectors along the joint will cause a normal force acting against the interface and thereby increasing the shear capacity, see Figure 5.8. Because cast-in reinforcement bars reach its yielding point at rather small displacement the normal force N_c can be determined from

$$N_c = A_s * f_{st} \quad (5\text{-}3)$$

where f_{st} = design tensile capacity for reinforcement steel

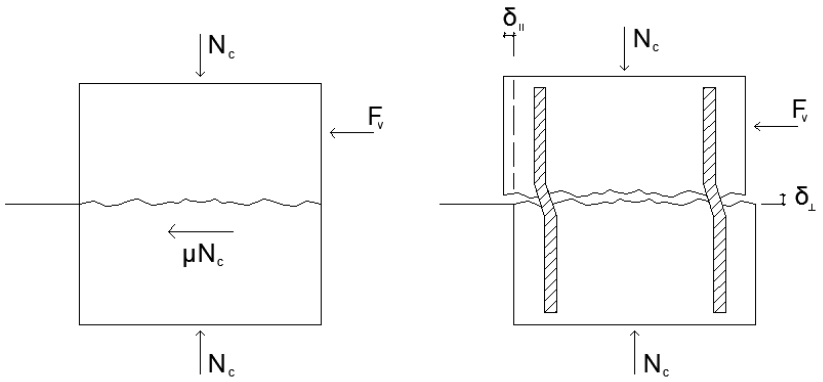

Figure 5.8 Force transfer through friction in the joints (Betongelementföreningen, 1998).

where N_c = the normal force acting perpendicular against the joints

and the shear capacity is

$$F_{vmax} = m' A_s' f_{st} + N_c \quad (5\text{-}4)$$

where m = a parameter depending on the concrete surface according to Boverket (2004), section 3.11.3

An illustration of when shear is transferred by dowel action is shown in Figure 5.9.

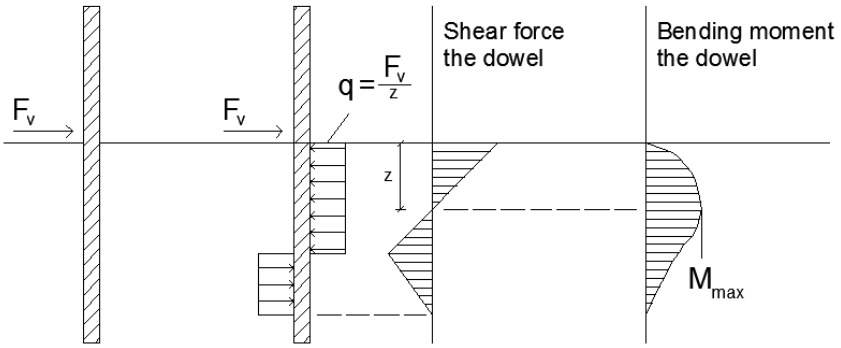

Figure 5.9 Force transfer by dowel action in a reinforcement bar, screw or a dowel (Betongelementföreningen, 1998).

This load case determines the shear capacity according to equation 6.8.3 in Boverket (2004), section 6.8.3 and is presented as

$$F_v = \emptyset^2 * \sqrt{f_{cc} * f_{st}} \quad (5\text{-}5)$$

where Ø = the diameter of the dowel

The shear capacity depends on how the dowel is fixed to the elements. In Figure 5.10 three different boundary conditions are compared and the shear capacity in the two left examples, a) and b), correlates to equation (5-5) while the example to the right, c), has 40% higher capacity. A higher capacity is obtained when one of the ends are fixed as illustrated in example c) where the dowel is fixed to a plate.

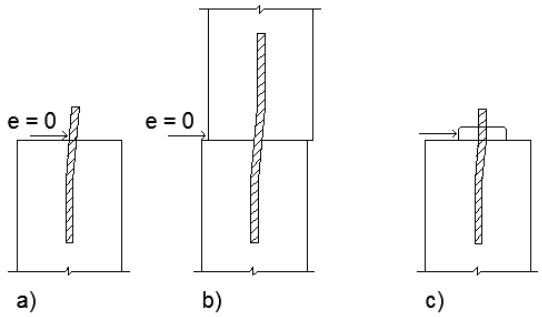

Figure 5.10 Shear transfer variation depending on the how the dowel is fixed. a) One part of the dowel end is casted in concrete. b) Both ends of the dowel is casted in concrete. c) One part of the dowel end is casted in concrete and the other is fixed (Betongelementföreningen, 1998).

If the force is applied with an eccentricity, the shear capacity will be reduced. Expression (5-5) will then be multiplied with the eccentricity factor expressed as

$$\left(\sqrt{1+\varepsilon^2} - \varepsilon\right) \quad (5\text{-}6)$$

where $\varepsilon = \frac{3 * e}{\emptyset} * \sqrt{\frac{f_{cc}}{f_{st}}}$

If both ends of the dowel is casted but a joint gap exists between the elements the shear capacity will be reduced. The shear force will be applied to the dowel with a higher eccentricity, see Figure 5.11. The eccentricity factor *e* will then be replaced with half of the joint gaps height (Betongelementföreningen, 1998).

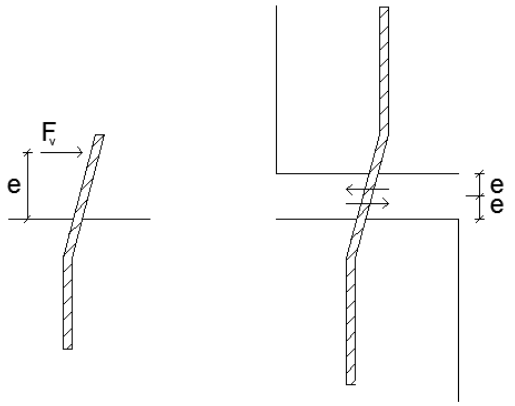

Figure 5.11 Shows how the force is applied with an eccentricity for a joint gap (Betongelementföreningen, 1998).

5.5 Reasons for restraints

Prefabricated elements minimize the construction time and the elements are typically assumed to be simply supported. This approach is generally also on the safe side when designing the elements and the structural system with respect to their load carrying capacity. However, the reality is more complicated than this simplified structural system. The design of the connection between the slab and the structural wall is of great importance and will determine the restraint degree and the magnitude will be defined with regard to the resilience of the connections, ductility and deformability. Restraint will appear both before and during free movements of the structure from long-term effects and could cause stress concentration and eventually cracks in the joint or in the slab.

Source of restraints in the connection between slabs and walls.

- Ties between the slabs and the supporting walls or a tying system between the slabs.
- Clamping of the slab. When the load from the upper wall is acting on the slab directly or indirectly it will be pinched between the supporting and the upper wall.
- Friction at the interface of the slab and the walls.
- Adhesive forces at the interface of the joint and the slabs.

5.5.1 Tying system

Variable load, shrinkage, creep, temperature- and humidity variation give rise to movements in the structural system. The need for movement is largest in the connection zone, and if the elements are strongly connected restraint forces will appear. Due to uncertainties regarding the estimation of movements and restraint degree, the need for movement is sometimes underestimated and the connection lacks capacity. A typical solution is to restraint the elements even more (Betongelementföreningen, 1998).

As the tying system allows the joints to transmit forces between the structural elements its properties will influence the stresses and force patterns. The ties could either be

anchored to the element by embedment of the joints, chases or other types of recesses. It is not unusual that the tying system consist of many different types of components which could affect the response (Betongelementföreningen, 1998).

5.5.2 Clamping

Structural elements which in the static design are regarded as simply supported, could be considered as partially or fully fixed depending on the configuration of the support. If the slab element is supported by a structural wall it will be clamped between the upper and lower wall and this will affect the boundary condition and also prevent the slab to move and rotate freely, causing a negative moment distribution over the support. According to Betongelementföreningen (1998) this depends partly on that the load from the upper wall will counteract the possibility for support rotation and prevents the slab to deform due to friction.

5.5.3 Friction

Clamping of the slab and the wall will result in friction forces which will limit horizontal movements. These forces depend on the magnitude of the load from the walls above and the surfaces and material of the elements. For more detailed description, see Section 6.2.4.

5.5.4 Adhesion

At the interface between the prefabricated element and the joint adhesive forces will arise. The adhesive forces could have a significant importance for the restraint and the capacity of the adhesive interface could correspond to the tensile capacity of the material used in the joint.

The effect from the adhesion and the tying system should not be considered at the same time. The ties do not become active until the restraint forces exceeds the adhesive capacity and cracks occur. The ties then become active and will restraint the structure.

6 Finite Element Analysis

This chapter describes how the non-linear finite element analysis has been performed using the FE-software DIANA (DIANA fea, 2017). Starting with a mechanical model, based on a physical model of reality, a finite element model was developed based on geometrical representation, material models, loads, boundaries and the finite element mesh. The modelling process is described, and modelling simplifications and assumptions are clarified in this chapter.

6.1 Introduction

DIANA is a finite element software for civil engineering, suitable for simulating the response of reinforced concrete subjected to different types of loading. The use of numerical simulations is necessary and plays an important part to predict reasonable and adequate response of a real behaviour. FE-software DIANA is according to DIANA (2017) appropriate for more advanced finite element techniques which contains analysis procedures, element libraries and a wide range of different material models.

There is normally a difference between what actually occurs in reality and what can be represented by the conceptual model of a structure. To simulate the behaviour as realistically as possible, the analysis procedure in DIANA was done in four phases.

1. The first phase represents when the concrete slab was tensioned in a precasting bed.
2. In the second phase the self-weight was applied to the slab element.
3. The third phase simulated the storage time at the factory.
4. The final phase was after the slab was mounted to the structure and represents its service life.

6.2 Modelling

6.2.1 Geometry

In this study, the structural system was simplified and two-dimensional models assuming plane stress was used. An example of such a model, consisting of prefabricated concrete slabs combined with the joints, reinforcement ties and structural walls is presented in Figure 6.1. In reality, out-of-plane stresses are expected since the distance between the prestressing tendons and ties can vary along the cross-section and due to long-term effects. The phenomena of out-of-plane stresses was disregarded due to simplicity and the model was made in 2D.

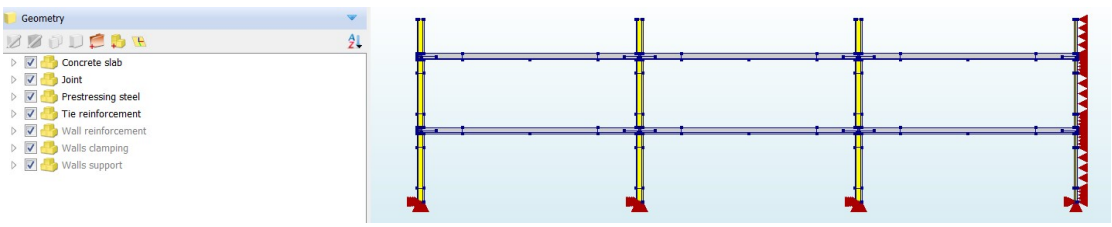

Figure 6.1 A 2D model of the structural system with three spans modelled in DIANA with symmetry lines.

The prestressed prefabricated concrete slab, the joint and the structural walls was modelled using plane stress elements with a prescribed out-of-plane thickness. The

prestressing tendons were modelled as embedded reinforcement bars in the concrete elements, with a prescribed tendon area and no slip between the reinforcement and the concrete. The reinforcement ties used to prevent progressive collapse were also modelled as embedded reinforcement bars in the concrete elements, with a prescribed cross-section area. The reinforcement ties were modelled to have a bond-slip interface to surrounding concrete. The ties were placed in the centre of the slab cross-section, extending from the joints into the slabs.

6.2.2 Supports and boundary conditions

The model was defined with different support conditions for each phase of the analysis. Supports were placed at certain points of the structure where displacements were assumed not to occur. The supporting walls was considered to be fully fixed to the foundation.

Since the structure is symmetric, the finite element model was reduced by implementing symmetry boundary conditions, see right part of Figure 6.1. The symmetry condition was used under the assumption that the other half of the structure would illustrate the same behaviour as the presented results from the modelled part of the structure.

The walls above the slab were included to half of their heights in the model to simulate the effect of clamping see Figure 6.1 and Figure 6.2. The floors of the building above this level were not included due to simplicity, but instead, their weight was added as line loads placed on the upper walls. Tyings were added to the upper edge of the upper walls, see Figure 6.2. The purpose of the tying's was to provide similar rigidity as the part of the building above this level would have given. The upper edges of the upper walls were restrained by preventing rotation i.e. the same vertical displacement was kept along the upper edges.

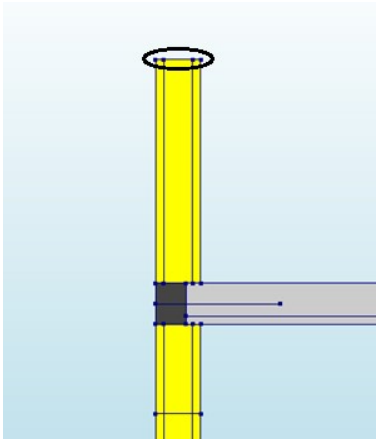

Figure 6.2 Attached tying.

6.2.3 Material models and reinforcement-concrete interaction

The material properties of the model should reflect the state of the physical structure. In the following sections the material models and how material parameters were specified for each material are described.

6.2.3.1 Concrete

A *Total Strain crack model* was used to model the non-linear response of concrete including cracking and crushing. In addition, models for *Shrinkage* and *Creep* was used to model the long-term response. Shrinkage and creep takes the surrounding environment, the age at the end of curing period and concrete age at loading into account. The Total Strain crack model is based on a smeared approach for the fracture energy and the properties of concrete is depending on its behaviour in compression and tension.

The material properties of the concrete were defined by specifying the material class according to to *Eurocode 2 EN 1992-1-1*, using the program option "*Concrete design codes*". The program then calculates all needed material properties based on Eurocode and default choices.

6.2.3.2 Prestressing tendon

The prestressing tendons were modelled as embedded reinforcement. The interface between the prestressing tendons and the concrete was therefore inseparable i.e. no bond slip could occur. The prestressing steel was modelled as linearly elastic – perfectly plastic, using von Mises plasticity with no hardening. Values for Young's modulus of elasticity, density and yield stress for the tendons were specified.

To be able to model prestressing correctly one aspect to include is bonding, see Figure 6.3. The prestressing tendons were not bonded to the mother element when the prestressing force was applied. This is similar to how it works in reality where the tendons are prestressed before contact is made to the concrete. As the concrete hardens, bonding is developed between the prestressed tendons and the concrete. This was modelled in DIANA by performing the analysis in different phases, where the tendon was unbonded in the first phase, when the prestressing load was applied, and bonded in the second phase, when the concrete was hardened and affected by the effect of prestressing.

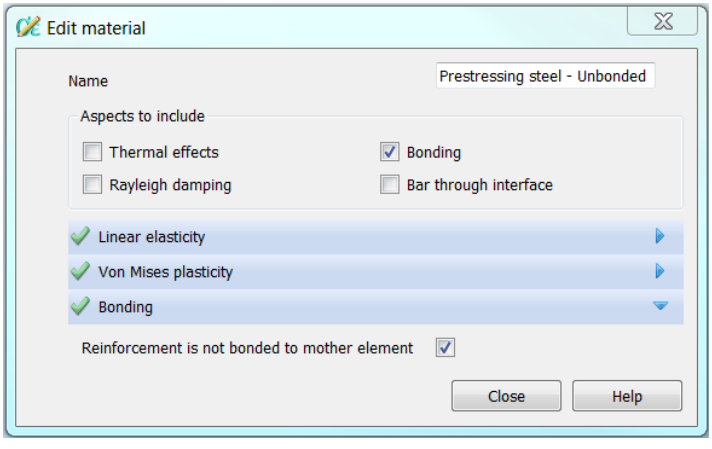

Figure 6.3 How to apply bonding between prestressing tendons and concrete in DIANA.

6.2.3.3 Reinforcement ties

Similar as for the prestressing tendons, the reinforcement ties were modelled as linearly elastic – perfectly plastic, using von Mises plasticity with no hardening. Values for Young's modulus of elasticity, density, and yield stress for the reinforcement ties were specified. The material properties of the ties were defined using the program option "*Reinforcement and pile foundation*", where also the bond-slip relation for the interaction with surrounding concrete was defined through the option *Bond-slip reinforcement*.

According to Tejchman and Bobinski (2014) there does not exist a fully correct way to model the phenomena of bond-slip since it depends on the boundary conditions of the whole system. Bond-slip can therefore be modelled in different ways depending on the complexity of the mechanical model. In this study, a bond-slip relation according to *local bond-slip relationship* from fib (2013) was used, assuming good bond conditions.

This user defined bond-slip model in DIANA is based on a friction stress-slip diagram according to fib (2013). This method takes into account that the tensile forces are transferred from the concrete to the reinforcing steel when cracking occur. When there is a difference in strains and displacement between the two materials, bond stresses arise. These stresses depends on the concretes' compressive strength, the surface and the localization of the reinforcement bars as well as the slip (Eriksen & Kolstad, 2016), see Section 3.4 and Figure 3.13. According to fib (2013) the bond-stress for each slip can be determined as

For $0 \leq s \leq s_1$:

$$\tau_0 = \tau_{max}\left(\frac{s}{s_1}\right)^{\alpha} \tag{6-1}$$

For $s_1 \leq s \leq s_2$:

$$\tau_0 = \tau_{max} \tag{6-2}$$

For $s_2 \leq s \leq s_3$:

$$\tau_0 = \tau_{max} - (\tau_{max} - \tau)\frac{s - s_2}{s_3 - s_2} \tag{6-3}$$

For $s_3 < s$:

$$\tau_0 = \tau_f \tag{6-4}$$

Table 6.1 Parameters for defining mean bond stress-slip curve (fib, 2013).

Pull-out failure		
	Good bonding conditions	**All other bonding conditions**
τ_{max}	$2.5\sqrt{f_{cm}}$	$1.25\sqrt{f_{cm}}$
s_1	$1.0\ mm$	$1.8\ mm$

s_2	$2.0\ mm$	$3.6\ mm$
s_3	c_{clear} [1)]	c_{clear} [1)]
α	0.4	0.4
τ_{bf}	$0.4\tau_{max}$	$0.4\tau_{max}$

[1)] c_{clear} is the clear distance between ribs

According to equation *(6-1)* - *(6-4)* and Table 6.1, the bond-slip curve indicated in Table 6.2 and illustrated in Figure 6.4 can be derived.

Table 6.2 Values for Bond-slip curve for C50/60.

Slip [mm]	Bond stress [MPa]
0	0
0,1	7,58
0,2	10,00
0,3	11,76
0,4	13,20
0,5	14,43
0,6	15,52
0,7	16,51
0,8	17,41
0,9	18,25
1,0	19,04
2,0	19,04
6,0	7,62
10,0	7,62

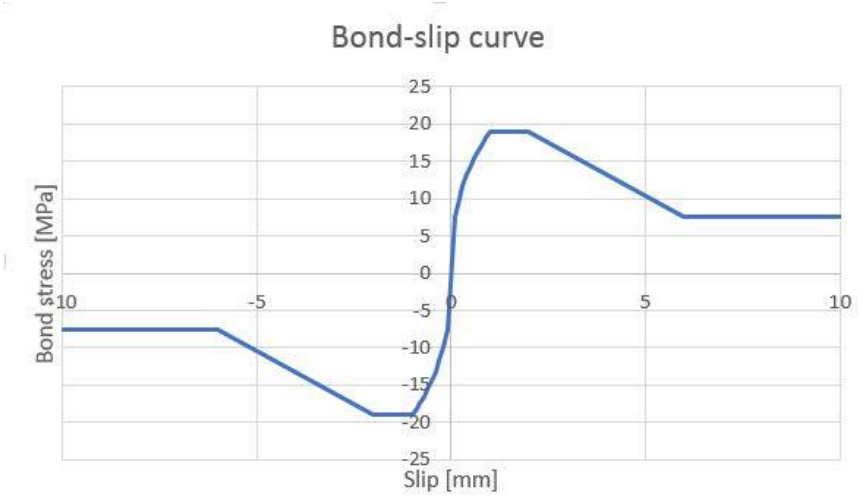

Figure 6.4 Bond-slip curve for C50/60.

When defining the material properties, also parameters of the bond-slip interface must be given, because when modelling bond-slip, certain relations regarding stiffnesses of bonds are needed. In DIANA, there are linear stiffnesses defined as shear stiffness and normal stiffness. These stiffnesses describes the behaviour between the shear- and

normal tractions and the shear- and normal displacements across the interface (DIANA fea, 2017). The shear stiffness (DSSX) can be explained as the tangent of the bond slip curve between the point where there is no slip and the first sampling point. The normal stiffness (DSNY) can be seen as the stiffness when the reinforcing steel is crushing the surrounding concrete (Eriksen & Kolstad, 2016).

In the model, the values for shear- and normal stiffness for bond-slip were calculated by the following expressions

$$DSSX = \frac{\tau_{b1}}{s_1} \tag{6-5}$$

$$DSNY = \frac{E_c}{\emptyset} \tag{6-6}$$

Specific element data for bond-slip reinforcement has to be specified. The description of the element data suitable for bond-slip reinforcement is *Bondslip Interface Reinforcement* which in DIANA is known as *INTERF*. With the use of INTERF, certain specifications follow regarding whether the reinforcement bar is a considered a truss or a beam. In this study, the truss condition was used since the reinforcement tie only should be exposed to uniaxial stresses where no shear or bending is assumed.

6.2.4 Interfaces between slab elements and in-situ concrete used in joints

The interfaces between the prefabricated concrete slabs and the in situ casted concrete joints were modelled with a constitutive model for sliding along rough macro-cracks, called *Crack dilatancy* in DIANA (2017). The same adhesive strength as the tensile strength of the concrete material was used in the joints. According to DIANA (2017) the model for Crack dilatancy is applicable to more advanced analysis of sliding along rough macro-cracks.

The friction model between the prefabricated concrete slabs and the joints and the structural walls are based on Coulomb friction. The behaviour of the Coulomb friction model is similar to the plasticity model of Mohr-Coulomb where the total relative displacement rate takes movement or displacement into account. The behaviour of Coulomb friction is further explained in Figure 6.5 which is modified from Lundgren (2007).

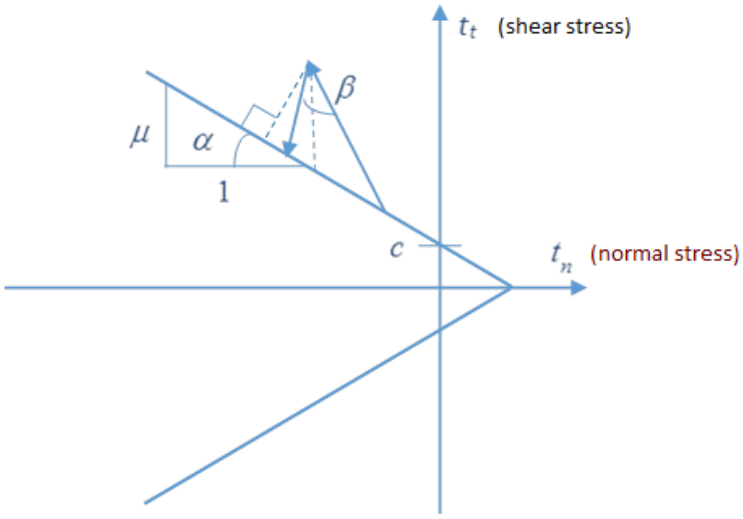

Figure 6.5 Friction model (Lundgren, 2007).

The friction angle α is defined by the friction coefficient μ and at which angle a material body slides without cohesion c. The shear stresses needed for the material body to slide needs to be larger than the cohesion capacity. The dilatancy angle β describes the relationship between shear stress and normal stress when the body slides. The magnitude of the dilatancy angle is between zero and the friction angle. The equation used for the cohesive capacity is equation (3-17)

For interfaces with zero thickness it is important to consider numerical instabilities and therefore not to use exceedingly high values for normal stiffness (K_{nn}) and shear stiffness (K_{tt}). According to Červenka (2016), these stiffnesses can be estimated as

$$K_{nn} = \frac{E_c}{t_I} \tag{6-7}$$

$$K_{tt} = \frac{G_c}{t_I} \tag{6-8}$$

where G_c = Shear modulus for concrete
t_I = Width of the interface zone, or element length

6.2.5 Loads

Three loads were applied in this analysis, a prestressing force to the tendons, self-weight of the structure and a vertical load from the stories above. The prestressing force is applied to the prestressed elements with a specific load type, *Reinforcement bar prestress,* and a corresponding stress. The self-weight is implemented by defining a global load. DIANA takes the material properties and the geometry into account and assigns a dead weight to the elements given a density in the model. Regarding the vertical load from the stories above, it is based on hand-calculation of self-weight and is applied as a line-load. No load combinations are used since this study only focus on characteristic values.

6.2.6 Mesh and element types

The element size and number of elements influence the computational time of the analysis. To get results regarding cracks, displacements and strains, recommendations for a maximum element size according to Rijkswaterstaat (2016) is expressed in Table 6.3

Table 6.3 Guidelines for size of element mesh (Rijkswaterstaat, 2016).

Slab Structure	Maximum element size
2D Modelling	$min\left(\frac{l}{50}, \frac{b}{50}\right)$
3D Modelling	$min\left(\frac{l}{50}, \frac{b}{50}, \frac{h}{6}\right)$

The prestressed prefabricated concrete slabs, joints and structural walls are modelled using plane stress element. The main element type used is denoted CQ16M, DIANA (2017). CQ16M is an eight-node quadrilateral isoparametric plane stress element. In areas with curvatures or corners also another mesh type was used, denoted CT12M. CT12M is a six-node triangular isoparametric plane stress element. The nodes of an isoparametric plane stress elements has two in-plane degrees of freedom per node.

In 2D modelling of interfaces, *structural line interface* elements of type CL12I were used, between two different lines placed on either side of the interface. These elements had 3 nodes along each interface line. The element type could therefore be shortened as CL12I – line 3+3. Each node has 2 degrees of freedom, an element therefore had a total amount of 12 degrees of freedom.

6.3 Analysis

6.3.1 Phases

The mechanical response of the slabs with regard to their connections to the joints was examined with a phase based analysis. A phased analysis is necessary when modelling a geometry which is changing during the analysis. The phases depend on the construction sequence and represent each part of the process from casting and tensioning to the end of service life. The response is linear until the concrete structure cracks. Cracking leads to redistribution of stiffness which results in a nonlinear behaviour and to simulate this a *structural nonlinear* analysis is needed in each phase. Various *Execution steps* are selected depending on what occurs in each phase.

- *Load steps* was used to simulate the application of a time independent load to the structure. The load was applied instantly but in specified increments to illustrate the response stepwise. Other elements were added to the structure after varying amount of time. Elements would not have been affected by the same magnitude of creep and shrinkage and load steps take this into account.
- *Time steps* are used to simulate time dependent response. Whether the structure is subjected to a new load or already has a load from a previous phase, this execution step can be used to simulate the change of behaviour over time. Total simulation time for this study was approximately 50 years, which is the normal

design service life for *Building structures and other common structures* according to CEN (2002), The time steps were shorter in the beginning of the service life and increased with time to replicate the long-term effects.

- *Start steps* are used in all phases except the first phase and takes the load from the previous phase into account.

The model was successively developed and became more complex during the analysis. The development of the model was defined based on changes of material properties, the application of loads and redefinition of boundary conditions. Each phase is explained further in Table 6.4 and the specification of each phase in DIANA can be seen in Figure 6.6.

Table 6.4 Phase development in the analysis.

Phase	
1	The first phase simulates the pretensioning of the tendons. Hence, only the prefabricated concrete slabs and the tendons are included. The slabs were modelled as simply supported. The prestressing tendons were modelled with no bond to get the effect of prestressing, and the prestressing load was applied in one increment in this load step. The prestressing load was the only applied load in this phase. Deformations occur as a result of prestressing.
2	In phase 2 the prestressing tendons were modelled as bonded and the self-weight was applied. This after an initial start step was used to ensure that the load from the first phase remained. The application of self-weight used 10 increments to illustrate how the slab behaves when the deformation due to prestressing was counteracted by the deformation from self-weight and equilibrium was obtained
3	Phase three resembles the storage time at the concrete factory. This is an important period since the long-term effects begin immediately after casting and the impact is largest in the beginning. In this time step increments with variable duration appropriate for the parametric study were used.
4	In the fourth and final phase, the slabs were connected to the structure and combined with the joints and the walls. The slabs were connected to the joints by a dilatancy crack interface. The slabs and the joints were connected to the lower walls using interface elements instead of being simply supported on point supports as in previous phases. The lower walls were modelled as fully fixed in the bottom. The slabs combined with the joints were clamped between the lower and the upper walls due to loading. The effect of clamping acted as a restraint and Coulomb friction interface elements were used between the combination of slabs/joints and the upper and lower walls. As prevention from progressive collapse, continuous reinforcement ties were added between the joints and the slabs. To resemble the service life of approximately 50 years, small increments were used in the beginning of this time step and were successively increased to reflect the long-term effects.

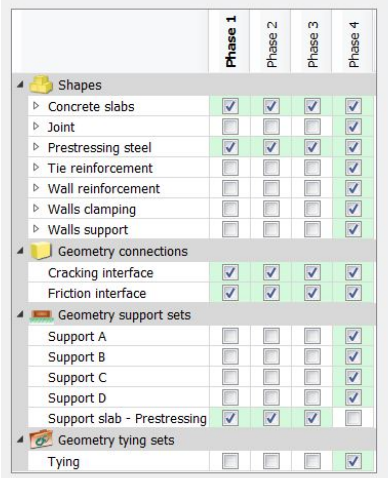

Figure 6.6 Phase structure in DIANA.

6.3.2 Iteration methods

Performing a nonlinear analysis requires a iteration method to find equilibrium within each iteration of the analysis, with respect to the unbalance between the internal and the external forces. A repeated iteration procedure is performed until this unbalanced force is removed and the internal and external force is in equilibrium (Rijkswaterstaat, 2016).

This study used the *Regular Newton-Raphson* iteration method which is based on quadratic convergence. This means that the final solution is obtained with rather few iterations, but the iterations themselves are relatively time consuming. The method is based on the stiffness relation which is calculated after each iteration (DIANA fea, 2017).

To achieve equilibrium in the iteration process, a relevant convergence criterion is needed. However, to achieve equilibrium it is not necessary for the unbalanced force to be absolutely zero and a tolerance is set to determine within what range equilibrium can be obtained, see Table 6.5. Convergence is obtained when at least one of three norms is fulfilled. For Regular Newton Raphson method, at least one convergence norm should be used, but for this case it is favourable to use an energy-norm simultaneously with a force- and displacement-norm to help avoid false convergence. Table 6.5 shows the tolerances used for the different norms in this study.

Table 6.5 Convergence tolerance (DIANA fea, 2017).

Convergence norm	Convergence tolerance
Energy	0,0001
Displacement	0,01
Force	0,01

6.4 Output

The investigation of this study's issue regarding restraint forces are based on following results:

- Total horizontal displacement
- Total strains
- Crack widths

To be able to analyse the results stated above, some specific outputs in DIANA were needed. These outputs are stated in Figure 6.7.

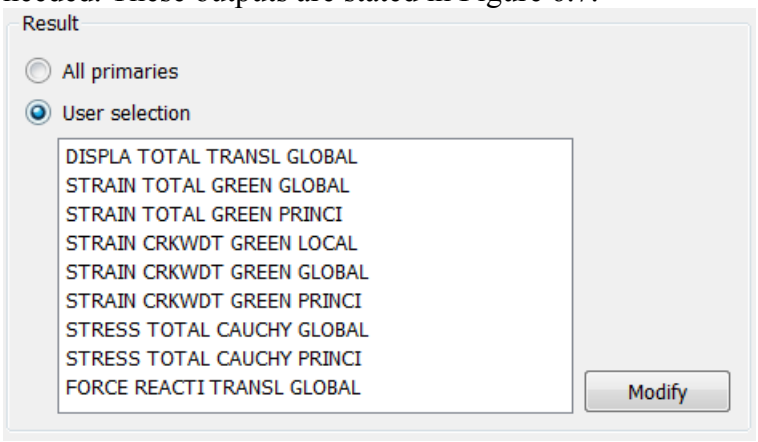

Figure 6.7 Output in DIANA.

6.5 Verification

To verify the model, different verification methods have been used simultaneously throughout the modelling process. Each step in the modelling process have been verified and evaluated thoroughly before the next step have started. To compare and ensure that the results are reasonable and consistent, another FEM software (PRE-Stress 6.5) and simplified hand calculations have been used. PRE-Stress 6.5 was chosen due to the fact that it handles prestressing and long-term effects in a similar way as DIANA. Hand calculations were used both to convert certain modelling techniques from one software to the other but also to compare the results from DIANA. This verification method was used to confirm that the modelling of the geometry, prestress and long-term effects was performed correctly. The comparison of the results from DIANA and PRE-Stress 6.5 are presented in Table 6.6 and illustrated in Figure 6.8 and Figure 6.9. Hand-calculations used in PRE-Stress 6.5 is found in the Appendix.

Table 6.6 Comparison between DIANA and PRE-Stress.

Case	Deformation in y-direction
DIANA	$5{,}59*10^{-3}$
PRE-Stress	$5{,}6*10^{-3}$

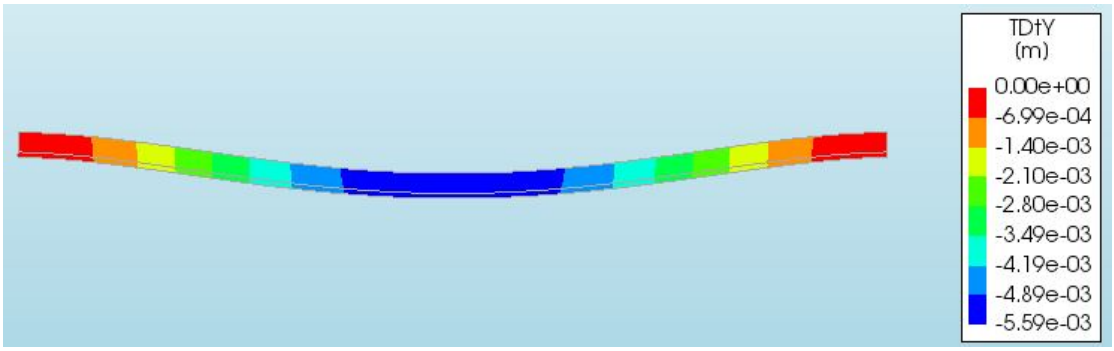

Figure 6.8 Vertical displacement of a prestressed slab in DIANA exposed to long-term effects.

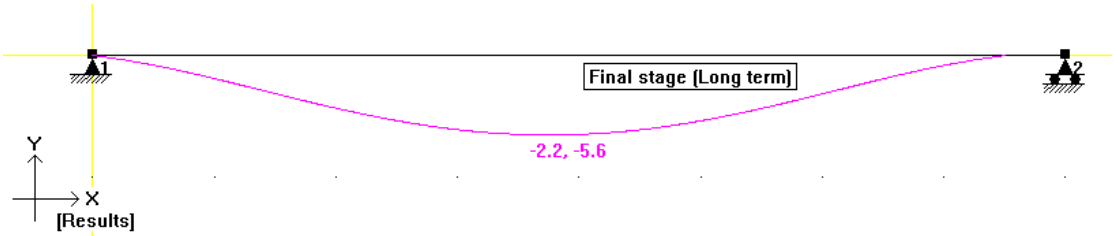

Figure 6.9 Vertical displacement of a prestressed slab in PRE-Stress 6.5 exposed to long-term effects.

A more complex and theoretical method was adopted concerning modelling of the connection between the slabs, joints and the walls. Since there does not exist a program which handle this type of connection with various restraints, it had to be modelled based on different assumptions and limitations. The verification tool for this part was very much based on theory of probability and simpler hand calculations where each restraint was analysed individually.

The effect of clamping due to friction is based on static friction. The friction coefficient combined with normal force (self-weight from stories above) result in a friction force and act as a restraint. The restraint will be active and the slab will not slide until the magnitude of the horizontal force overcome the frictional force. The slabs are prevented to deform freely due to restraints and due to increasing long-term effects a cumulative force appear within the slab. The cumulative force corresponds to the horizontal force and when it is larger than the frictional force the slab starts to slide. The cumulative forces decrease when the slab slides. Also, when the tensile stresses become larger than the tensile capacity, cracking will occur and stresses within the material, and consequently the cumulative force, will decrease.

As a simplification, the friction interface was therefore tested with an application of load instead of the effect from shrinkage and creep. The model is presented in Figure 6.10 where interfaces, normal force and horizontal force are presented.

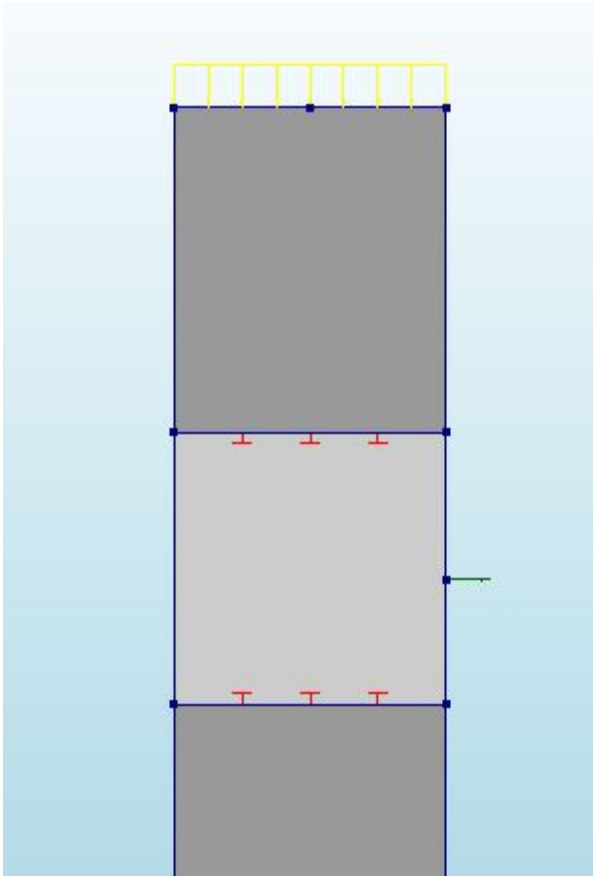

Figure 6.10 Friction model in DIANA. The yellow lines represent a distributed line load, the red marks the friction interface between the slab and the joint and the green line represent a prescribed deformation.

The horizontal force was applied as a prescribed deformation. Using prescribed deformations in DIANA requires a support located in the same node as the prescribed deformation. The support reaction correlates to the load that the prescribed deformation correspond to. When the support reaction from the prescribed deformations is of the same magnitude as the total frictional force it will not increase any further and the elements starts to slide. The size of the compressive force was $1*10^6$ N/m and the wall thickness was 0.25 m with two frictional surfaces. This resulted in a total frictional force of 500 kN. The development of the support reaction is presented in Figure 6.11.

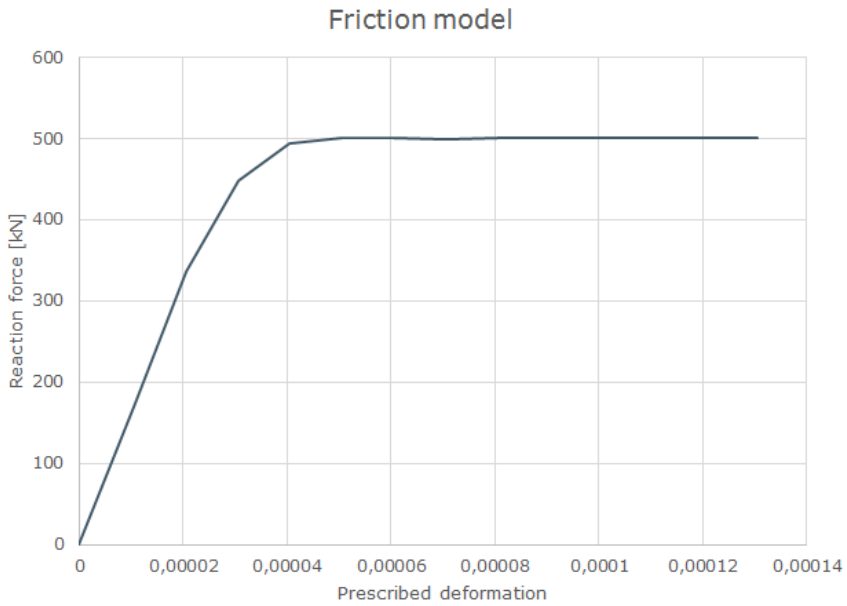

Figure 6.11 Friction model with prescribed deformation-reaction force relationship.

The tie reinforcement preventing progressive collapse was modelled with bond-slip material properties. The stiffness of the tie reinforcement will increase the stiffness of the structural system and combined with concrete it will act as one unit. This was verified by modelling a concrete rod with reinforcement bar in the centre of the cross-section exposed to a tensile force, see Figure 6.12.

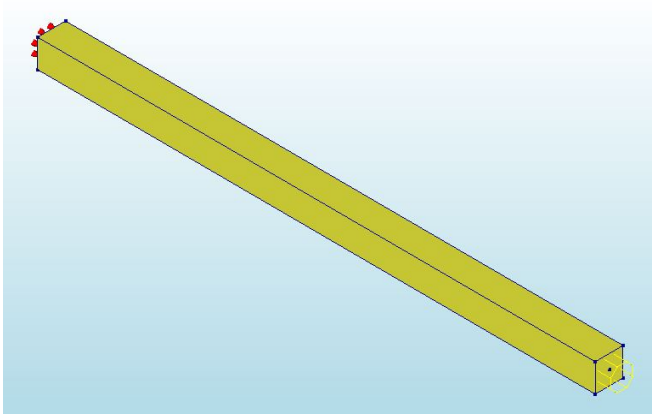

Figure 6.12 Concrete rod with bond slip reinforcement in DIANA.

Figure 6.12 illustrates how the geometry, loads and boundary conditions are applied and the Figure 6.13 presents the deformations.

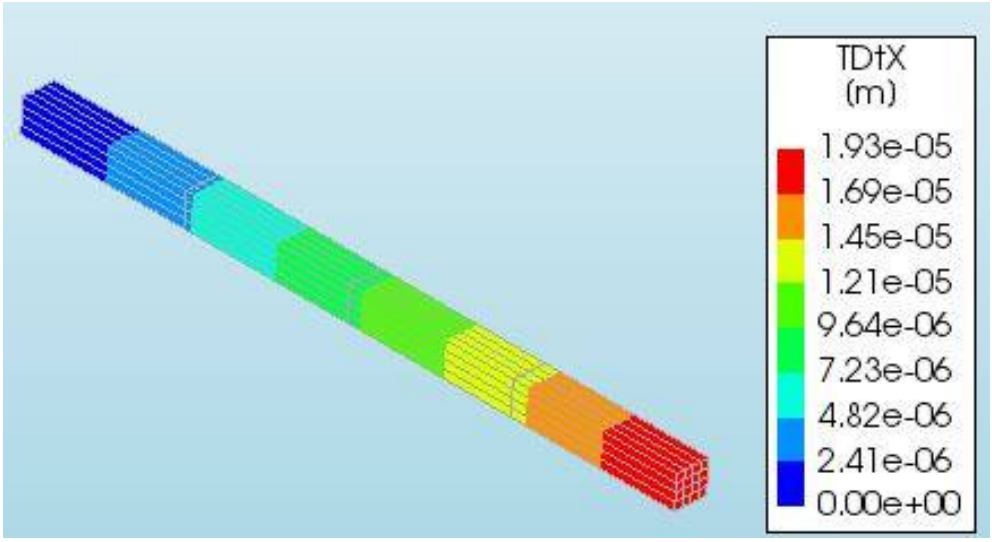

Figure 6.13 Deformation of the concrete rod in DIANA.

The results from DIANA was compared to hand calculations, see the Appendix. The area of the reinforcement bar was recalculated to an effective concrete area and the hand calcul1ations were based on calculating the deformations of a concrete rod. Table 6.7 presents the deformation from both methods.

Table 6.7 Comparison of results from DIANA and hand calculations.

Case	Deformation
DIANA	$1.93*10^{-5}$ m
Hand calculations	$1.88*10^{-5}$ m

By calculating an effective concrete area, it is assumed that the whole rod has the same stiffness. This was not the case when performing the analysis in DIANA due to bond-slip between the rod and the concrete. The rod in the hand calculations was therefore stiffer than the rod in DIANA which is the reason why the result between the two methods differ. The deformation in DIANA was therefore larger which also was expected.

7 Parametric study

To analyse the problem and to understand its origin, it is important to study the impact of certain parameters separately. Therefore, a parametric study was performed. This makes it possible to evaluate appropriate parameters, decide their range with respective design constraints and study the influence of each parameters. This approach allows for optimization by further refining the design until satisfaction.

In order to perform a parametric study, a reference object was selected, see Section 7.1. From these basic conditions, the following parameters were evaluated with regard to cracks: storage time, number of stories, numbers of spans and span lengths. Throughout the FE analysis each parameter was simulated numerous times with varying properties and its effect was evaluated. Firstly, storage time, number of stories and number of spans was examined and compared to the reference object. Secondly, the same reference values were used but different span lengths were applied in order to evaluate its effect on the final result.

After the analysis, the necessary results were post processed. The impact of each parameter was investigated and comparisons between the parameters were made. Regarding the results, outputs such as displacements, crack widths and strains were considered to be most interesting for this study. In the following sections the reference object is presented as well as the influence of each parameter mentioned above.

7.1 Reference object of the parametric study

The model which was used in the study, was a structure with load bearing slabs, walls and its connection and was designed based upon a reference object provided by COWI. This design served as a basis in the parametric study. The parameter values for the reference object is presented in Table 7.1. The properties for the reference object corresponds to the material and environmental conditions provided by COWI.

Table 7.1 Parameters for the reference object.

Parameter	**Value**
General	
Temperature [°C]	20
RH of surroundings [%]	50
Service life [years]	50
Concrete age at loading [days]	28
Concrete age at end of curing period [days]	0
Compressive force from stories above [kN/m]	739,5
Storage time	30 days
Number of storeys	5
Concrete	
Concrete class [-]	C50/60
Cement type [-]	Normal hardening
Young's modulus according to DIANA [MPa]	38629
Poisson’s ratio [-]	0,2

Density [kg/m³]	2450
Tensile strength [MPa]	2,9
Compressive strength [MPa]	50
Fracture energy [N/m]	152
Prestressing steel	
Total prestressing tendon area [mm²]	350
Prestressing force [MPa]	1300
Young's modulus [GPa]	200
Yield stress [MPa]	1860
Tie reinforcement steel	
Tie reinforcement diameter [mm]	2ø12
Total tie reinforcement area [mm²]	226
Tie reinforcement density [kg/m³]	7500
Young's modulus [GPa]	200
Normal stiffness [N/m³]	$3,22*10^{12}$
Shear stiffness [N/m³]	$7,58*10^{10}$
Slab	
Thickness [m]	0,23
Width [m]	1
Span length [m]	8
Number of spans	6
Joint	
Thickness [m]	0,09
Height [m]	0,23
Wall	
Thickness [m]	0,25
Height [m]	2,5
Reinforcement [mm²/m]	197,92
Friction interface	
Normal stiffness [N/m³]	$1,93*10^{12}$
Shear stiffness [N/m³]	$8,04*10^{11}$
Cohesion [MPa]	8,02
Friction coefficient [-]	1
Friction angle [°]	45
Dilatancy angle [°]	0
Interface	
Normal stiffness [N/m³]	$1,93*10^{12}$
Shear stiffness [N/m³]	$8,04*10^{11}$
Cube compressive strength [MPa]	50
Tensile strength [MPa]	2,9
Maximum aggregate size [m]	0,016

The conditions for long-term effects are based on indoor environment, concrete class, concrete age at loading and end of curing period. Selected values for concrete age at loading and end of curing period were recommended by DIANA (DIANA fea, 2017).

Values for normal- and shear stiffness for reinforcement and interfaces were calculated separately according to equation (6-5) to (6-8). Regarding Coulomb friction, values for cohesion, friction- and dilatancy angle are based on a friction model and plasticity

theory. Cohesion is found by equation (3-17), friction angle is calculated based on the friction coefficient and the dilatancy angle is recommended to be as low as possible with regard to the stability of the calculations.

The main purpose of this study is to understand where cracks occur due to long-term effects and how different parameters affect the response. Therefore, focus was on adjusting parameters regarding storage time, number of stories, span length and numbers of span. However, other parameters may also have a large impact but was not included in this study.

In Figure 7.1, areas of interest with respect to cracking are marked 1 to 5 and was evaluated and assessed in the parametric study.

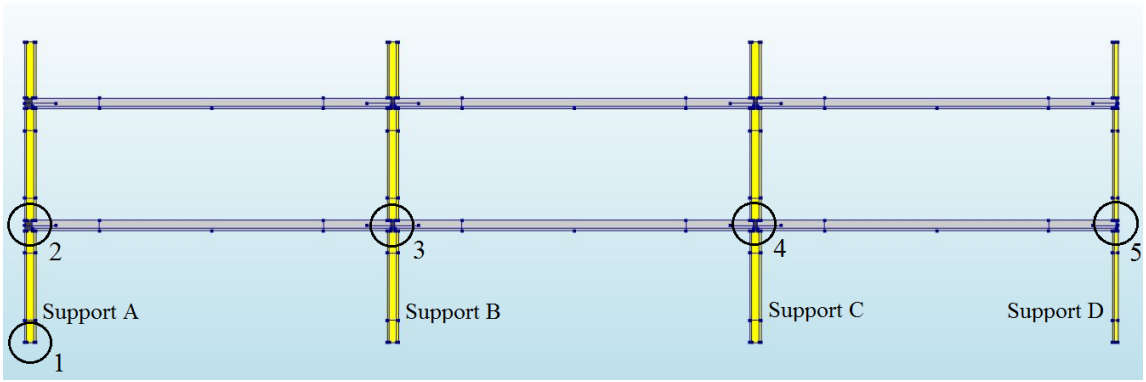

Figure 7.1 Reference object in DIANA where specific areas that will be studied in the parametric study are circled.

- The supporting walls, which are assumed to be fully fixed in the bottom, will be exposed to a negative bending moment. Therefore, it is interesting to investigate the distribution of cracks at point 1 with regard to tensile stresses.
- At point 2, the total deformation in the horizontal direction was measured in the outermost joint. The response of the connection zone was also studied at this point. Focus was on the development of strains, where zones with high strain concentration indicate where cracks might occur.
- The response with regard to strain development was also studied at point 3, 4 and 5. Even though most restraint is assumed to act at point 5, the structural behaviour is influenced also by other connection zones and it is therefore essential to observe their behaviour as well.

An overall observation with respect to when and where cracks become too large was performed and regarding the slabs, focus was on the response close to the joints. Since the elements are exposed to indoor conditions there are no requirements for crack limitations. However, limitations for crack width was assumed to be 0,4 mm and 1 mm. A crack width of 0,4 mm can be considered noticeable while cracks of 1 mm can be considered as large cracks.

7.2 Influence of storage time

The results in this study depends largely on the response of long-term effects; the time between casting and mounting is therefore of great importance. As mentioned in Section 4.5 and 4.6, shrinkage and creep develops over time, with their largest impact

in the early days of the structure and they reach their final value after long time. By simulating different storage times, restraint forces associated with long-term effects will be affected.

The influence of storage time was studied by varying the time before mounting of the prefabricated elements between 1 week and 6 months. 1 week is not optimal, but certain circumstances at the construction site could require fast delivery. Another case could be that the factory stores element which has a later delivery date, and this corresponds to the assumed storage time of 6 months. It is hard to predict the storage time since it varies largely in real-life construction. However, a storage time of 1 week to 6 months was considered to cover the most common interval.

7.2.1 Horizontal deformation

The structure deforms in the horizontal direction as a consequence of long-term effects. Figure 7.2 illustrates how the total horizontal deformation, at point 2, see Figure 7.1, is affected by various values of storage time during service life.

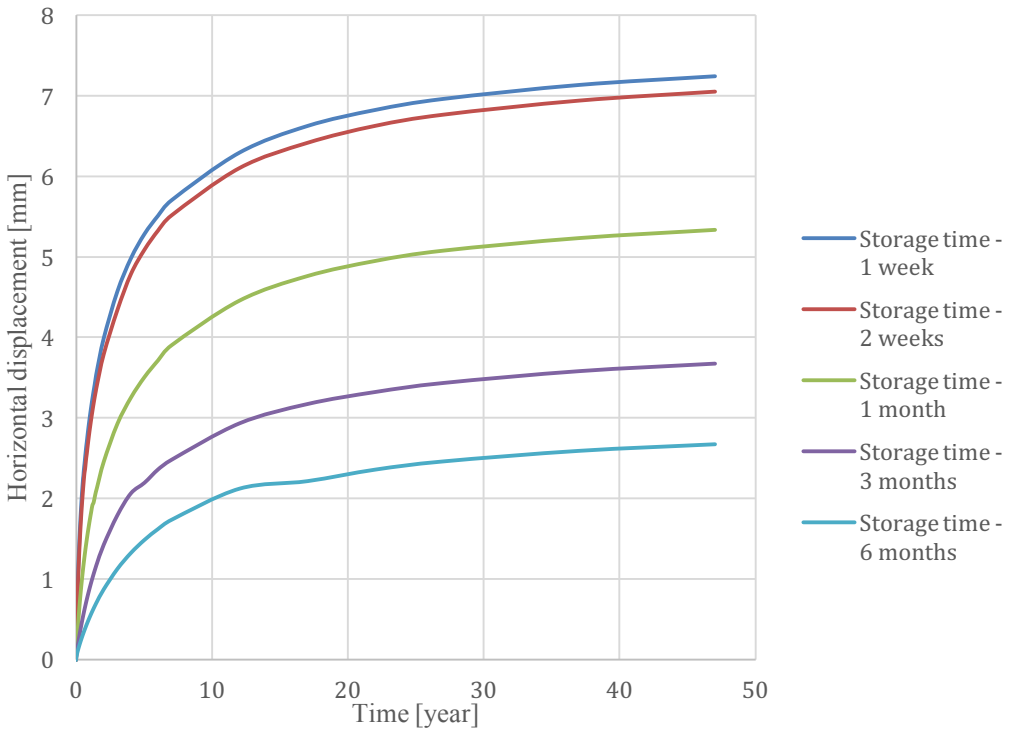

Figure 7.2 Deformation in the horizontal direction based on varying storage time.

As Figure 7.2 illustrates, the deformation in the horizontal direction decreases when the storage time increases. The change can be considered to be dependent of time and has greatest impact in the first 3 months. It can be noted that the deformation can be halved if the slab elements are stored in 3 months instead of 1 or 2 weeks. However, storing it for a further 3 months will not have the same effect. The deformation which occur from approximately 16 years to the end of service life is similar for all curves which also indicates that longer storage time in the beginning affect the total deformation.

Figure 7.3 illustrate how the reference object eas deformed at the end of service life.

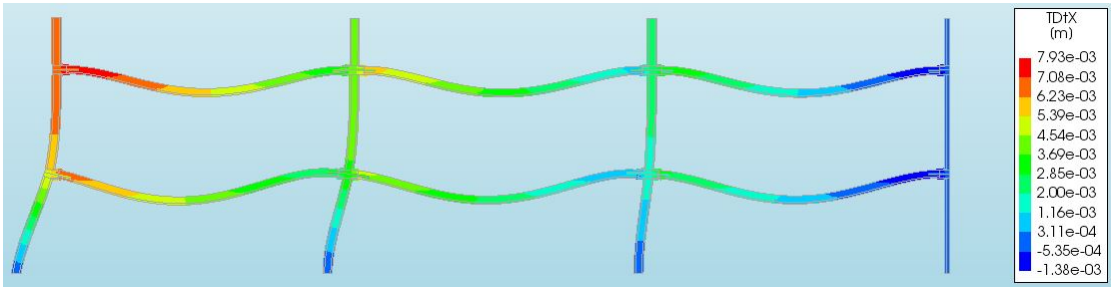

Figure 7.3 Horizontal deformation in DIANA corresponding to 1 month of storage time.

7.2.2 Cracking in the bottom corner of the exterior wall

For point 1 in Figure 7.1, large tensile stresses will appear near the support. How these stresses affect the cracking behaviour over time with respect to storage time are presented in Figure 7.4.

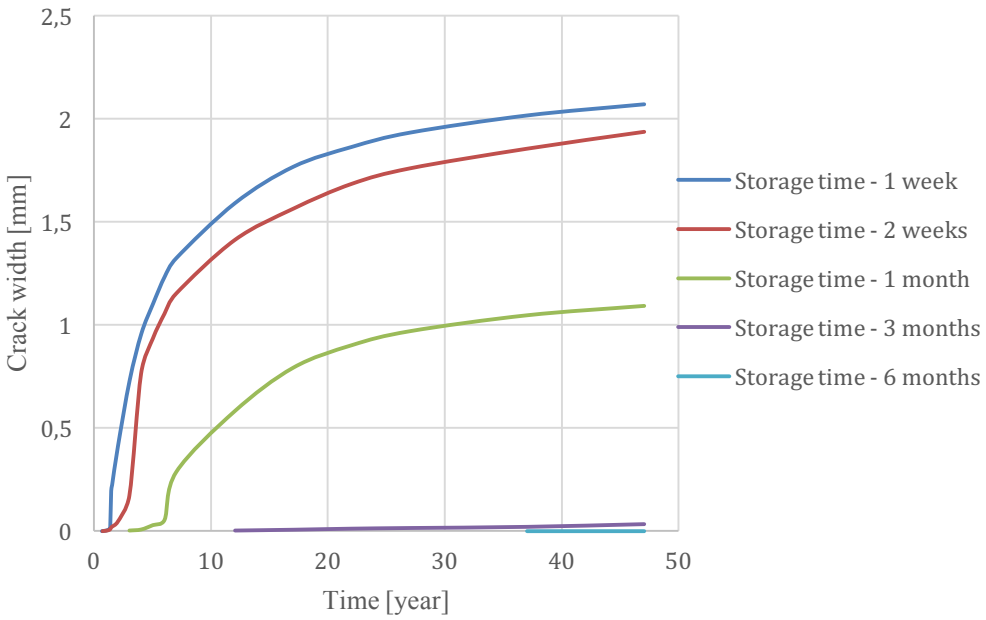

Figure 7.4 Crack development in the exterior wall near the support based on varying storage time.

The crack development is connected to the deformation in the horizontal direction. As Figure 7.4 illustrates, a larger crack is developed with shorter storage time and larger horizontal deformation, see Figure 7.2. The magnitude of the cracks that appear with elements stored less than one month are not acceptable with regard to the design codes. Particularly not since point 1 in Figure 7.1 corresponds to an exterior wall which has certain requirements regarding water tightness. However, if the storage time is 3 months or longer, cracks in the exterior wall can be avoided for the reference object.

7.2.3 Strain development in connection zones

Cracks occured where the maximum principal strains exceed the limit of $7.5*10^{-5}$ for a C50/60 concrete. Figure 7.5 presents the range of the maximum principal strains presented for each connection zone in figures 7.6 to 7.10.

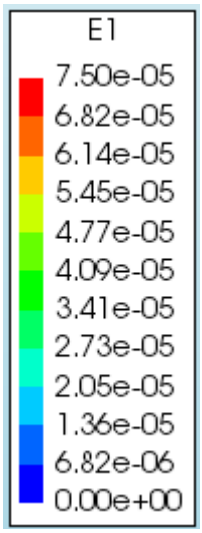

Figure 7.5 Strain legend for figures 7.6 to 7.10.

Figure 7.6 – Figure 7.10 illustrates how the principal strains developed in the connection zones when the storage time was varied from 1 week up to 6 months.

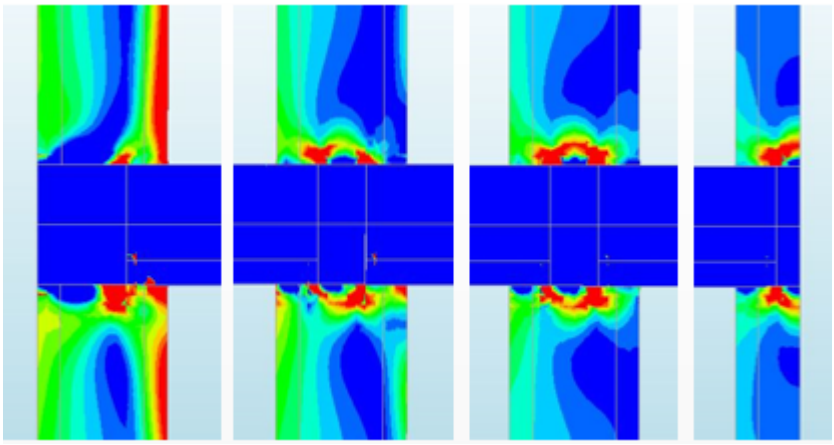

Figure 7.6 Strain development in connection zones 2-5 - Storage time 1 week.

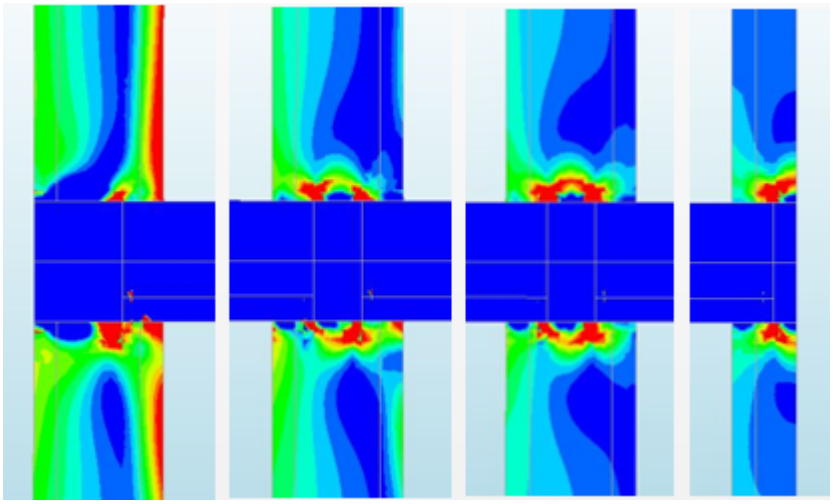

Figure 7.7 Strain development in connection zones 2-5 - Storage time 2 weeks.

Figure 7.6 and Figure 7.7 shows that large principal strains and cracks will develop at the inside of the exterior wall for storage times of 1-2 weeks. Still, a noticeable difference in strain pattern of the exterior wall can be seen as the strains decrease when the storage time increase from 1 to 2 weeks.

Short storage time results in larger long-term deformations after the slabs have been mounted. Larger deformations combined with effect of clamping from the structural walls causes larger strains in the walls. The values of the principal strains in the walls indicate that cracks have occurred and the results from 1 and 2 weeks of storage time are similar.

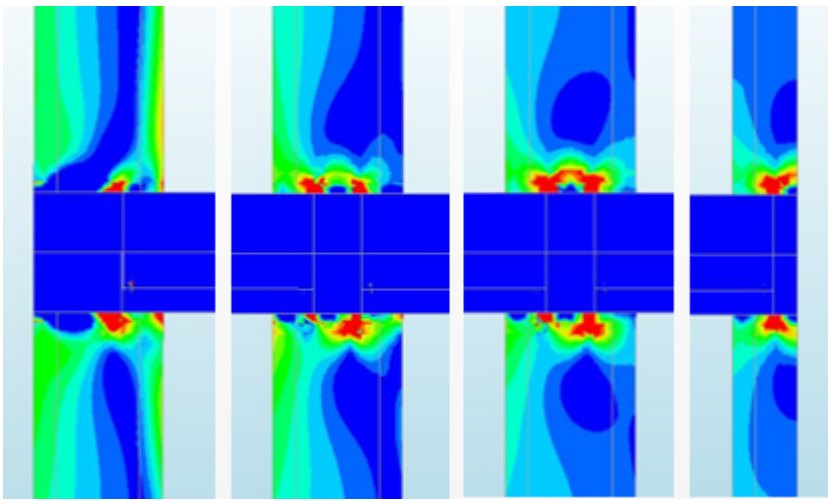

Figure 7.8 Strain development in connection zones 2-5 - Storage time 1 month.

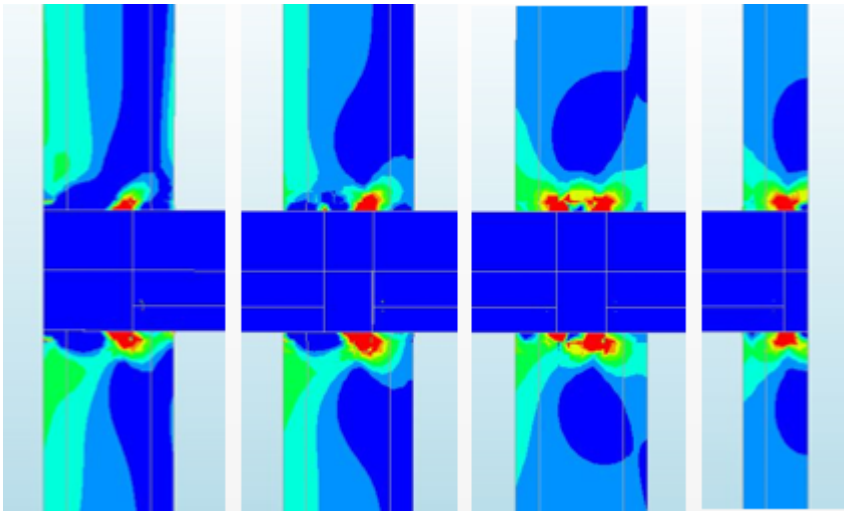

Figure 7.9 Strain development in connection zones 2-5 - Storage time 3 months.

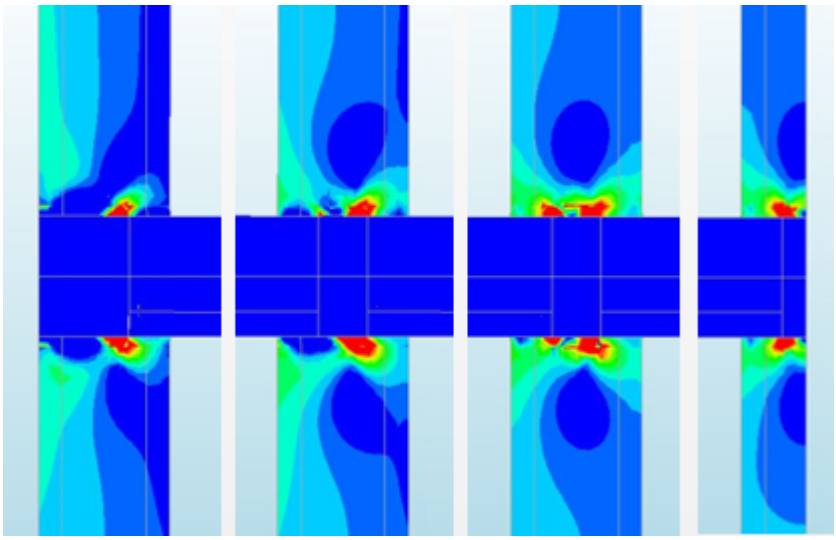

Figure 7.10 Strain development in connection zones 2-5 - Storage time 6 months.

Figure 7.8 - Figure 7.10 demonstrates that a storage time of 1 to 6 months also gives a similar behaviour. With 1 month of storage time, the principal strain is still large enough to cause cracking in the exterior walls at the connection to the slab. However, the cracked area does not have the same extent as with a storage time of 1 or 2 weeks. With longer storage time cracks do not develop at the surface of the walls.

For a storage time of 1 to 6 months, small zones in all of the structural walls are exposed to too large strains. However, it is possible to see that the strains in the structural walls decrease as the storage time increase. In Figure 7.11, the crack width in point 5 (see Figure 7.1) is presented for the different storage times.

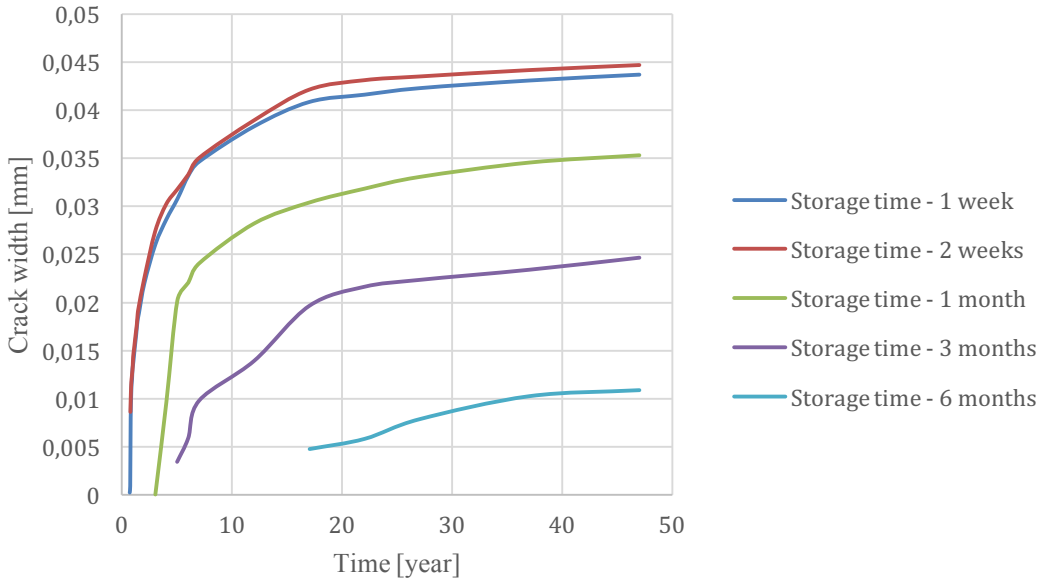

Figure 7.11 Development of cracks in structural walls at point 5.

Figure 7.11 confirms the importance of longer storage time with regard to long-term effects.

7.3 Influence of number of stories

Since the effect of clamping increases with number of stories above the studied slab, it will have an impact on the restraint degree at the connection between the slab and the walls. As specified in Section 4.1, the restraint degree increases with the vertical load. Therefore, it is interesting to investigate what effect the number of stories above the slab has on the structural behaviour, especially in the connection zone.

As specified in Table 7.1 the total number of stories of the building for the reference object was 5. However, to simulate different composition of buildings, a variation of 3 to 15 stories were analysed. The load from each story represent the self-weight of the structural elements and no variable load is included.

7.3.1 Horizontal deformation

To simulate the clamping effect, analyses were made with varying loads to resemble different number of stories. The horizontal deformation at point 2 (see Figure 7.1) is presented in Figure 7.12.

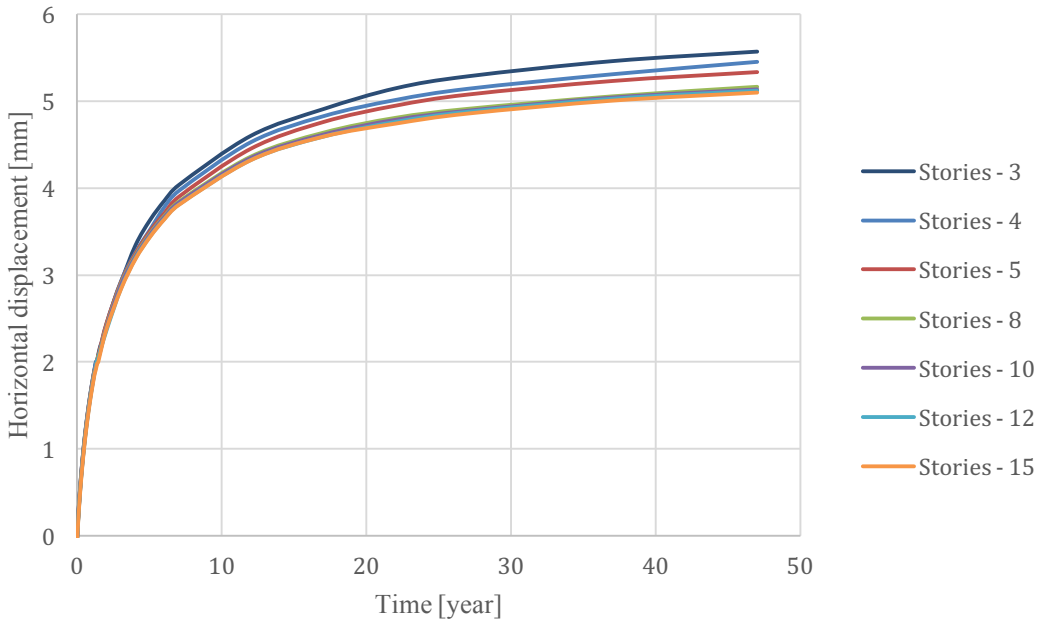

Figure 7.12 Deformation of point 2 (see Figure 7.1) in the horizontal direction for varying number of stories.

Figure 7.12 shows that the horizontal deformation decreases with increasing number of stories. For the first 3 years, the deformation is (more or less) the same independent of the number of stories, but the analysis demonstrates differences in the final deformation. Up to eight stories the graph shows reduced deformations with increasing number of stories, but for more stories the difference in deformation is negligible independent of number of stories. The final deformation value only differs approximately 0,5 mm between 3 and 15 stories.

7.3.2 Cracking in the bottom corner of the exterior wall

The crack width at point 1 (see Figure 7.1) is illustrated as a function of time for different number of stories in Figure 7.13.

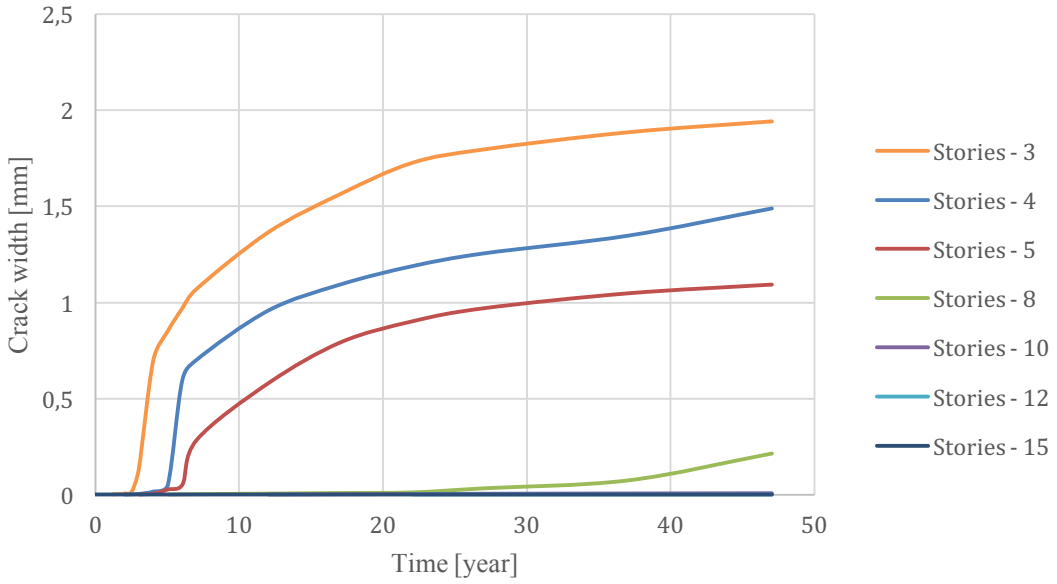

Figure 7.13 Crack width development in the exterior wall near the support based for varying number of stories.

That the restraint caused by the clamping effect from 3 to 5 stories, is not sufficient to prevent cracking in the bottom corner of the wall. When the slab deforms it will to some extent deform the supporting wall as well and therefore cracks will appear in the bottom corner of the wall in buildings with stories. If the clamping effect is large enough, as the for buildings with 10 or more stories, no cracks will occur. The figure also indicates that the cracks will occur at a later stage and that the crack width decrease as more stories are applied.

7.3.3 Strain development in connection zones

Figure 7.14 – Figure 7.20 illustrates how the maximum principal strains developed with respect to the clamping effect from increasing number of stories in the building studied.

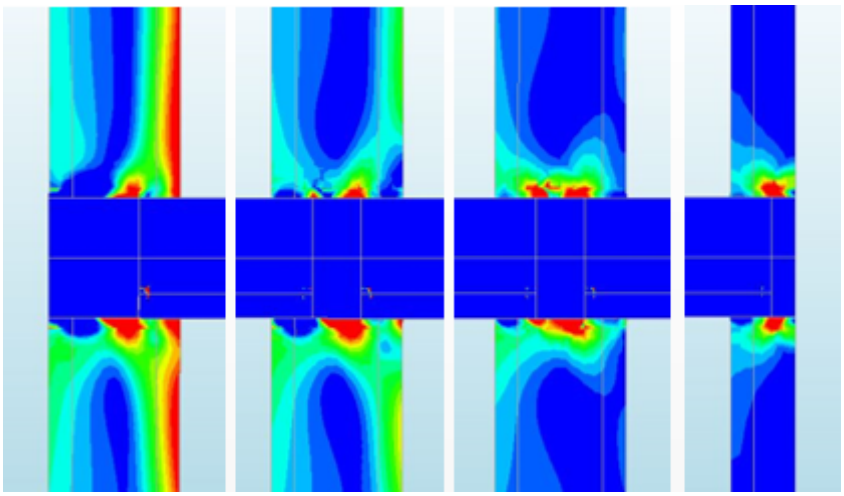

Figure 7.14 Strain development in connection zones 2-5 - 3 stories.

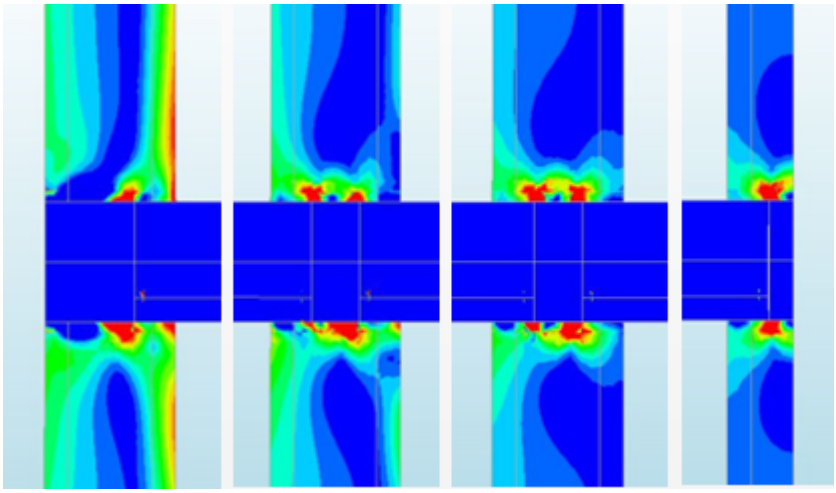

Figure 7.15 Strain development in connection zones 2-5 - 4 stories.

Figure 7.14 and Figure 7.15illustrates that cracks occured at the inside of the exterior walls This means that the clamping force from 3 and 4 stories, respectively, are not large enough to prevent cracking at the inside of the exterior walls. The force from long-term effects caused the slab to slide and, as a result, small areas with principal strains exceeding the cracking strain were developed in the walls close to the connection zone.

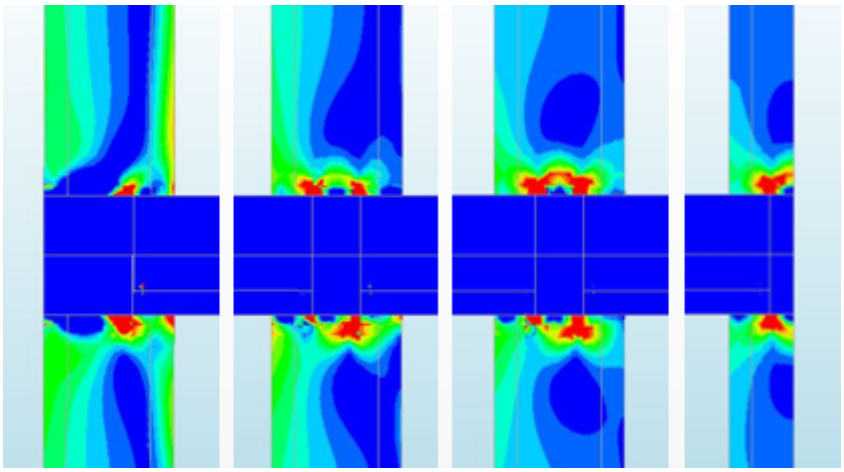

Figure 7.16 Strain development in connection zones 2-5 - 5 stories.

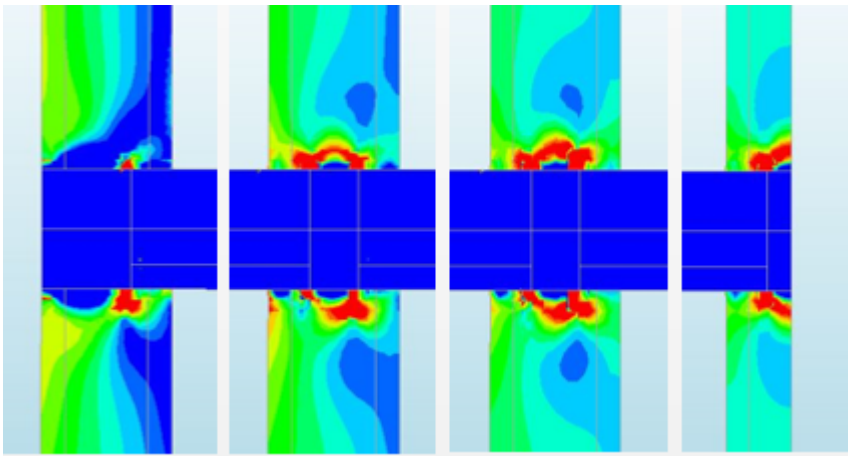

Figure 7.17 Strain development in connection zones 2-5 - 8 stories.

Compared to the cases with 3-4 stories, the buildings with 5 and 8 stories have a more limited possibility to deform as the possibility to deform decreases due to the effect of clamping, larger principal strains were developed inside the structural walls causing larger and/or more internal cracks.

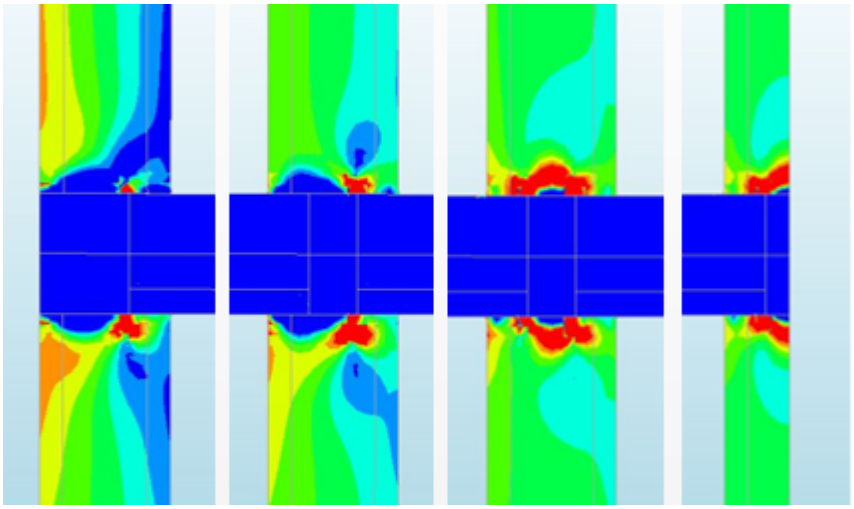

Figure 7.18 Strain development in connection zones 2-5 - 10 stories.

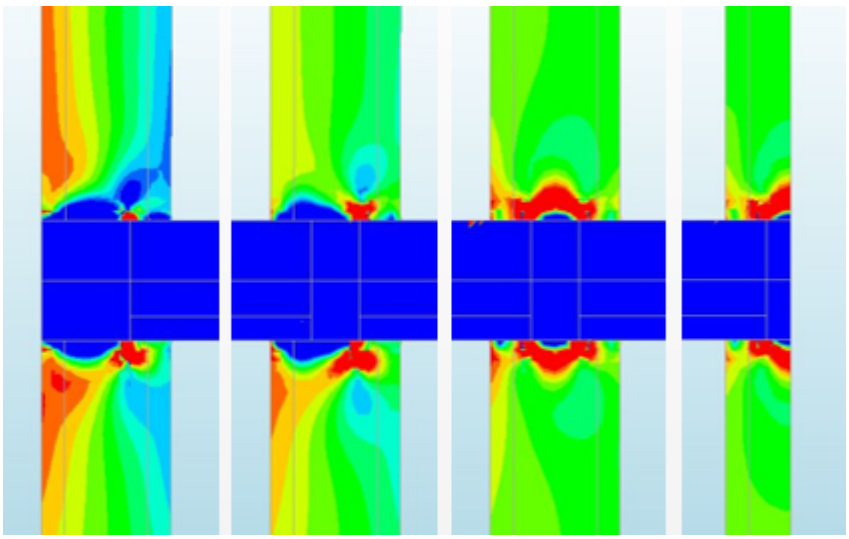

Figure 7.19 Strain development in connection zones 2-5 - 12 stories.

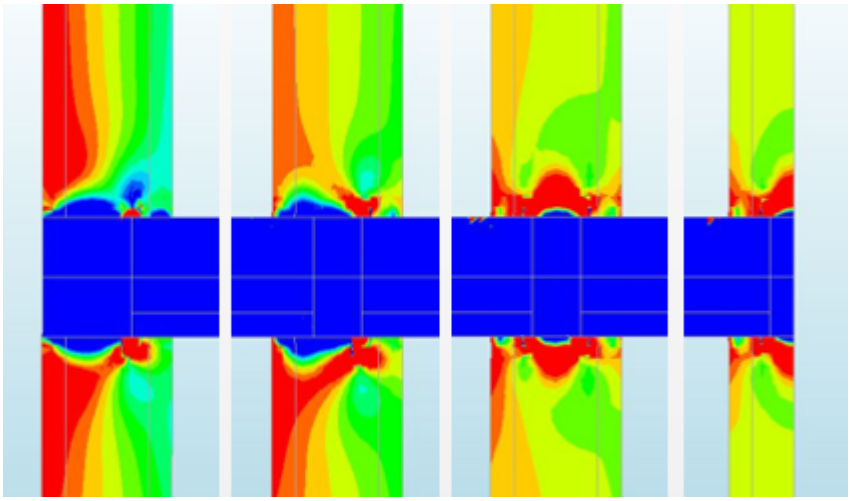

Figure 7.20 Strain development in connection zones 2-5 - 15 stories.

Figure 7.12**Fel! Det går inrte att hitta någon referenskälla.** illustrated that when the building exceeds 10 stories, the number of stories does not influence the long-term deformation of the slabs. The clamping force is large enough to prevent free deformation of the slabs, which will induce large principal strains in the structural wall elements, see Figure 7.18 to Figure 7.20. Figure 7.18 and Figure 7.19 shows increasing areas with principal strains larger than the cracking strain for 10 and 12 stories, respectively, but for 15 stories, see Figure 7.20 the cracked areas were substantially large. It should also be noted that for more than 8 stories the results indicates that cracks will emerge on the inner walls and for 15 stories cracks from spalling will start from the slab to the wall surface.

Smaller cracks were developed in the upper edge of the slab. The size of the cracks in the slabs were limited as the structural wall elements cracked as well, allowing the slab to deform and it should not be considered as fully fixed. Buildings which contains more than 8 stories develop too large strains in the outer side of the exterior wall.

Figure 7.21 presents how the the maximum crack width was developed in the central supporting wall at point 5, see Figure 7.1.

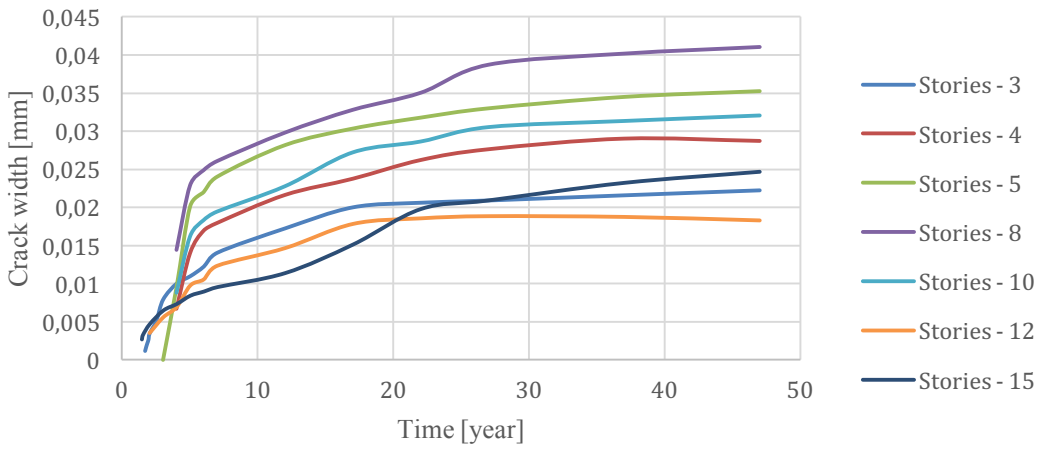

Figure 7.21 Crack development in the structural wall in point 5.

The size of the crack increased with increased number of stories up till 8 stories. For 10, 12 and 15 stories the crack size becomes smaller compared to 8 stories since extensive areas of strains larger than the cracking strain indicates that large cracks occur in other locations, causing the cracks in point 5 to be smaller.

7.4 Influence of number of spans

The total length of the building is dependent on the number of spans. An increased length will also increase the restraint forces which could have an impact on the results in terms of deformation and cracking. Based on experience from existing buildings, the parameter study was decided to represent buildings with lengths varying between approximately 30 and 80 meters.

7.4.1 Horizontal deformation

To simulate the varying building length, seven different FE models were analysed. In Figure 7.22 the horizontal deformation at point 2, see Figure 7.1, is presented as a function of time for different number of spans.

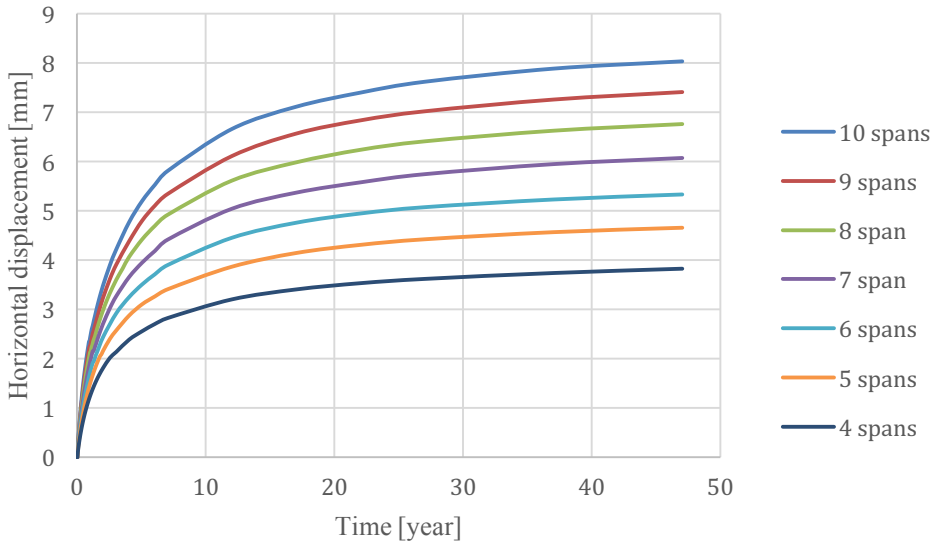

Figure 7.22 Deformation in the horizontal direction based on varying number of spans.

Figure 7.22 indicates that the horizontal deformation increases with increasing number of spans. The deformation developed differently based on the number of spans. It should be noted that the largest part of the deformation occurred during the first 10 years.

7.4.2 Cracking in the bottom corner of the exterior wall

With increased number of spans, the exterior wall was positioned further away from the symmetry line of the building. How this affects the largest crack width at point 1, see Figure 7.1, is illustrated in Figure 7.23.

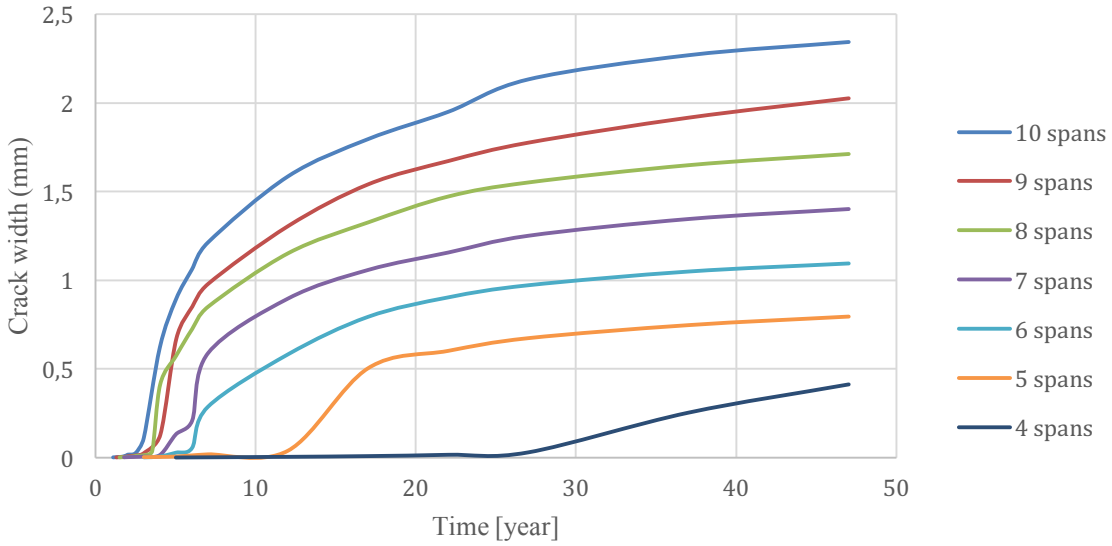

Figure 7.23 Crack development in the exterior wall near the support based on varying number of spans.

Based on the relation between crack width and number of spans, Figure 7.23 shows that the exterior wall was more exposed to wide cracks with more spans. All curves illustrate a similar behaviour but the crack initiated at different time steps and it growed faster in size with increasing number of spans.

7.4.3 Strain development in connection zones

Increased number of spans brings more supports and connection zones, which results in more possible restraints. Figure 7.24 – Figure 7.30 illustrates the development of maximum principal strains for buildings with 4 to 10 spans.

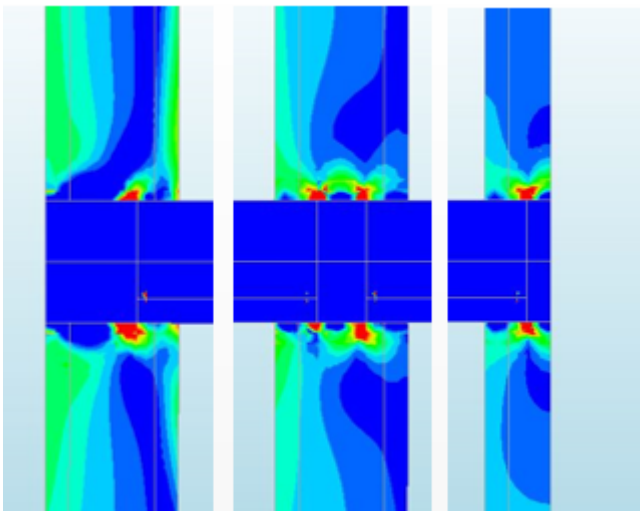

Figure 7.24 Strain development in connection zones - 4 spans.

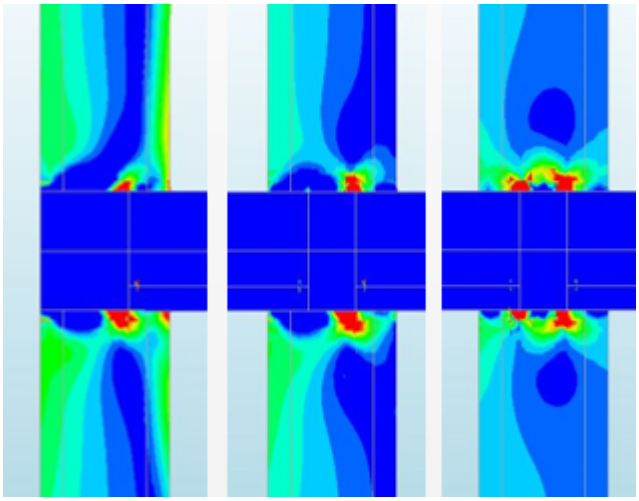

Figure 7.25 Strain development in connection zones - 5 spans.

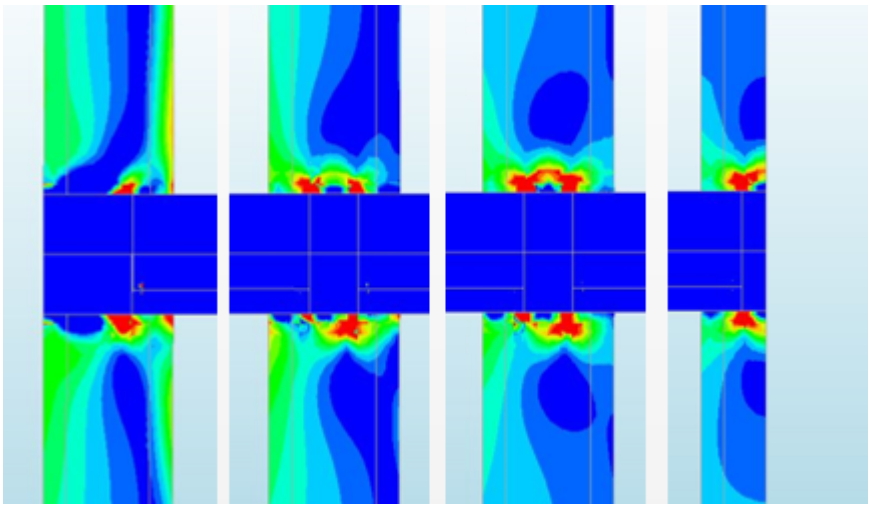

Figure 7.26 Strain development in connection zones - 6 spans.

Figure 7.24 – Figure 7.26 show how the strains varied for 4 to 6 spans. The strain in the structural walls increased when more spans and longer buildings are made were studied. When 6 or more spans were analysed it was possible to see that cracking starts to develop over a larger part of the inside of the exterior wall but also that larger strains concentration in the outer part of the exterior wall started to develop. Increasing strains, leading to cracks starting from the end of the slab elements, were also detected inside the structural walls as the number of spans increased.

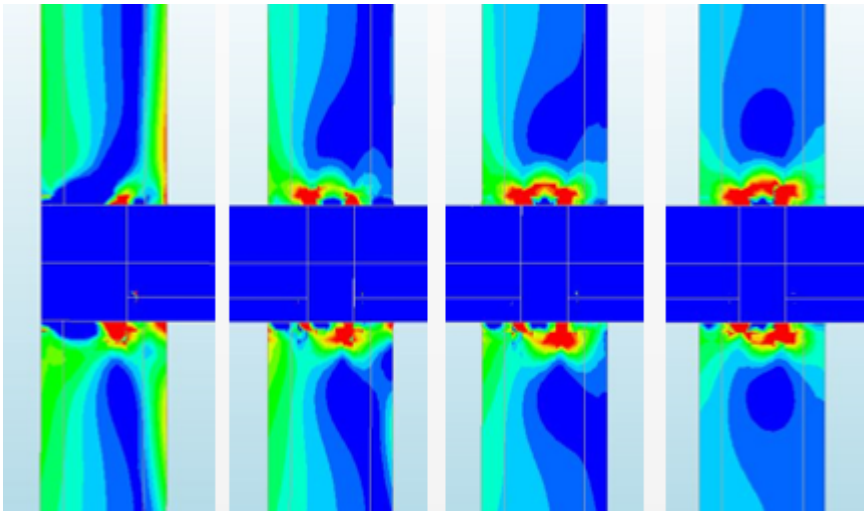

Figure 7.27 Strain development in connection zones - 7 spans.

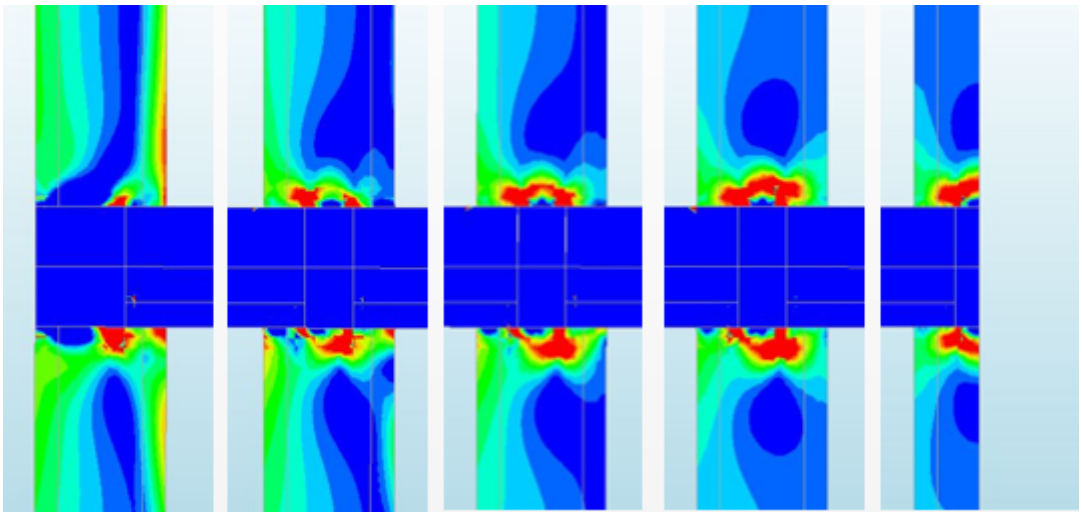

Figure 7.28 Strain development in connection zones - 8 spans.

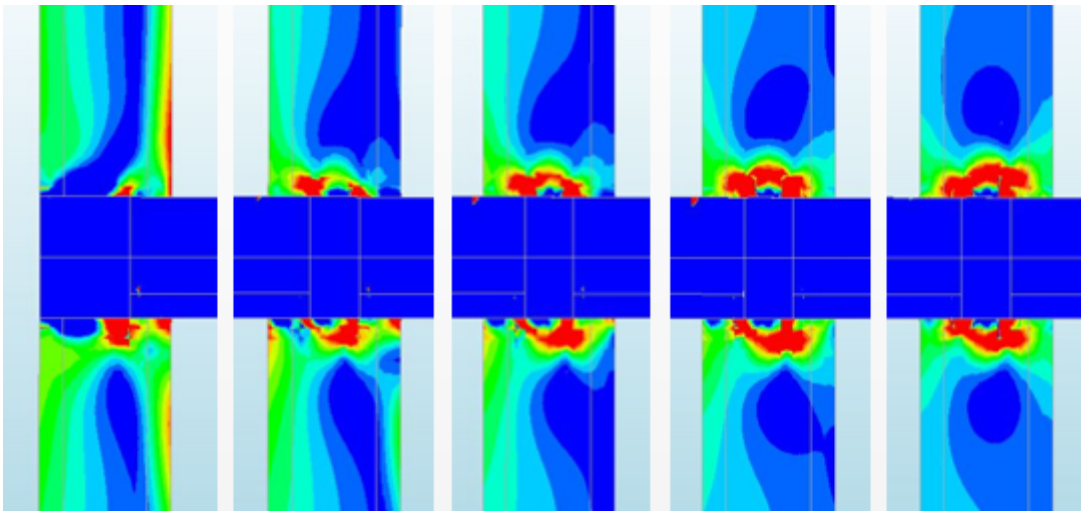

Figure 7.29 Strain development in connection zones - 9 spans.

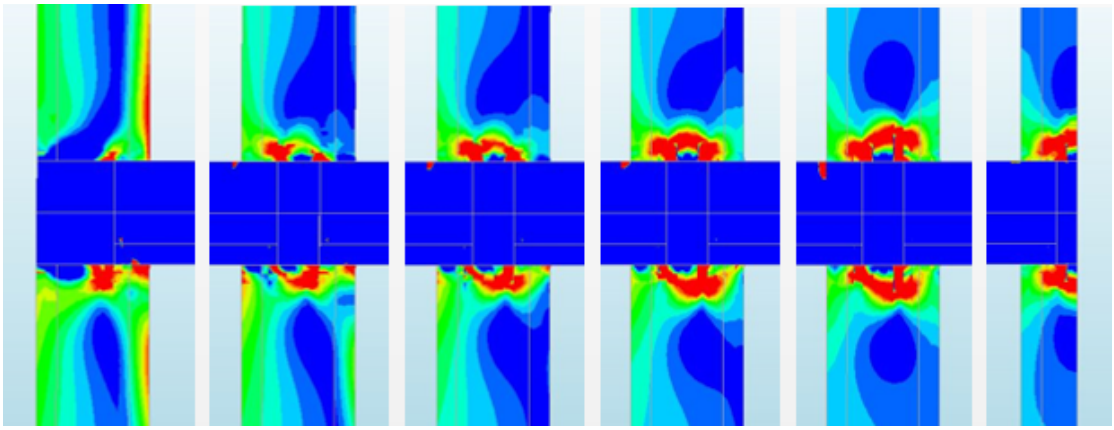

Figure 7.30 Strain development in connection zones - 10 spans.

With 7 to 10 spans, larger strains in the exterior wall and cracks seems inevitable. The slab also started to crack in its upper edge as the total amount of spans exceed 7 spans. Larger cracks were also found inside the walls closer to the centre of the building. This was expected since the supports in the centre of the building are exposed to the largest restraint force. The walls which were not in the centre of the building had the possibility to "bend" when the slabs were deformed, and therefore not as restrained as the centre wall.

7.5 Influence of span lengths

Since different span length are used in the production it is necessary to investigate the effect of their lengths. As the length of the elements increases, the restraint forces will increase in proportion. However, as the length of each span increases, the fewer spans are needed to fulfil the desired length of the building and vice versa. As a continuation of the parametric study, different span lengths were therefore investigated to see the impact of this parameter.

Since this study was performed in cooperation with COWI, focus was on using the same lengths as they usually work with in design, i.e. 7 m, 8 m, 9 m, and 10 m. During the investigation 28 different analyses were performed with specified span lengths and varying number of spans. During these analyses, all other parameters were kept unchanged, as stated in Table 7.1.

7.5.1 Horizontal deformation

For each span length, the final horizontal deformation is presented in Figure 7.31 for a building length varying from 27 to 81 meters. The horizontal deformation was measured in the outer joint in point 2, see Figure 7.1.

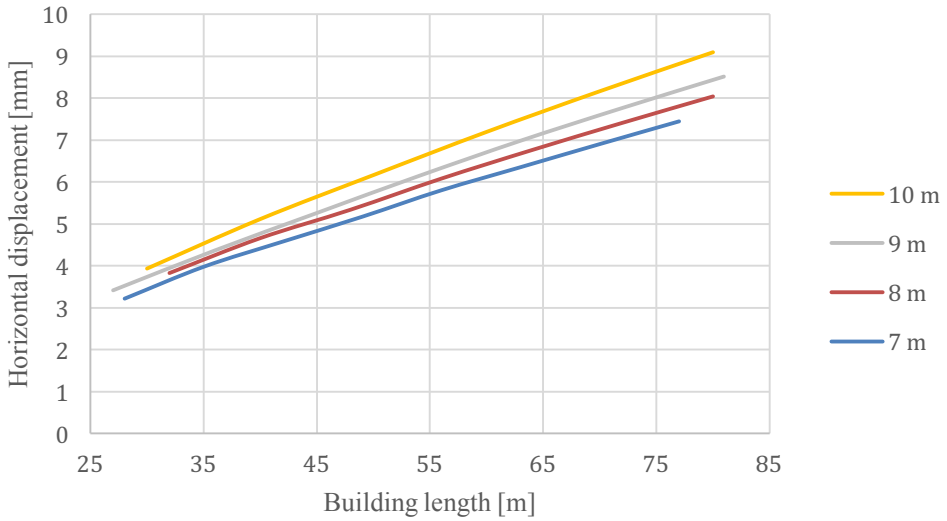

Figure 7.31 Deformation in the horizontal direction of point 2, see Figure 7.1, as a function of the building length for varying span lengths.

Figure 7.31 illustrates a rather linear relation between the final horizontal deformation and the total length of the building for each span length. It also displays a gradual increase in deformation with increasing span length, as well as a greater difference between the span lengths as the building becomes longer. From the point of view of horizontal deformation, the figure indicates that it is beneficial to use smaller span lengths although it requires more spans.

7.5.2 Cracking in the bottom corner of the exterior wall

The final value for crack width at the bottom corner in point 1, see Figure 7.1, was compared for different span lengths, for increasing total length of the building, see Figure 7.32.

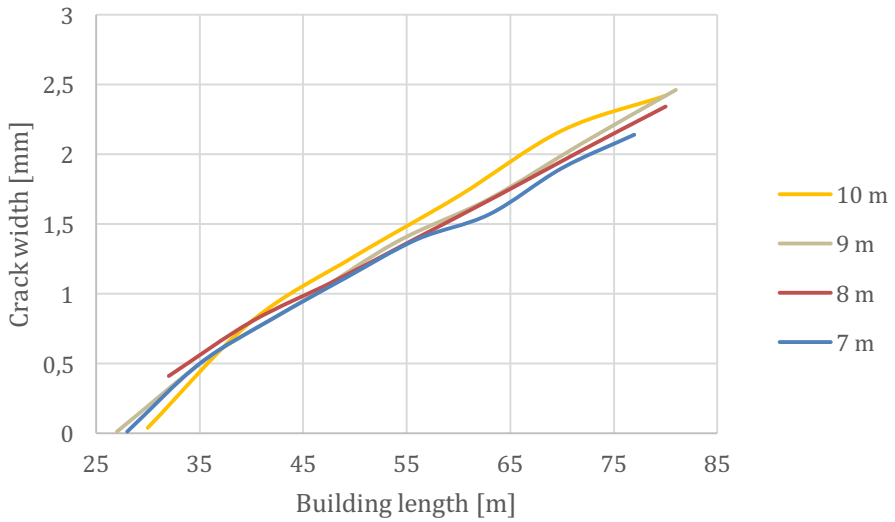

Figure 7.32 Crack width in the exterior wall near the support as a function of the building length, for varying span lengths.

Figure 7.32 indicates that the final values for crack width is roughly the same regardless of span length. The crack widths for longest span length of 10 m is slightly wider than for the other span lengths which all show similar values for the same building length. If this this deviation depends on the FE-model or corresponds to the real response is hard to judge.

7.5.3 Cracking in the upper edge of the slabs

During the FE-analyses cracks were observed at the upper edge in each slab. The cracks only developed at one side of the slab, the one closest to the symmetry line. The largest cracks were also discovered in the slab closest to the symmetry line and therefore an investigation was made to compare the size of these cracks, depending on different length of the building and for varying span length, see Figure 7.33.

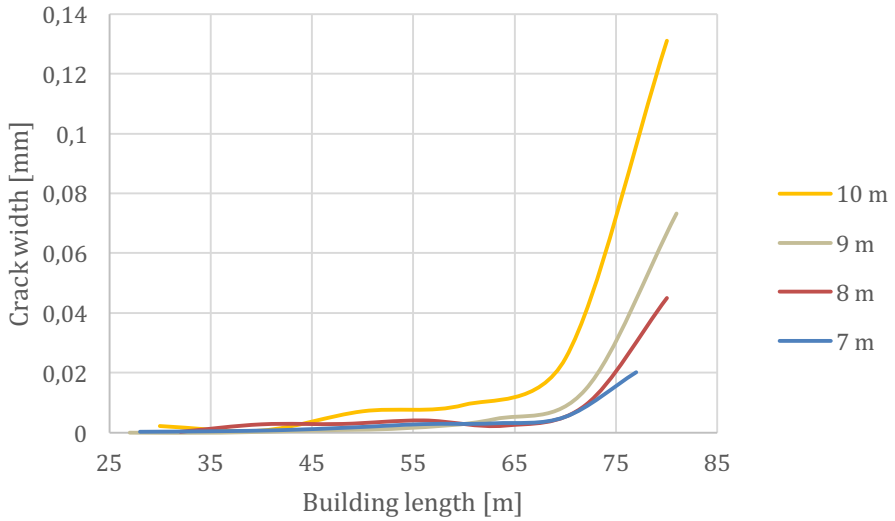

Figure 7.33 Crack widths in the upper edge of the slab near the symmetry line as a function of the building length, for varying span lengths.

Figure 7.33 illustrates a similar behaviour, but with different magnitudes, for the different span lengths. As each building reaches the length of approximately 70 meters, an increase of crack widths occurs for all cases. For buildings with longer spans, the crack widths are remarkably wider.

7.6 Observations

As shown in Section 7.2 – 7.5, the behaviour is infuenced by each parameter. However, a general remark is that the cracking behaviour is similar, with similar crack patterns, independently of the variation of the parameters, but that the size of the cracks depends on the values of each parameter.

For the reference object in this parametric study, the first major crack (with a crack width larger than 0,4 mm) emerged in the exterior wall, at the interface between the wall elemetns and the joint, see Figure 7.34.

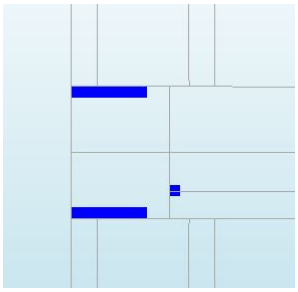

Figure 7.34 The first major crack between the wall elements and the joint at the exterior connection zone.

When the crack had propagated through the interface at the exterior wall, cracking appeared in the other connection zones. The cracks appeared at the top of the joint according to Figure 7.35.

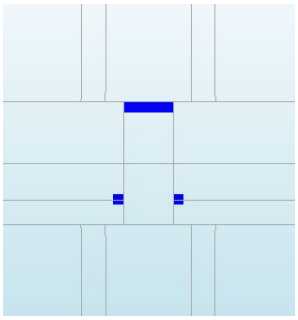

Figure 7.35 Major crack in the top of the joint at the connection zones.

As the time progress, cracking also spread to the wall elements as well as to the interfaces between of the slabs and the joints for all connection zones. If stresses were high enough, cracks developed in the upper edge of the slab for all connection zones except at the exterior wall, see Figure 7.36.

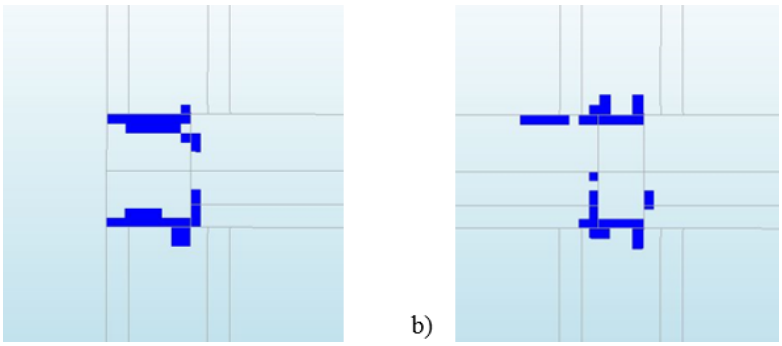

Figure 7.36 a) Cracks developed in the connection zone at the exterior wall at the end of service life. b) Cracks developed in the inner connection zones at the end of service life.

For the supporting walls, cracking started later than in the connection zones and the lower part of the exterior walls was most exposed. The cracking started to develop from the outer corner and the crack region extended upward in the wall. With time, the crack in the bottom of the wall propagated through the wall, see Figure 7.37. Similar behaviour can be expected for neighbouring walls, but at a later stage.

a) 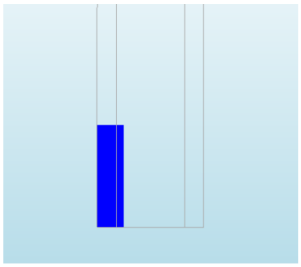 b) 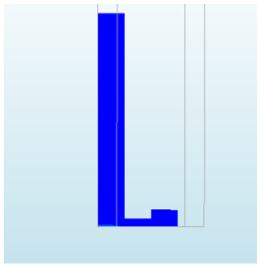

Figure 7.37 Crack pattern at the bottom corner at the exterior wall. a) The first region with major cracking. b) Complete crack pattern at the end of service life.

Following this general behaviour, each parameter will affect when specific cracks occur. Table 7.2 – 7.4 present at which time the crack width exceeds the crack width limitation for varying storage time, number of stories and number of spans, respectively.

Table 7.2 Time, in year [yr], when the crack width exceeded the crack width limitation given in the table heading, for varying element storage times.

	Cracks 0,4mm				Cracks 1mm
Storage time	Support A [yr]	Support B [yr]	Connection zone at support A [yr]	Other connection zones [yr]	Support A [yr]
1 week	0,7	2	0,41	0,45	5
2 weeks	0,73	2,1	0,41	0,58	6
1 month	3	7	0,41	0,75	-
3 months	12	-	0,41	0,87	-
6 months	37	-	0,41	0,93	-

Table 7.3 Time, in year [yr], when the crack width exceeded the crack width limitation given in the table heading, for varying number of stories

	Cracks 0,4mm				Cracks 1mm
Number of stories	Support A [yr]	Support B [yr]	Connection zone at support A [yr]	Other connection zones [yr]	Support A [yr]
3	1,2	3	0,39	0,66	7
4	2	5	0,41	0,74	12
5	3	7	0,41	0,75	-
8	5	-	0,46	0,87	-
10	12	-	0,48	0,91	-
12	22	-	0,49	0,96	-
15	-	-	0,51	0,97	-

Table 7.4 Time, in year [yr], when the crack width exceeded the crack width limitation given in the table heading, for varying number of spans

	Cracks 0,4mm						Cracks 1mm	
Number of spans	Support A [yr]	Support B [yr]	Support C [yr]	Support D [yr]	Connection zone at support A [yr]	Other connection zones [yr]	Support A [yr]	Support B [yr]
4	5	-	-	-	1	1,7	-	-
5	3,1	22	-	-	1	1,6	-	-
6	3	7	-	-	0,43	0,75	-	-
7	1,8	4	-	-	0,43	0,75	17	-
8	1,5	3	12	-	0,41	0,75	12	-
9	1,3	2,5	6	-	0,41	0,7	12	50
10	1,2	1,9	4	27	0,41	0,7	6	22

Table 7.2 – 7.4 shows that more restraint induces larger and more cracks. Longer storage time as well as fewer stories and spans results in smaller and fewer cracks due to less restraints.

8 Discussion

8.1 Modelling process

Since many analyses were to be performed, an early decision was made to work with a 2D model to reduce the computational time. If a 3D model would have been used then it would illustrate the total behaviour of the cross-section, i.e. it would have included long-term effects in more than one direction, i.e. also in the transversal direction. By using a 2D model, the transverse connection between the slabs and the dowel effect in the connection zone were ignored. Since the dowel's primary task is to prevent a vertical collapse, an assumption was made that the effect from the tie reinforcement and the clamping has a greater impact on the horizontal restraint than the dowel. The dowel would have only increased the stiffness of the joint and possible made a small contribution to the restraint degree. By choosing a 2D model, out-of-plane stresses was also disregarded which could have some impact further away from the tie reinforcement, if the ties are placed too far apart, then the restraint in those areas are only due to clamping.

A simplification was made to model the building with symmetry lines and only two stories with tyings and a distributed load to simulate additional stories. This was also done to minimize the computational time since several analyses were to be performed. A comparison was made between the reference object (with tyings and distributed load) and a complete model of 5 stories. Both methods showed similar behaviour and outcome. Based on this, it was judged that this simplification was feasible, even though various combination of parameters will affect the restraint and final result differently. Since the structure will deform differently with different geometry, the position of the tyings would need to be adjusted in order to resemble the behaviour correctly. As an approximation, the tyings were placed at a level corresponding to the section with no curvature in the case of 5 stories to resemble how the structural wall elements are expected to deform in average.

By doing an analysis in different phases, DIANA added elements to the model at different times. In each new phase, elements from previous phases already contained deformations, stresses and strains. This could become a problem: since the interfaces were already attached to the deformed elements they caused initial stresses to additional elements added to the interfaces in a later phase. This is not the case in reality, since the additional elements are mounted to the structure with zero initial stresses. In DIANA it is possible to adjust the initial stresses with an option called DEFORM IMPORT (DIANA fea, 2017). DEFORM IMPORT is added manually in a DAT.file but it is relatively time consuming and after the deformation is added it is not possible to adjust anything in the model. Therefore, a comparison was made regarding the impact of adjusting the initial stresses with this option. Based on this, a choice was made to ignore the initial stresses in the added elements since they had no major impact on the final results and since the initial deformations were considered to be relatively small. For example, it had a negligible effect on the strain distribution compared to the effect of storage time, that had a large effect on the initial stresses and strains. Shorter storage time resulted in smaller initial deformations and less initial stresses but lead to development of larger strains in the end. This can be compared to longer storage time which resulted in larger initial deformation and larger initial stresses but to smaller strains at the end of service life, see Section 7.2.3.

The verification of the model was made step-wise, to check that the behaviour of each modelled part would have a response that correspond to the reality. The reason for this was that if each modelled part had a correct response, they would also provide as real behaviour as possible combined. It could be mentioned that a verification of response of the friction model was made in this study because the restraint force due to long-term effect acts in cycles and is accumulated with time. As the slab is affected by shrinkage and creep, normal forces are developed within the element. The slab is clamped together between the walls and a frictional force holds the slab still. As the effect of shrinkage and creep increases, the magnitude of normal force within the element has accumulated and as the normal force gets larger than the frictional force, the slab slides horizontally. As the slab slides, the accumulated normal forces within the element decreases as the tensions gets released due to sliding.

8.2 Parameters affecting the response of the structure

During the investigation, it became clear that the horizontal long-term deformation of the slab affected the development of cracks at the bottom of the exterior wall. As the slab deforms, tensile forces will increase due to the fact that the supporting walls are fixed to the foundation and will bend when the slab contracts. Longer storage time and fewer spans are therefore beneficial in order to prevent these cracks. However, even if a building consists of many spans with elements that had a short storage time, the results indicates that cracks can be prevented if the building have enough stories to provide large enough clamping forces in the walls. In addition to preventing the slab to slide, the effect from large enough clamping is that the cracks at the bottom will be avoided since the supporting walls will have compression stresses in the whole cross-section.

The result from Section 7 indicates that the development of strains is highly dependent on each parameter investigated. Shorter storage time resulted both in larger restraint forces and horizontal deformations compared to the reference building; this caused cracks in the interior part of the exterior wall. Similar response was predicted if a building consisted of 3 or 4 stories since the effect of clamping was not large enough to prevent the slab to slide. If the same building had its prefabricated elements stored for 1 month, it approximately had the same horizontal deformation as a building with 5 stories and 1 or 2 weeks of storage time. These configurations also entailed similar crack patterns in the exterior wall. The results also show that the cracking in the interior part of the exterior wall increases with more spans since more restraint forces are restrained by the supports.

A typical crack pattern occurred in the structural walls at the connection to the slabs. These cracks were dependent on the combination of storage time and the total amount of stories. With longer storage time, the slabs had less need to deform after they had been mounted to the structure. On the other hand, even with a large effect of clamping, strains and cracks will develop in the walls if large long-term deformations are expected due to short storage time. Therefore, the effect of clamping is more crucial for these cracks, but the response is still very dependent on the storage time. It was shown that a building consisting of several spans with a lot of stories exposed to a short storage time is not an appropriate combination with regard to restraint cracks.

Even though the span lengths usually are decided with regard to the buildings' design, Section 7.5 suggest that shorter span lengths could be worth considering with regard to long-term displacement and restraint cracks. This indicates that the length of the slab elements affects has a greater negative impact on the construction when subjected to restraint than the number of elements.

Of all the parameters investigated, storage time is the only parameter that can be adjusted without changing the design of the building. It is therefore considered to be the simplest adjustment that can be made in the production in order to reduce restraint forces and crack risks. Furthermore, Section 7.2 indicates that this might also be the parameter that has the greatest impact.

8.3 Structural response with regard to cracks

The result of the parametric study shows that the cracks affect the structural response of the building. The large cracks at the bottom of the exterior wall affect the effective boundary condition at the support; in a linear analysis, this can be considered as partially fixed or hinged instead of fully fixed, depending on the number of stories. The likelihood of this assumption having a negative effect of the global structural response is relatively small since other components such as elevator shafts and shear walls most likely are used to stabilize the building.

Since all structural walls were reinforced with regard to a reference object for prefabricated walls according to COWI, no special regard was taken considering crack widths with regard to corrosion in the exterior wall. However, with regard to certain requirements, the results imply that additional reinforcement might be needed for the exterior wall.

The cracks developed in the structural walls at the connection zones to the slabs were more crucial to the capacity of the structure. If the effect from clamping is large it will increase the restraint forces in the structure. Larger restraint forces will induce stresses and strains in the structural wall elements as it prevents the slab to deform. As the strains in the walls increase, cracks start to develop in the walls and, as a result, release the slab and allow it to deform. The effect of clamping needs to be taken into account in design, otherwise it could lead to too large strains in the wall sections and the stiffness of the wall might decrease.

When the result from Section 7 were compared to actual damages in real structures, it looks quite similar. For the reference object, larger cracks were initiated within the structure after approximately 5 years in the analysis and this was also the case for the corresponding building in reality. The probability of spalling and cracking of concrete are therefore high and is likely to damage the building. The comparison to observations in real buildings indicates both that the model has been correctly defined, but also that the influences of the parameters are reasonable.

8.4 Effect of boundary conditions

As the effect of clamping increases, the slabs ability to rotate decreases and could be considered as a fixed connection. Eventually, cracks were developed in the upper edge of the slabs but these were limited as the structural wall elements cracked as well. If the

wall elements would not crack, more severe cracks in the upper edge of the slab can be expected. Since the boundary conditions of the slabs elements are considered to be simply supported in design, some additional reinforcement might be required to be able to limit the crack width in the upper edge of the slab, in addition to what is directly obtained from the design calculations.

In this study, only the first story's slab and connected walls were studied in detail. For the slabs and walls above, which only were treated as loads, different patterns of strains and cracking possibly could develop. No special boundary conditions were attached to the wall elements except from the tyings, the walls therefore presented the same deformation as the walls on the second story would have in reality. The walls on the used in the model, defined in Section 6, had one side exposed to tensile stresses and one side exposed to compression as the amount of stories didn't exceed 8 stories. If more than 8 stories are used in a building, the cross-section of the walls used in the model are expected to be only in compression resulting in crushing of concrete.

9 Conclusion

This study investigated damages such as cracks and spalling due to long-term effects in long and narrow buildings consisting of prestressed prefabricated concrete slab elements. In a parametric study, the influence of the following parameters was investigated: storage time, number of stories, number of spans and span lengths.

The most significant result was that damages are likely to appear during service life, but that some damages can be prevented if only certain parameters are adressed in design. The study showed that all parameters in the parametric study have a distinctive impact on the structural response and it is therefore of great importance to take the response from each parameter into account individually in design.

The following conclusions can be drawn from this study:

The parametric study revealed that the parameter with greatest impact on reducing structural damages is storage time. Longer storage time allows the slabs to deform freely and less intrinsic deformation are expected. Therefore, less restraint forces are induced within the structure. If storage time would be considered in design then fewer actions concerning maintenance and repair would be needed in the future. Storage time would not affect the structural design but rather the need of storage space as well as waiting time before the elements could be assembled.

In the structural walls, certain damages in form of spalling and crushing of concrete will develop. It was concluded that the risk of spalling increase with shorter storage time and if a building consists of several spans. As more spans are used, more possible restraint forces within the structure are induced. Therefore, the influence of storage time determines the magnitude of restraint forces in each connection which, if large enough, could cause spalling. Spalling could to some extent be prevented if storage time is considered in design. The corner of the structural wall elements is crushed as it prevents the slab to rotate. If the corner of the wall would be redesigned as more round and smooth then the stress concentration would be more distributed.

The effect of clamping is one of the main reasons for the origin of restraint forces. In design, it is very important to consider the clamping effect for a multi-storey building because otherwise cracks are most certainly inevitable. The results clearly indicate that the frictional force in each interface is dependent on the effect of clamping. This means that certain requirements with respect to cracks in structural wall elements needs to be considered as the friction force prevent the slabs to slide and therefore develop stresses and strains in the walls as it deforms with the slabs.

The observations from the parametric study shows that number of spans and span length affected the intrinsic deformations do to number and size. However, Section 7.6 indicates that they do not have the same impact as storage time and number of stories.

Regardless of how the parameters studied are varied, the first crack will occur between the exterior wall and the joint already during the first year, followed by cracks in the other joints.

A hypothesis before this study was that the connection between the slab and the joint was the weakest part since the elements were casted in different steps and at various time. The result from the parametric study clearly supported this hypothesis and proved that the restraint from the tie reinforcement only becomes active after the first crack has occurred.

As a final remark the parametric study concluded that a combination of shorter storage time, more stories and longer and more spans could result in larger cracks which will affect the structural behaviour.

Regarding finite element modelling, DIANA proved to be an efficient software that handles both long-term effects and restraint well. This was proved by verification and supported by theory and facts. For that reason, the results from the FE-model can be considered credible and something that should be taken into account in future design. Although it has brought attention to restraints, some simplifications were made and only limited numbers of parameters were investigated and therefore a continue research would be of great value.

9.1 Future research

For future research with regard to restraint forces there are a lot of development opportunities which concerns current codes, FE-modelling and more advanced studies where various parameters are studied.

For future research with respect to FE-modelling, a 3D-model could be used concerning restraint forces. A 3D-model could take into account:

- Effect of long-term effects also in the transversal direction.
- More advanced modelling of connections with regard to tie reinforcement and dowels.
- A complete model with all stories.
- Use DEFORM IMPORT to start with zero initial stresses in the joint and structural walls.

Future research could also focus on the effect of storage time which in our study seemed to be the most decisive parameter. Future research with regard to storage time could study:

- How longer storage times can be made possible in the industry, without compromising time and efficiency demands
- The possibility to utilize a storage climate which accelerates the effect of long-term effects.
- Use alternative materials such as rapid hardening concrete to minimise the long-term deformations after assembly of the slab elements.

10 References

Červenka, V., Červenka, J., & Jendele, L. (2016). *ATENA Program documentation Part 1 - Theory.* Prague, Czech Republic: Červenka Consulting.

Al-Emrani, M., Engström, B., Johansson, M., & Johansson, P. (2011). *Bärande konstruktioner del 2* (1 ed.). Göteborg: Chalmers University of Technology.

Al-Emrani, M., Engström, B., Johansson, M., & Johansson, P. (2013). *Bärande konstruktioner Del 1* (1 ed.). Göteborg: Chalmers University of Technology.

Antona, B., & Johansson, R. (2011). *Crack control of concrete structures subjected to restraint forces.* Göteborg, Sweden: Chalmers University of Technology.

Betongelementföreningen. (1998). *Bygga med prefab.* Bromma: Betongelementföreningen.

Bobinski, J., & Tejchman, J. (2014). *Continuous and Discontinuous Modelling of Fracture in Concrete Using FEM.* Gdansk, Poland: Springer-Verlag Berlin and Heidelberg GmbH & Co. K.

Boverket. (2004). *Boverkets handbok om betongkonstruktioner, BBK 04.* Karlskrona, Sweden: Boverket.

Brattström, N., & Hagman, O. (2017). *Reinforced concrete subjected to restraint forces.* Stockholm: Royal Institute of Technology.

Burström, P. (2007). *Byggnadsmaterial* (2 ed.). Lund: Studentlitteratur AB.

CEN. (2002). *Eurocode - Basis of structural design.* Brussels, Belgium: European Committee for Standardization.

CEN. (2004). *Eurocode 2: Design of concrete structures - Part 1-1: General rules and rules for buildings.* Brussels, Belgium: European Committee for Standardization.

CEN. (2006). *Eurocode 1 - Actions on structures - Part 1-7: General actions - Accidental actions.* Brussels, Belgium: European Committee for Standardization.

Danielsson , H., & Malmgren, L. (2006). *Utformning av byggnader för säkerhet mot fortskridande ras.* Lund: Lunds Tekniska Högskola.

Department of Defense (DOD). (2016). *Design of buildings to resist progressive collapse.* USA: Unified Facilities Criteria (UFC) 4-023-03.

DIANA fea. (2017). *https://dianafea.com*. Retrieved April 18, 2018, from https://dianafea.com/manuals/d102/Diana.html

Engström, B. (2011). *Design and analysis of prestressed concrete structures* (7 ed.). Göteborg: Chalmers University of Technology.

Engström, B. (2014). *Restraint cracking of reinforced concrete structures.* Göteborg: Chalmers University of Technology.

Eriksen, M., & Kolstad, M. (2016). *Investigation of Cracking Behavior in Reinforced Concrete Panels with Bond-slip Reinforcement.* Trondheim, Norway: Norwegian University of Science and Technology.

Eriksson, M., & Fritzson, E. (2014). *Crack control of extended concrete walls.* Göteborg: Chalmers University of Technology.

fib. (2013). *Model Code for Concrete Structures 2010.* Berlin, Germany: Wilhelm Ernst & Sohn, Verlag für Architektur und technische Wissenschaften GmbH & Co. KG.

Fritzson, E. (2018, 05 18).

Heinrich, T. (1991). *Creep, relaxation and shrinkage of structural concrete.* Aachen, Germany: Technical University Aachen.

Hermodsson, T. (1992). *Bjälklagskryss av prefabricerade väggelement och förespända håldäckselement.* Lund: Lund Institute of Technology.

Lundgren, K. (2007). Lap splice over a grouted joint in a lattice girder system. *Magazine of Concrete Research, 59*, 713–727.

Plos, M. (2000). *Finite element analyses of reinforced concrete structures.* Göteborg: Chalmers University of Technology.

Rijkswaterstaat. (2016). *Guidelines for Nonlinear Finite Element Analysis of Concrete Structures.* Netherlands: Rijkswaterstaat Centre for Infrastructure.

Starossek, U. (2014). *Progressive collapse of structures.* ICE Publishing.

The Daily Telegraph. (1968). *Wikipedia*. Retrieved 04 20, 2018, from https://en.wikipedia.org/wiki/Ronan_Point#/media/File:Ronan_Point_-_Daily_Telegraph.jpg